

Detection and Speciation of Silver in Freshwater Containing Triclosan
and Thyroid Hormone T₃

by

Patricia Lillian Collins
B.Sc., University of Victoria, 1997

A Thesis Submitted in Partial Fulfillment
of the Requirements for the Degree of

MASTER OF SCIENCE

in the School of Earth and Ocean Sciences

© Patricia Lillian Collins, 2010
University of Victoria

All rights reserved. This thesis may not be reproduced in whole or in part, by photocopy
or other means, without the permission of the author.

Supervisory Committee

Detection and Speciation of Silver in Freshwater Containing Triclosan
and Thyroid Hormone T₃

by

Patricia Lillian Collins
B.Sc., University of Victoria, 1997

Supervisory Committee

Dr. Jay T. Cullen, School of Earth and Ocean Sciences
Supervisor

Dr. Kevin Telmer, School of Earth and Ocean Sciences
Departmental Member

Dr. Caren C. Helbing, Department of Biochemistry and Microbiology
Outside Member

Abstract

Supervisory Committee

Dr. Jay T. Cullen, School of Earth and Ocean Sciences

Supervisor

Dr. Kevin Telmer, School of Earth and Ocean Sciences

Departmental Member

Dr. Caren C. Helbing, Department of Biochemistry and Microbiology

Outside Member

In freshwater, there is more opportunity for silver (Ag) to interact with organic ligands than in seawater. Triclosan is an antibiotic agent which resembles thyroid hormone T_3 and is finding its way into aquatic systems. Preliminary toxicology studies for the frogSCOPE program suggest that triclosan and nanosilver (nanoAg), also used as an antibiotic agent, may be chemically interacting, as they seem to synergistically increase the endocrine-disrupting abilities already observed independently in each chemical. Ag speciation methods can be used to determine if triclosan or thyroid hormone T_3 are interacting with Ag ion (Ag^+), which gets released over time by nanoAg. To fully utilize Ag speciation methods, however, total Ag in the sample must also be independently analyzed. Here we investigated a new total Ag analysis using cadmium sulfide quantum dots (CdS QDs) as fluorescence probes in solution. This method promises results in a fraction of the time of the established competitive ligand equilibration-solvent extraction (CLE-SE) technique utilizing PDC^- and DDC^- to bind Ag and bring it out of solution. Following this investigation were a series of experiments using CLE-SE for total Ag and Ag speciation in well water used to house bullfrog tadpoles in frogSCOPE Ag exposure studies. CLE-SE for Ag speciation was also applied to well water samples containing the two levels of nanoAg or Ag^+ used in frogSCOPE

Ag exposures, and used in ligand competition experiments to examine the potential of triclosan or T_3 to act as strong Ag-binding ligands, as compared to glutathione and EDTA, two known Ag-binding ligands. The results of the latter experiments could be used to determine if either of these could be forming complexes with Ag which increase or decrease their delivery to amphibian cells.

The fluorometric method using CdS QDs showed no ideal analytical response to nanomolar Ag^+ , even when commercial QDs were modified and used, so it could not be applied to our samples. Using CLE-SE for total Ag, the well water used as a base for toxicity studies in frogSCOPE contained Ag below the method detection limit of 5 pM. Using the speciation variation of the CLE-SE method, no evidence of naturally-occurring ligands which could produce extractable (hydrophobic) or non-extractable (hydrophilic) Ag complexes was found in this well water. EDTA and glutathione responded as model Ag-binding ligands to form non-extractable hydrophilic Ag complexes in fresh water. T_3 behaved like these model ligands, while triclosan enhanced the extractability of Ag in the presence of certain concentrations of the added ligand, DDC⁻. In another set of experiments, coordination of Ag by triclosan or T_3 was not detectable within that analytical window. These results suggest that ionic Ag released over time by nanoAg may be binding T_3 and preventing it from reaching its receptor, but confirming the interaction of triclosan and Ag^+ will require additional experiments using different analytical windows.

Table of Contents

Supervisory Committee	ii
Abstract	iii
Table of Contents	v
List of Tables	vii
List of Figures	viii
List of Abbreviations	ix
Acknowledgments.....	xi
Dedication	xii
Chapter 1: Introduction	1
1.1 References.....	9
Chapter 2: Total Silver in Aqueous Solutions using CdS Quantum Dots	13
2.1 Introduction.....	13
2.2 Methods.....	18
2.2.1 Synthesis of CdS QDs for use as probes for Ag ⁺	19
2.2.2 Functionalizing commercial CdS QDs for use as probes for Ag ⁺	20
2.2.3 Preparation of standards and samples for fluorometric analysis	21
2.3 Results.....	22
2.3.1 Quantum dot synthesis and functionalization	22
2.3.2 Synchronous Fluorescence Spectra.....	22
2.3.3 pH and toluene effects on quenching, enhancement of fluorescence	29
2.4 Discussion	32
2.5 Conclusions.....	42
2.6 References.....	43
Chapter 3: Using Competitive Ligand Exchange-Solvent Extraction to Examine Silver Interaction in Well Water Containing Triclosan and Thyroid Hormone T ₃	46
3.1 Introduction.....	46
3.2 Methods.....	59
3.2.1 Total Ag using PDC ⁻ /DDC ⁻	60
3.2.2 Qualitative competitive ligand exchange experiments	61
3.2.3 Titrations of Ag into well water used in frogSCOPE	64
3.3 Results.....	65
3.3.1 Total Ag using PDC ⁻ /DDC ⁻	65
3.3.2 Qualitative competitive ligand exchange experiments	67
3.3.3 Titrations of Ag into well water used in frogSCOPE	72
3.4 Discussion	81
3.4.1 Characterization of well water used collected from PESC.....	81
3.4.2 Qualitative interaction of model ligands, triclosan, and T ₃ with Ag	83
3.4.3 Interpretation of titrations of Ag into well water	86
3.5 Conclusions.....	89
3.6 References.....	91
Chapter 4: Conclusions	95
4.1 References.....	101

Appendix I: Cleaning protocols for equipment used in trace silver analysis	103
AI.i Definition of “clean”	103
AI.ii Glassware, low-density polyethylene (LDPE), and polypropylene (PP)	103
AI.iii Teflon-FEP bottles, sample vials, and separatory funnels	104
AI.iv References	105
Appendix II: Fluorometric Method for Total Silver using CdS Quantum Dots	106
AII.i Experiments involving synthesized quantum dots (QDs)	106
AII.i.i Synthesis of CdS QDs via controlled colloidal precipitation.....	106
AII.i.ii Preparation of other reagents	108
AII.i.iii Sample preparation and fluorometric analysis.....	109
AII.ii Experiments involving commercial CdS quantum dots (QDs).....	110
AII.ii.i Functionalization of commercial CdS QDs with mercaptoacetic acid (MAA)	110
AII.ii.ii Preparation of other reagents	112
AII.ii.iii Sample preparation and fluorometric analysis.....	113
Appendix III: Organic Extraction Method for Total Silver and Silver Speciation.....	114
AIII.i Total silver experiments.....	114
AIII.i.i Sample preparation	114
AIII.i.ii Preparation of other reagents	117
AIII.ii Silver speciation experiments	123
AIII.ii.i Sample preparation	123
AIII.ii.ii Collection of well water and preparation of other reagents.....	126
AIII.iii Method Limitations	135
AIII.iv References.....	138
Appendix IV: Data Tables	139

List of Tables

Table 1: Anticipated function of chemicals used in the synthesis of CdS quantum dots, in order of their addition to the reaction vessel.....	36
Table 2: Equations used to take experimental data and quantify Ag species in freshwater using DDC ⁻ as the added ligand.....	50
Table 3: ICP-MS instrument parameters for total Ag and Ag speciation methods.	62
Table 4: Regression analysis of well water titrations.	76
Table 5: Summary of information attained from Langmuir linearizations shown in Figure 22.....	78
Table 6: Regression analysis of frogSCOPE Ag exposure sample titrations.	82
Table 7: Titration set-up for total silver in milli-Q water.	122
Table 8: Titration set-up for competitive ligand exchange experiments with well water from PESC.	128
Table 9: Details on frogSCOPE samples examined by competitive ligand exchange. .	131
Table 10: Details of reagent scaling for different concentration factors required by frogSCOPE samples, as compared with “usual” samples in the pM range (grey).	132
Table 11: Titration set-up for competitive ligand exchange experiments with frogSCOPE samples.....	133
Table 12: Opportunities for Ag loss and gain during sample preparation and analysis.	136

List of Figures

Figure 1: Schematic of cellular uptake and bioavailability of dissolved silver.	3
Figure 2: Overlay of fluorescence emission and excitation maxima for commercial CdS QDs, 2×10^{-4} M, buffered using HEPPS.	17
Figure 3: TEM image of synthesized CdS QDs.....	23
Figure 4: TEM images of commercial CdS QDs.....	24
Figure 5: Synchronous fluorescence spectra for several Ag^+ standards.	26
Figure 6: Selected synchronous fluorescence intensities at 304 nm when CdS exposed to solutions of Ag^+ ranging from 0.5-5 nM.	27
Figure 7: Effect of 0.5-10 nM Ag^+ on synchronous fluorescence of CdS QDs at 304 nm using $\Delta\lambda = 305$ nm.	28
Figure 8: The effect of adding solutions containing 2% HNO_3 to buffered solutions containing 2×10^{-4} M CdS on pH.	30
Figure 9: Synchronous fluorescence intensity at 304 nm over time with the addition of 5 nM Ag^+ to a blank solution containing 2×10^{-4} M commercial CdS QDs.	31
Figure 10: Effect of concentration of mercaptoacetic acid (MAA) on synchronous fluorescence intensity at 304 nm in blanks and 4 nM Ag^+ made with commercial CdS..	33
Figure 11: A possible mechanism for the formation of CdS from thioacetamide and cadmium chloride.....	37
Figure 12: Diagram of functionalized commercial CdS QDs (circles) and some possible interactions with silver ions.	40
Figure 13: Appearance of ligands and Ag-ligand complexes formed in the experiments.	48
Figure 14: Schematic representation of titration curves for natural samples titrated with Ag^+ at a set concentration of DDC^-	51
Figure 15: Comparison of blanks using the total Ag method involving APDC/NaDDC, and the Ag speciation method involving 10^{-6} M DDDC.	66
Figure 16: Comparison of ICP-MS counts from a series of external standards and a series of APDC/NaDDC extractions on acidified water.	68
Figure 17: Effect of equilibration time with CHCl_3 on percent recovery of Ag ion using an APDC/NaDDC ligand mixture.	69
Figure 18: Standard additions curve for total Ag on well water collected from PESC on May 10, 2010.	70
Figure 19: Comparison of effect of $[\text{DDC}^-]$ on Ag^+ recovery.	71
Figure 20: A comparison of percentage recoveries of 100 pM Ag^+ in freshwater (Fraquil and well water) containing DDC^- and other competitive ligands.	73
Figure 21: Titration curves for PESC well water used as a medium in frogSCOPE toxicity studies.	75
Figure 22: Titration plots (left) and Langmuir linearizations (right) for well water containing 100 μM EDTA (a) and 30 $\mu\text{g/L}$ triclosan (b).....	77
Figure 23: Titrations of frogSCOPE samples.	80

List of Abbreviations

Ag	silver
Ag ⁺	silver ion
APDC	1-pyrrolidinecarbodithioic acid, ammonium salt
CdS	cadmium sulfide
CLE-SE	competitive ligand exchange-solvent extraction
DDDC	diethyldithiocarbamic acid, diethylammonium salt
DDC ⁻	diethyldithiocarbamate ion
EDTA	ethylenediaminetetraacetic acid
FEP	fluorinated ethylene polypropylene
FIM	free-ion model (of metal toxicity)
frogSCOPE	frog Sentinel species Comparative “Omics” for the Environment
GFAAS	graphite furnace atomic absorption spectrometry/spectrometer
HEPPS	3-[4-(2-hydroxyethyl)-1-piperazinyl]propanesulfonic acid
ICP-MS	inductively-coupled plasma-mass spectrometry/spectrometer
LDPE	low-density polyethylene
LOQ	limit of quantification
MAA	mercaptoacetic acid
MDL	method detection limit
MQ	milli-Q (water)
NaDDC	diethyldithiocarbamic acid, sodium salt
nanoAg	nanosilver

PDC ⁻	1-pyrrolidinecarbodithioate ion
PESC	Pacific Environmental Science Centre
PMT	photomultiplier tube
PP	polypropylene
QD	quantum dot
T ₃	3,3',5-triiodothyronine
TEM	transmission electron microscope
TRβ	thyroid hormone receptor beta

Acknowledgments

A big thank you to J. T. Cullen, for inviting me to be a part of your lab group, then giving me both the guidance and the independence I needed to do this work. Members of the Cullen Lab Group, thank you for being there throughout the joys and frustrations of life and research.

To my committee: C. C. Helbing, thank you for inviting the Cullen Lab to be a part of your multi-disciplinary project, frogSCOPE, and for your ongoing input. Also a big thanks to A. Hinthner, N. Veldhoen, and A. Carew, members of your group who have provided chemicals, samples, results, and other technical support along the way. K. Telmer, thank you for your ongoing support of my timeline and help with GWB software.

Kudos for technical support: thank you, M. Moffitt, for sharing your expertise with quantum dots and generously sharing your lab space; D. Berry and N. Taylor, for your fluorometer expertise and instrument time; B. Gowan, for your TEM expertise and instrument time; J. Spence, not only for help during the long and drawn-out lab move, but also for your ICP-MS expertise and instrument time; G. Catalano and D. Harrison at Science Stores, for your consistently prompt, friendly delivery of much-needed supplies, and R. Skirrow at PESC, for all your help coordinating sampling.

Finally, I must thank my friends and family. Your ongoing presence during the difficult years of this degree has made this accomplishment all the more precious.

Dedication

This thesis is dedicated to the students and instructors in Academic Upgrading at Keyano College in Fort McMurray, Alberta. Your passion for lifelong learning and motivation to overcome barriers inspired me to embark on this adventure as a mature student in the middle of an already fulfilling career.

Chapter 1: Introduction

In addition to natural sources, silver (Ag) is introduced to the aquatic environment via human activity through mining, sewage, the photographic industry, and the use of AgI for seeding clouds in arid areas. As a result, elevated Ag in natural waters can be used as a tracer of anthropogenic impacts on the aquatic environment (Bruland & Lohan, 2003). Today, Ag usage goes beyond its precious metal status: although it has been used as currency, jewellery, and flatware for centuries, it has recently seen increased usage as a germicidal agent in hand sanitizers, antibacterial soaps and lotions, and odour-eliminating textiles and sterile medical plastics (Blaser, Scheringer, MacLeod, & Hungerbühler, 2008). Given recent fears over an H1N1 influenza pandemic and the push for more “natural” alternatives to “harsh chemicals”, germicidal Ag is becoming an increasingly popular antibiotic in over-the-counter consumer products.

However, as a heavy metal ion, Ag ion (Ag^+) is acutely toxic to organisms, second only to mercury (Ratte, 1999). As the ionic form is the most biologically accessible, the speciation of Ag appears to be just as important as its total concentration in assessing Ag toxicity (Ratte, 1999). For example, silver nitrate (AgNO_3) is very toxic because it completely dissociates in water to yield Ag^+ and NO_3^- (Choi et al., 2008; Ratte, 1999). In contrast, silver thiosulfate (AgS_2O_3^-), although soluble, remains a complex and is not highly toxic, because it does not release free Ag^+ (Ratte, 1999). Silver chloro complexes (AgCl_x^-) and insoluble Ag precipitates, such as Ag_2S , also appear to have diminished toxicity, for the same reasons (Choi et al., 2008; Ratte, 1999). Thus, the *form*

of Ag is more important in determining toxicity than the absolute total concentration of Ag in a natural water sample, though knowledge of both parameters is important.

Observations on toxicity of these inorganic Ag species support the free-ion model (FIM) of metal uptake by aquatic organisms (Hudson, 2005; Phinney & Bruland, 1997). The FIM suggests that bioavailability (and therefore toxicity) of metals is proportional to the concentration of free (hydrated) metal ions as well as the number of surface transport sites on the cell membrane (Phinney & Bruland, 1997). The model is based on studies where metal ions, complexed with organic ligands such as EDTA to form kinetically inert, hydrophilic, charged complexes (e.g. AgEDTA^{3-}), temper interaction with algal cell membranes and therefore reduce metal uptake by the cell (Phinney & Bruland, 1997). Free ions are toxic because they can get into the cell easily: they are attracted to surface transport proteins (e.g. Na^+/K^+ ATP-ase, the “sodium-potassium pump”) embedded in the cell membrane, and are small enough to pass into the cell through these conduits. Larger charged species, however, are not toxic because they cannot pass through these conduits, and being charged, they also cannot simply diffuse through the lipophilic cell membrane (Figure 1).

However, not all potentially toxic compounds adhere to the FIM. In experiments with fungicidal metal-dithiocarbamates, Phinney and Bruland (1997) found that these fungicides were not only able to pass into algal cells, but they were also able to undergo metal exchange reactions in water containing added Cu and Pb ions, allowing for these

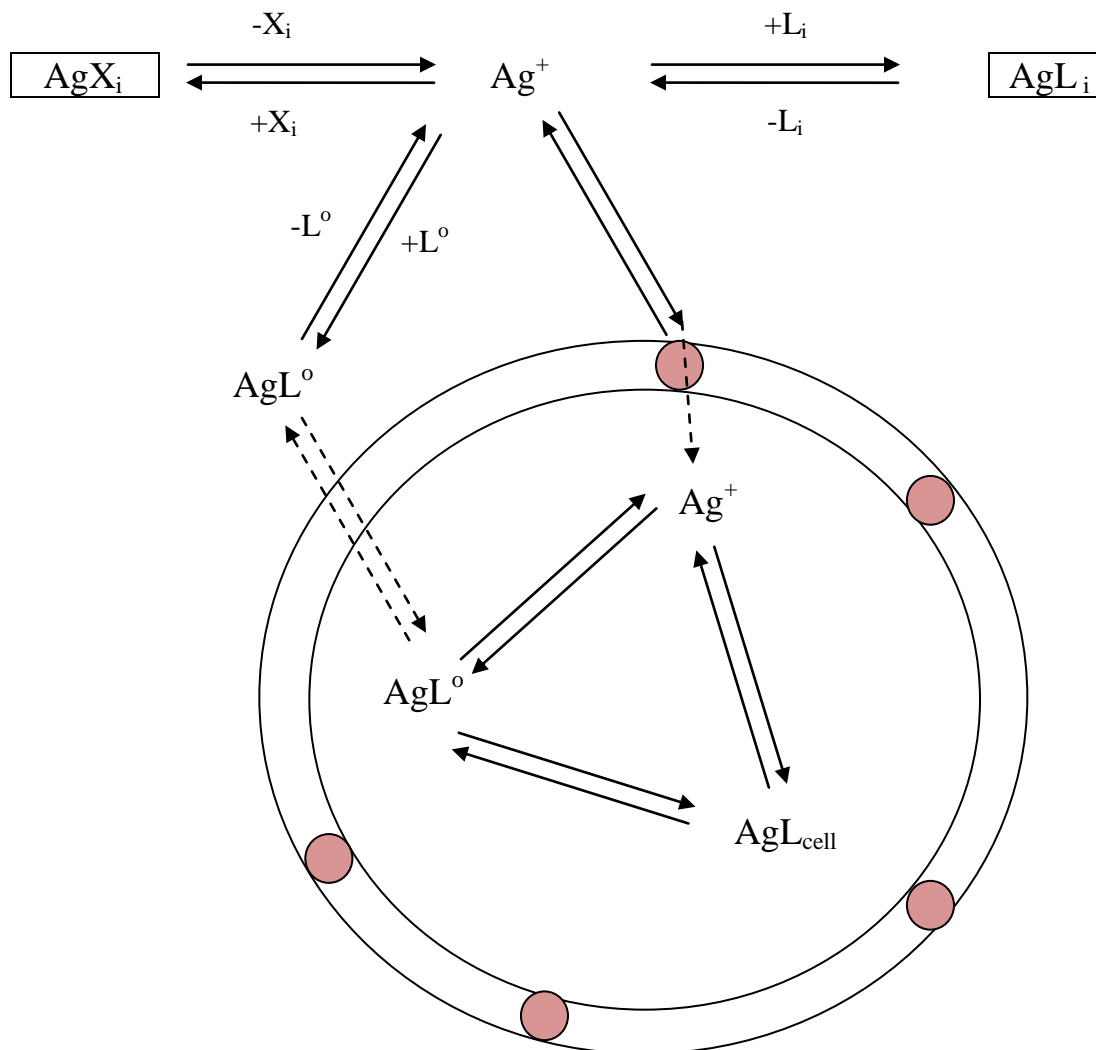


Figure 1: Schematic of cellular uptake and bioavailability of dissolved silver.

Metal ions are thought to enter cells in one of two ways: as “free” (hydrated) ions (Ag^+) which can pass through the protein channels embedded in the cell membrane (pink circles), or as small neutral, lipophilic complexes (AgL^o) which can pass directly through the lipid bilayer of the cell membrane. Once inside the cell, Ag^+ can be released to interact with ligands in the cell (AgL_{cell}). Inorganic complexes (AgX_i) and hydrophilic organic complexes (AgL_i) are charged, so they cannot pass through the cell membrane, but are too large to pass into the cell via protein channels. Adapted from Phinney & Bruland (1997) *Estuaries* Vol. 20 No. 1, p 74.

metals to be taken up by the cells. If hydrophobic metal-ligand complexes are small enough, and soluble enough in organic solvents (i.e. if their octanol-water partition coefficients, K_{ow} , are large, such as for $\text{Cu}(\text{DDC})_2$, which is $10^{2.8}$), then it is highly probable that they can passively diffuse through the lipophilic cell membrane into the algal cell, thus bringing in metal via a second mechanism (Phinney & Bruland, 1997). If we are examining a particular organic ligand and its interaction with Ag^+ , then we need to know if it forms a neutral complex, which could potentially increase Ag uptake and therefore increase toxicity, or if it forms a charged complex, which could potentially decrease Ag uptake and therefore decrease toxicity.

Since Ag speciation in marine waters is dominated by AgCl_x^- complexes (Valverde, Costas, Pena, Lavilla, & Bendicho, 2008), marine organisms have some protection against the toxic Ag^+ ion, as well as hydrophobic organic complexes which cannot form due to intense competition by high chloride ion (Cl^-) concentrations. The same cannot be said for fresh waters. As a result of low Cl^- levels, there is more opportunity for Ag^+ to both exist freely or to bind organic ligands or other inorganic anions in freshwater (Valverde et al., 2008). Phinney and Bruland's (1997) results suggest that the toxicity of organo-Ag complexes would depend on whether or not they were charged. Techniques do exist to qualitatively determine how much Ag speciation is associated with organic ligands in solution, as well as the effect of these ligands on recovery of Ag into an organic solvent, but these methods cannot determine the identity of organic ligand(s) in the sample coordinated with Ag^+ (Miller & Bruland, 1995;

Valverde et al., 2008). However, these methods would be useful in examining the effect of known ligands which are suspected to interact with Ag^+ .

While it is well known that Ag^+ is toxic to a wide range of organisms at relatively low levels (Ratte, 1999), synthetic nanosilver (nanoAg) represents a new form of Ag with distinct physical and chemical properties and heretofore underappreciated toxic effects. NanoAg, tiny Ag particles with a diameter of less than 100 nm, have demonstrated the ability to kill a wide range of bacteria and are the Ag species of choice in germicidal consumer products (Choi et al., 2008). As these nanoparticles get washed out of treated plastics and textiles, nanoAg ends up in municipal sewage effluent and sludge, which can eventually end up back in rivers, lakes, and oceans (Blaser et al., 2008). Over time, nanoAg releases Ag^+ , but its own toxicological effects on eukaryotes, particularly on vertebrates, are just beginning to be understood (Choi et al., 2008; Handy et al., 2008). The mechanisms of toxicity of nanoAg and Ag^+ in eukaryotes may be a result of interference with proteins and hormones. Silver is a “soft” cation, and has a strong affinity for thiol (-SH) groups, as is demonstrated by its large conditional stability constant with glutathione ($\log K' = 33.15$; (Miller & Bruland, 1995). This suggests that Ag^+ could bind cysteine, a thiol-containing amino acid, preventing the formation of the cysteine-cysteine linkages important in maintaining the conformation of many proteins. NanoAg has also been reported to change protein conformation by aggregating with proteins, again through thiol groups, perhaps creating the stress response observed by Hinthner et al. (in review). As a hormone-disrupter, very low levels of nanoAg have been shown to perturb 3,3',5-triiodothyronine (T_3)-mediated signaling in frog tadpole tissue by

increasing thyroid hormone receptor β transcription (Hinther et al., in review). The mechanism for this disruption, however, is unknown.

The effects of hormone-disrupting antibiotics, including nanoAg, on amphibians are currently being evaluated using novel molecular assays. frogSCOPE (Frog Sentinel species Comparative “Omics” for the Environment) is the name given to this three year, multi-disciplinary research program. An overview of the program can be found at <http://www.genomebc.com/portfolio/projects/environment-projects/current/frogSCOPE-frog-sentinel-species-comparative-omics-for-the-enviro/>. Two of the many goals of frogSCOPE are to determine Ag speciation in the well water used for the Ag and nanoAg toxicity studies on bullfrogs, and to determine if Ag forms any strong associations with low levels of triclosan, a known frog thyroid hormone disrupting compound (Veldhoen et al., 2006). Triclosan, which is structurally similar to the thyroid hormones T₃ and T₄ found in all vertebrates, can be increasingly found in wastewater, municipal, and well water supplies as the usage of the chemical becomes more widespread. Some preliminary frogSCOPE test results (C. C. Helbing, unpublished data) also suggest that the presence of nanoAg enhances the thyroid hormone disruption capabilities of triclosan reported by Veldhoen et al. (2006). This suggests that these two antibiotics are somehow working synergistically, and that Ag is finding its way into frog cells. In this case, it is important to tease out whether or not this is a nanoparticle effect, or an interaction/association of Ag⁺ with organic ligands that would act to increase the metal and potentially the ligands’ bioavailability.

Experiments are needed in order to examine whether nanosilver particles or the Ag ions they release over time are the more likely culprits in creating the hormone disruption and oxidative stress observed by Hinthner et al. (in review) and C. C. Helbing (unpublished data). We will be focusing on the interaction of potential organic ligands with ionic Ag. Within this scope, two scenarios are likely to explain the increased hormone disruption in frog cells: chemical modification of thyroid hormone T₃ or triclosan by Ag⁺, or increased lability of the Ag-triclosan or Ag-T₃ compound, which increases Ag uptake into the cells. Traditional approaches to aquatic toxicology do not always consider such interactions, and as more diverse chemicals end up in our wastewater streams, more unanticipated interactions of mixtures of chemicals in wastewater effluents are likely, making such studies increasingly important.

Model ligand experiments, which allow for the measurement of organic Ag species, could be used to determine if either of these scenarios is even possible, shedding some light on potential reasons for the observation that the presence of nanoAg increases endocrine disruption by triclosan. However, measuring such organic Ag species in natural water samples is a two-part, time-consuming process requiring large samples of water. One portion of sample must be acidified and allocated for total Ag analysis, while another portion must be set aside, unacidified, for speciation studies. Total Ag analysis is itself difficult because Ag in natural water samples is usually only at the parts-per-trillion (picomolar) level (Bruland & Lohan, 2003). Traditional spectrophotometric techniques for Ag (AAS, ICP-OES, ICP-MS) simply do not have the detection limits required to directly analyze picomolar Ag in natural water samples, so samples must be pre-

concentrated either through anion exchange resins (Ndung'u, Ranville, Franks, & Flegal, 2006) or through complexation with strong organic ligands followed by extraction into an organic solvent such as chloroform (Bruland, Coale, & Mart, 1985; Bruland, Franks, Knauer, & Martin, 1979; Kinrade & Van Loon, 1974).

Although there are actually a number of total Ag analysis techniques being investigated which would allow for a simplified sample preparation and analysis using smaller volumes of sample (Javanbakhta et al., 2009; Pendyala & Koteswara Rao, 2009; Wang et al., 2008), there are, as of yet, few alternatives to using organic extraction methods for Ag speciation. Ag speciation experiments involve ligand exchange and employ similar organic extraction techniques as total Ag (Miller & Bruland, 1995), so if one is using organic extraction techniques for both total Ag and Ag speciation experiments, then at least 500 mL of sample are required just for one replicate. Unless large volumes of sample are collected, replicate analysis will not be possible. This can be disastrous if the sample preparation is compromised. Though reliable when everything goes right, the many steps of sample handling involved in these extraction-based methods present many opportunities for sample loss or contamination. By using another method for total Ag analysis, while still using the same speciation method, one can reduce these negative occurrences while also reducing preparation time.

The ultimate goal of this thesis is to contribute to understanding the behavior of Ag in freshwater containing triclosan through Ag speciation experiments. To address the goal, and reflect the two-part nature of such experiments, this thesis has two parts.

Chapter Two discusses the investigation of a fluorometric method for total Ag analysis which promises smaller sample volumes and simpler sample preparation. This method suggests that using of CdS quantum dots in an aqueous medium to attract Ag^+ creates a linear enhancement of fluorescence output in Ag standards ranging from 1-6 nM, covering the low-medium exposures of the frogSCOPE toxicological studies (Wang et al., 2008). The results of quantum dots synthesized as per Wang et al. (2008), and commercial quantum dots functionalized to these same specifications, will be compared for the first time. Chapter Three reports Ag speciation in the well water samples used in frogSCOPE, and examines whether or not triclosan and T_3 can compete as strong organic ligands for Ag. This will be the first time Miller and Bruland's (1995) speciation technique will be used to examine these as potential Ag-binding ligands. This type of experiment should become more important as common antibiotic agents increasingly end up in waste and natural waters, interacting in unforeseen ways with metal ions and resulting in increased toxicity for aquatic organisms.

1.1 References

- Blaser, S. A., Scheringer, M., MacLeod, M., & Hungerbühler, K. (2008). Estimation of cumulative aquatic exposure and risk due to silver: Contribution of nano-functionalized plastics and textiles. *Science of The Total Environment*, 390(2-3), 396-409.
- Bruland, K. W., Coale, K. H., & Mart, L. (1985). Analysis of seawater for dissolved cadmium, copper, and lead: an intercomparison of voltammetric and atomic absorption methods. *Marine Chemistry*, 17, 285-300.

- Bruland, K. W., Franks, R. P., Knauer, G. A., & Martin, J. H. (1979). Sampling and analytical methods for the determination of copper, cadmium, zinc, and nickel at the nanogram per liter level in sea-water. *Analytica Chimica Acta*, *105*(1), 233-245.
- Bruland, K. W., & Lohan, M. C. (2003). Controls of Trace Metals in Seawater. In H. Elderfield (Ed.), *Treatise on Geochemistry* (Vol. 6, pp. 23-47). Oxford: Elsevier Ltd.
- Choi, O., Deng, K. K., Kim, N.-J., Ross Jr., L., Surampalli, R. Y., & Hu, Z. (2008). The inhibitory effects of silver nanoparticles, silver ions, and silver chloride colloids on microbial growth. *Water Research*, *42*, 3066-3074.
- Handy, R., von der Kammer, F., Lead, J., Hasselov, M., Owen, R., & Crane, M. (2008). The ecotoxicology and chemistry of manufactured nanoparticles. *Ecotoxicology*, *17*(4), 287-314.
- Hinther, A., Vawda, S., Skirrow, R. C., Veldhoen, N., Collins, P., Cullen, J. T., et al. (in review). Nanometals induce stress and alter thyroid hormone action in amphibia at or below North American water quality guidelines.
- Hudson, R. J. M. (2005). Trace metal uptake, natural organic matter, and the free-ion model. *J. Phycol.*, *41*, 1-6.
- Javanbakhta, M., Divsar, F., Badiei, A., Fatollahi, F., Khaniani, Y., Ganjali, M. R., et al. (2009). Determination of picomolar silver concentrations by differential pulse anodic stripping voltammetry at a carbon paste electrode modified with phenylthiourea-functionalized high ordered nanoporous silica gel. *Electrochimica Acta*, *54*, 5381-5386.

- Kinrade, J. D., & Van Loon, J. C. (1974). Solvent extraction for use with flame atomic absorption spectrometry. *Analytical Chemistry*, 46(13), 1894-1898.
- Miller, L. A., & Bruland, K. W. (1995). Organic Speciation of Silver in Marine Waters. *Environmental Science & Technology*, 29, 2616-2621.
- Ndung'u, K., Ranville, M. A., Franks, R. P., & Flegal, A. R. (2006). On-line determination of silver in natural waters by inductively-coupled plasma mass spectrometry: influence of organic matter. *Marine Chemistry*, 98, 109-120.
- Pendyala, N. B., & Koteswara Rao, K. S. R. (2009). Efficient Hg and Ag ion detection with luminescent PbS quantum dots grown in poly vinyl alcohol and capped with mercaptoethanol. *Colloids and Surfaces A: Physicochemical and Engineering Aspects*, 339(1-3), 43-47.
- Phinney, J. T., & Bruland, K. W. (1997). Trace metal exchange in solution by the fungicides Ziram and Maneb (dithiocarbamates) and subsequent uptake of lipophilic organic zinc, copper, and lead complexes into phytoplankton cells. *Environmental Toxicology and Chemistry*, 16(10), 2046-2053.
- Ratte, H. T. (1999). Bioaccumulation and toxicity of silver compounds: a review. *Environmental Toxicology and Chemistry*, 18(1), 89-108.
- Valverde, F., Costas, M., Pena, F., Lavilla, I., & Bendicho, C. (2008). Determination of total silver and silver species in coastal seawater by inductively-coupled plasma mass spectrometry after batch sorption experiments with Chelex-100 resin. *Chemical Speciation and Bioavailability*, 20(4), 217-226.
- Veldhoen, N., Skirrow, R. C., Osachoff, H., Wigmore, H., Clapson, D. J., Gunderson, M. P., et al. (2006). The bactericidal agent triclosan modulates thyroid hormone-

associated gene expression and disrupts postembryonic anuran development.

Aquatic Toxicology, 80(3), 217-227.

Wang, L., Liang, A.-N., Chen, H.-Q., Liu, Y., Qian, B.-b., & Fu, J. (2008). Ultrasensitive determination of silver ion based on synchronous fluorescence spectroscopy with nanoparticles. *Analytica Chimica Acta*, 616(2), 170-176.

Chapter 2: Total Silver in Aqueous Solutions using CdS Quantum Dots

2.1 Introduction

Traditional analytical methods employing graphite furnace atomic absorption spectrometry (GFAAS) and inductively-coupled plasma mass spectrometry (ICP-MS) have shown consistent, robust linear responses to increasing concentrations of silver (Ag) in many types of sample. However, Ag levels in natural water samples are so far below the detection limits of these instruments that it is not possible to directly measure Ag without some method of pre-concentration. Pre-concentration methods, including organic extraction (Bruland et al., 1985; Bruland et al., 1979; Kinrade & Van Loon, 1974; Miller & Bruland, 1995) and ion-exchange resins (Ndung'u et al., 2006), require large sample volumes and can magnify even the smallest sources of contamination. The large amount of time required to prepare the samples, and the inability to do replicate analysis without collecting comparatively large volumes of water, are significant limiting factors in the utility of current Ag analysis methods.

Ag ion (Ag^+) is not a fluorescent species, so there is not currently a standard method that might involve fluorometry in measuring total Ag in natural waters. However, fluorometric methods for low-level Ag determination have been receiving a revived interest in recent years. Fluorometry has several advantages over GFAAS and ICP-MS: a simple sample introduction system; the potential to be adapted from batch mode to a flow-injection system; compact size, and a robust detector. A reliable way to

make Ag fluoresce, and show an increase (or decrease) in fluorescence which is proportional to concentration, is an analytically-favorable approach to Ag sensing in natural waters.

To make Ag^+ fluoresce, it must interact with some type of fluorophore. Traditional organic fluorophores such as bright-green fluorescein or bright-pink rhodamine derivatives are showing some promise in quantitative response (Swamy et al., 2009). Even better are inorganic fluorophores, such as the semiconductor quantum dots (QDs) CdSe, CdTe, and CdS, because they more easily dissolve in aqueous solutions, and have a longer photoluminescent shelf life in the presence of light, than organic fluorophores (Murphy, 2002). The spectral output of QDs can also be superior, since QDs within a narrow size range produce much narrower fluorescence peaks than organic fluorophores (Murphy, 2002). This is because the band gap energy (energy difference between the valence band and conduction band) of QDs is entirely dependent on size, so all QDs of a certain size will emit at the same energy, creating a fluorescence emission peak whose narrow width is solely determined by minute deviations from perfect spherical shape (Murphy, 2002).

Semiconductor QD fluorescence intensity can be dramatically affected by metal species in solution; hence, there is interest in using them to detect certain metals, such as Ag. The idea for using QDs as probes for ions in solution probably came from studies which illustrated the changes in fluorescence behaviours as these semiconductor QDs were placed in proximity to either metal nanowires or nanoparticles, such as in studies by

Kulakovich et al. (2002) and Song et al. (2005). Quenching of fluorescence can occur when a metal particle is either directly bonded to the QD surface, or close enough for non-radiative energy transfer directly from the QD to the metal (Brolo et al., 2006; Kulakovich et al., 2002). On the other hand, fluorescence enhancement can occur if the metal particle is in a “sweet spot”, a location far enough away to avoid non-radiative energy loss but close enough for the metal particle to act like an antenna (Brolo et al., 2006; Song, Atay, Shi, Urabe, & Nurmikko, 2005). Studies have shown that semiconductor QDs can be “tuned” to create either fluorescence enhancement or fluorescence quenching by attaching surface ligands to control the spacing between the QD and a desired metal particle (J.-L. Chen & Zhu, 2005; Y. Chen & Rosenzweig, 2002). This ligand attachment is known as functionalization. When functionalizing QDs, the choice of ligand also creates selectivity of these QDs to specific metal ions in solution, such as Zn versus Ag (Y. Chen & Rosenzweig, 2002). Soft ligands, particularly thiol-containing substances like mercaptoacetic acid (MAA), have already been used to functionalize QDs which can then selectively attract Ag (J.-L. Chen & Zhu, 2005; Wang et al., 2008).

Unique in the limited supply of fluorescence studies with QDs and metal ions, Wang et al. (2008) collected synchronous fluorescence spectra from the interaction of MAA-functionalized CdS QDs with Ag^+ . In normal fluorescence analysis, the sample is excited at a certain wavelength (λ_{ex}) and is scanned over a certain emission wavelength range, producing an emission spectrum with one or more maxima (λ_{em}). The peak height(s) of the emission maxima can be measured and then related to concentration, in

order to see if there is a useful analytical response. In synchronous fluorescence, instead of scanning just the emission wavelength, both the excitation and emission wavelengths are varied while maintaining a fixed wavelength interval ($\Delta\lambda$) between them, meaning that the fluorescence response can be selective for one substance (Vo-Dinh, 1978; Wang et al., 2008). This is because for each emission maximum that a fluorescent substance produces, there is a corresponding excitation maximum at which the substance absorbs energy (Figure 2). The difference between these, the Stokes shift, may be chosen as the wavelength interval $\Delta\lambda$ for synchronous fluorescence, or the experimenter may examine and choose from the difference between any two emission or excitation peaks in the spectrum for a particular substance (Vo-Dinh, 1978). The resulting synchronous fluorescence spectrum will therefore be specific for one substance, and show a single peak which can then be studied and related to concentration, similar to the conventional fluorescence emission peak approach. With synchronous fluorescence, the sensitivity (peak height) is increased, and the resulting spectra are greatly simplified, since only signals due to the substance of interest will be produced (Vo-Dinh, 1978; Wang et al., 2008).

The Wang et al. (2008), synchronous fluorescence method first requires a straightforward CdS QD synthesis which creates 20-25 nm particles in aqueous medium (Wang et al., 2008). Next, a small aliquot of this QD solution is added to several solutions containing varying nanomolar concentrations of Ag and a small amount of pH buffer. This is the only sample manipulation required, and only 8.5 mL of sample are needed. Wang et al. (2008) demonstrated that increasing concentrations of Ag produced

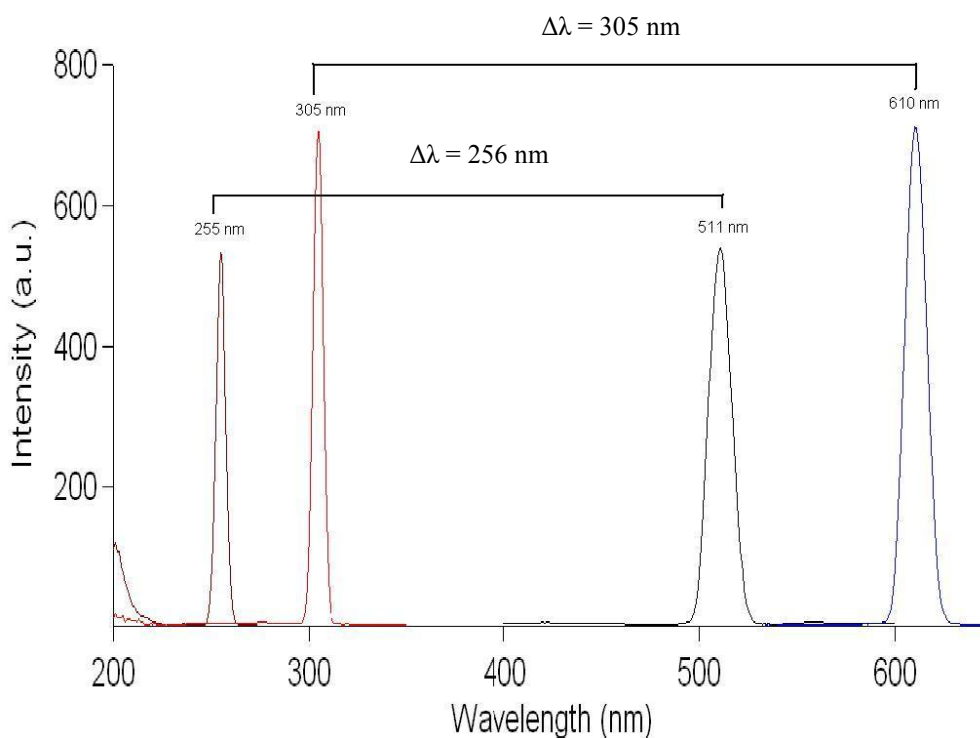


Figure 2: Overlay of fluorescence emission and excitation maxima for commercial CdS QDs, 2×10^{-4} M, buffered using HEPPS.

Excitation at 255 nm (λ_{em}) resulted in the emission maximum at 511 nm (λ_{ex}); excitation at 305 nm resulted in the emission maximum at 610 nm. Emission peaks observed in these experiments are red-shifted with respect to Wang et al. (2008), who observed an emission at 470 nm from the 255 nm excitation peak. The Stokes shifts for this sample would be $\Delta\lambda = 256$ nm and $\Delta\lambda = 305$ nm for each pair of $\lambda_{em}/\lambda_{ex}$, respectively. Other non-Stokes $\Delta\lambda$ values which could be used in synchronous analysis of this sample include the difference between the 511 nm and 305 nm peaks, or the 610 nm and 255 nm peaks. PMT = 600 V; slit widths = 5 nm (ex), 10 nm (em).

a roughly linear synchronous fluorescence enhancement effect on CdS QDs between approximately 0.08 and 15 nM Ag^+ , with a detection limit of 0.04 nM. This suggests that there might be a simple fluorometric method which may be able to detect picomolar Ag in natural water samples.

Our goal was to confirm that MAA-functionalized CdS QDs do, in fact, respond in an analytically-useful way to Ag^+ concentrations in the range studied by Wang et al. (2008), then see if the method was capable of detecting the picomolar quantities of total Ag in solution which would be found in real freshwater samples. We set out to use the CdS QD synthesis outlined by Wang et al. (2008), but also chose to investigate functionalizing commercially-available CdS QDs as our Ag^+ probes. No studies using these ready-made CdS QDs as Ag^+ probes have yet been reported. Using commercial CdS QDs would have three main advantages over in-house synthesis. First, time and resources could be focused on analysis, not QD synthesis; second, using commercial QDs should eliminate potential interferences due to unreacted sulfide species and other by-products of synthesis; third, the size of commercial QDs should be smaller and more uniform, giving narrower fluorescence peaks due to uniform band gap energies and potentially more even distribution of Ag across the QDs, leading to more reproducible results.

2.2 Methods

Synchronous fluorescence analysis was carried out on a Cary Eclipse spectrofluorometer, with PMT set to 600 V. pH measurements were made with a Thermo ORION 720A+ pH meter, with a Ross Sure-Flow Combination Electrode calibrated using pH 4, 7, and 10 buffers from VWR. Chemicals used in synthesis and commercial CdS functionalization were all reagent ACS grade or higher. All bottles used to store reagents and samples were trace metal-clean LDPE (see Appendix I). All solutions were made with Milli-Q (MQ) water (Millipore ELEMENT/Elix purification system). Commercial Lumidot™ CdS QDs in toluene (Sigma-Aldrich, 5 mg/mL CdS) were stored refrigerated, under nitrogen, and were always opened and handled under nitrogen in a glove bag. Solution preparation for experiments involving commercial CdS took place in a Class 100 clean space at the University of Victoria. Batches of synthetic and commercial CdS QDs were examined on a Hitachi H-7000 transmission electron microscope (TEM). For full details on chemical and sample preparation, please refer to Appendix II.

2.2.1 Synthesis of CdS QDs for use as probes for Ag⁺

Synthesis followed Wang et al. (2008) and is based on the controlled colloid precipitation method as described by Li et al. (2005). 200 mL of 0.01 M CdCl₂ and 200 mL of 0.1 M thioacetamide solutions were added to a 500 mL three-neck round-bottom flask and purged with nitrogen for 20 minutes. 20 mL of 0.1 M sodium hexametaphosphate were added to the mixture via syringe, and the mixture was stirred vigorously. The initial pH of the mixture was approximately 6.5. Approximately 45 mL

of 0.1 M NaOH was required to bring the pH of the solution up to 8.5. As pH adjustment occurred, the solution turned from clear and colourless to pale yellow to cloudy yellow. At the end of pH adjustment, there was yellow precipitate suspended throughout the solution. The mixture was stirred for 75 minutes following pH adjustment, and 67.9 μL of mercaptoacetic acid were added. The solution was made up to approximately 500 mL using MQ water, and was stirred for an additional 30 minutes under nitrogen. At the end of synthesis, the reaction vessel was capped and covered in aluminum foil for storage. The final concentration of CdS in the matrix was approximately 4×10^{-3} M.

2.2.2 Functionalizing commercial CdS QDs for use as probes for Ag^+

1.16 mL of CdS QDs in toluene (Sigma-Aldrich, 5 mg/mL CdS) were pipetted into a 50 mL round bottom flask inside a glove bag, under nitrogen. Initially, this entire aliquot, including the toluene, was treated with the chemicals described below; in later experiments, a stream of nitrogen was used to evaporate the toluene from the QDs, leaving a sticky yellow coating on the glass of the flask. 141 μL of 100X diluted (0.98%) mercaptoacetic acid (MAA) were added to the flask, loosening the yellow material from the glass and dissolving it slightly. 9.83 mL of 4×10^{-3} M sodium hexametaphosphate solution (adjusted to pH 10.5) were added, and the flask was placed on a shaker for at least 24 hours to allow for the QDs to be functionalized by MAA. The final pH of the CdS in matrix was 8.61; the final concentration of CdS was approximately 4×10^{-3} M.

2.2.3 Preparation of standards and samples for fluorometric analysis

For initial experiments, 10.00 mL Ag standards ranging from 0.5 nM through 10 nM and a blank were prepared volumetrically by adding the following solutions to 30 mL LDPE bottles, in the order listed: 500 μL of 2×10^{-3} M CdS solution, 1.00 mL of buffer (0.067 M PBS buffer for first six experiments; 1 M HEPPS for the remainder), various aliquots of 1000 nM or 100 nM Ag^+ solution (made from successive dilution of a SPEX Certi-Prep, 996 mg/mL Ag^+ ICP standard in MQ water), and 8.5 mL of MQ water. Standards were shaken and then typically allowed to equilibrate 20-30 minutes before analysis. Later experiments involved creating individual 10.00 mL water “samples” containing between 0.5 and 15 nM Ag^+ . Samples and a blank were prepared at the fluorometer by measuring 500 μL of CdS, 1.00 mL of buffer, and 8.5 mL of the prepared sample (or MQ water for the blank). The samples were shaken for 1 minute, followed by 10-minute equilibration prior to analysis. All samples prepared in these experiments would have a final concentration of 1×10^{-4} M MAA, and 2×10^{-4} M CdS.

A 10 mm x 10 mm quartz cuvette was rinsed with a small quantity of solution to be analyzed, before 3.00 mL of sample solution were pipetted into the cuvette. The cuvette was wiped carefully to remove any interfering dust or drops, placed in the fluorometer, and analyzed. For each sample, a blank was analyzed for emission and excitation spectra, followed by three replicate runs of synchronous fluorescence at 304 nm with $\Delta\lambda = 305$ nm.

2.3 Results

2.3.1 Quantum dot synthesis and functionalization

Synthesis of CdS QDs following Wang et al. (2008) formed clear, pale yellow solutions without any QDs visible in the TEM images. However, when the concentration of thioacetamide was 10-fold in excess of the cadmium chloride, a bright yellow solution with a lot of deep yellow precipitate formed. TEM analysis showed distinct QDs in the 20-25 nm range, along with large, irregularly-shaped clumps of smaller QDs of about 5 nm size (Figure 3). Commercial LumidotTM CdS QDs had an oleic acid coating to make them soluble in toluene, and were a uniform 5 nm in size (Figure 4a). As these QDs were not soluble in our mercaptoacetic acid-sodium hexametaphosphate matrix, even after agitation and sonication, we sought a way to exchange the surface oleic acid ligands with mercaptoacetic acid (MAA). Using guidelines from Sigma-Aldrich (http://www.sigmaaldrich.com/etc/medialib/docs/Sigma-Aldrich/General_Information/lumidot_faqs.Par.0001.File.tmp/lumidot_faqs.pdf), we sought to treat the CdS QDs with MAA, as per section 2.2 (Methods), to induce ligand exchange. The resulting solution was the same depth of yellow colour as the solution of synthetic CdS QDs, and TEM analysis revealed particles ranging from 20-250 nm in size.

2.3.2 Synchronous Fluorescence Spectra

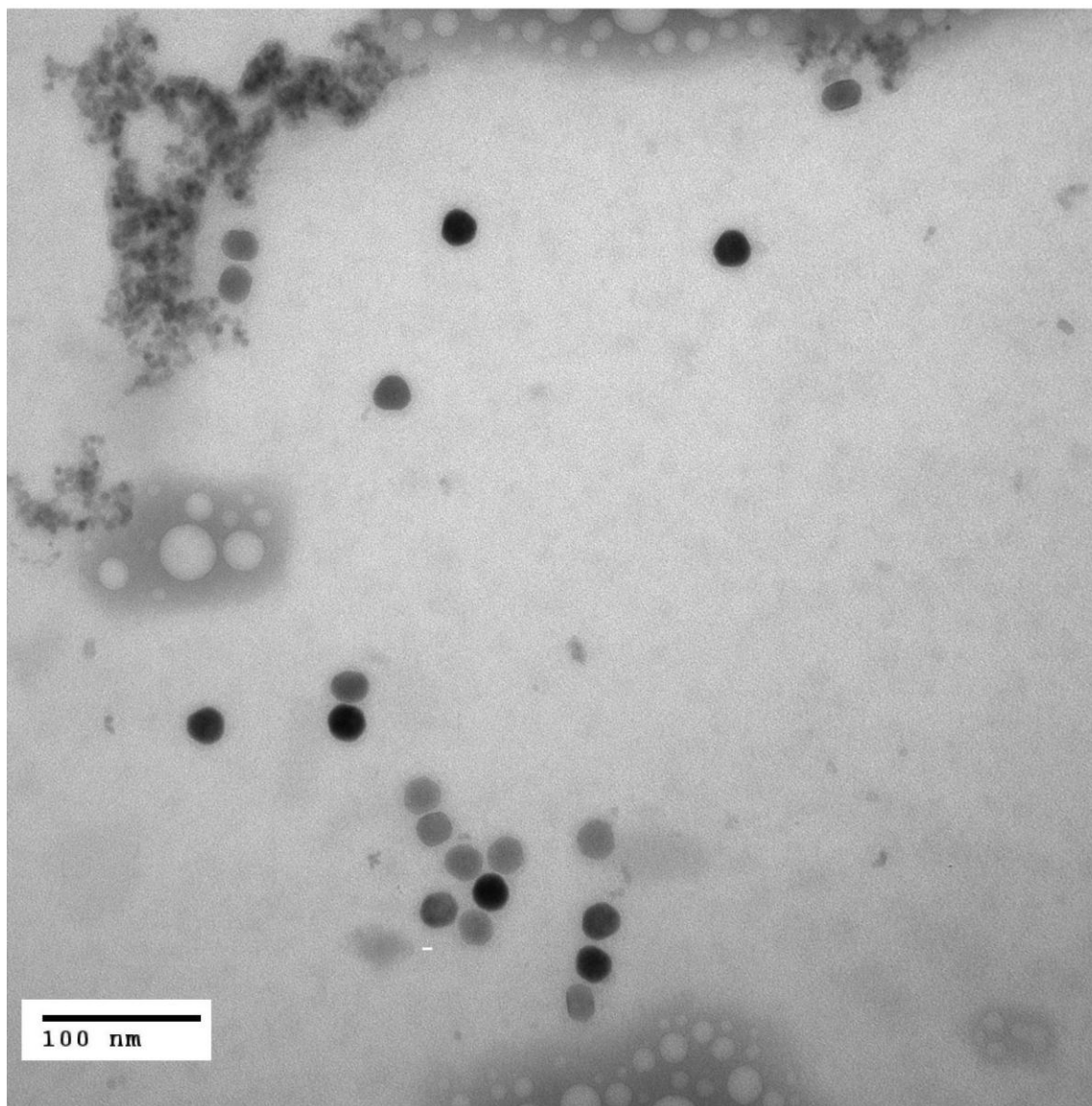


Figure 3: TEM image of synthesized CdS QDs.

These QDs were synthesized as per Wang et al. (2008) with one change: using a 10X excess of thioacetamide (0.1 M instead of 0.01 M). A 0.01 M solution produced no QDs after two synthesis attempts.

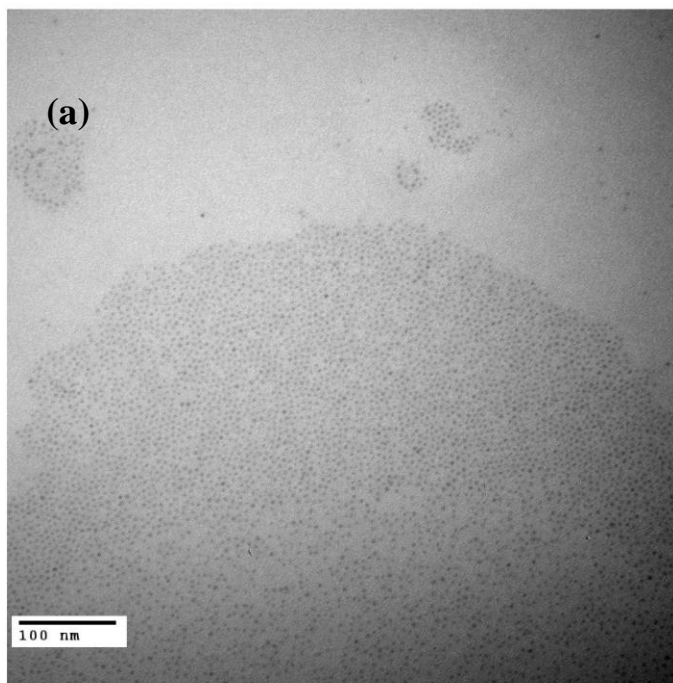
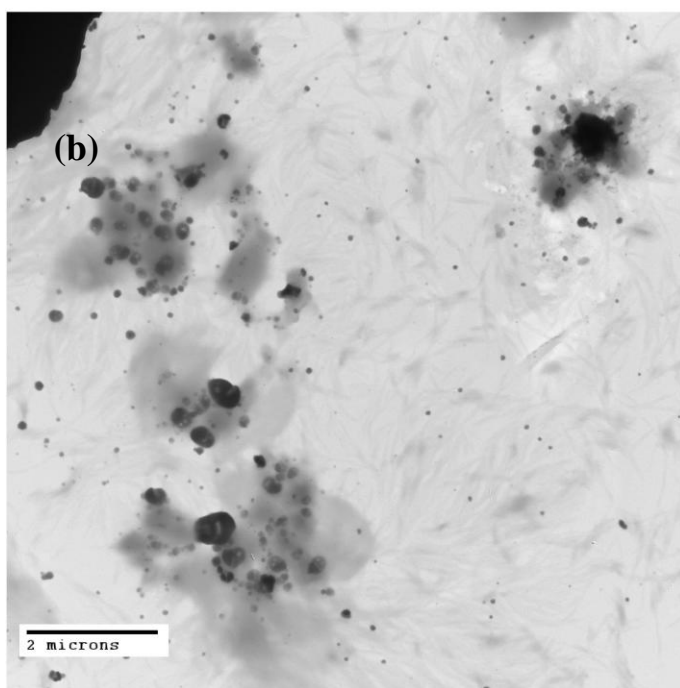


Figure 4: TEM images of commercial CdS QDs.

(a) Diluted to 4×10^{-3} M CdS, in toluene. Uniform particle shapes and sizes of approximately 5 nm.



(b) 4×10^{-3} M CdS, after treatment to evaporate toluene, functionalize with mercaptoacetic acid, and make soluble in a sodium hexametaphosphate matrix, pH 8.6. Non-uniform particle shapes, ranging from 20-250 nm in size.

Wang et al. (2008), reported a synchronous fluorescence peak at 304 nm using a $\Delta\lambda$ of 215 nm. In our initial analyses, no peak was noted at this $\Delta\lambda$. After identifying the key wavelengths which excited CdS and were emitted by CdS (Figure 2), a number of $\Delta\lambda$ values were investigated, corresponding to the differences between the four main excitation and emission peaks seen in Figure 2. Only $\Delta\lambda$ of 256 nm and 305 nm, both corresponding to Stokes shifts for our CdS mixtures (Figure 2), showed any appreciable changes with increasing Ag concentration. The peak at 304 nm, resulting from $\Delta\lambda$ of 305 nm, was chosen for further studies, because it was narrower and showed a greater response to increasing Ag concentration. Appendix IV summarizes the synchronous fluorescence data collected in all experiments.

The peak centered at 304 nm was definitely affected by Ag^+ concentration, though not in the way expected (Figure 5, 6). When compared to the blank, the vast majority of experiments showed a quenching of the signal when Ag^+ was present in the lowest standard (Appendix IV). The very first experiment using synthesized CdS QDs involved Ag stocks prepared without nitric acid, and was one of the few experiments which suggested enhancement (Figure 6b). Since the response was non-linear over the range of standards tested, it was suspected that the silver may have been lost to adsorption on container walls in stock solutions, so subsequent analyses employed Ag stocks containing 2% nitric acid to keep the Ag^+ stable. Using this Ag stock, the next experiment with synthesized CdS QDs suggested quenching of the signal, though again the response was not linear over the range of standards tested (Figure 5a). The first time commercial quantum dots were used, the toluene in which they were suspended was not

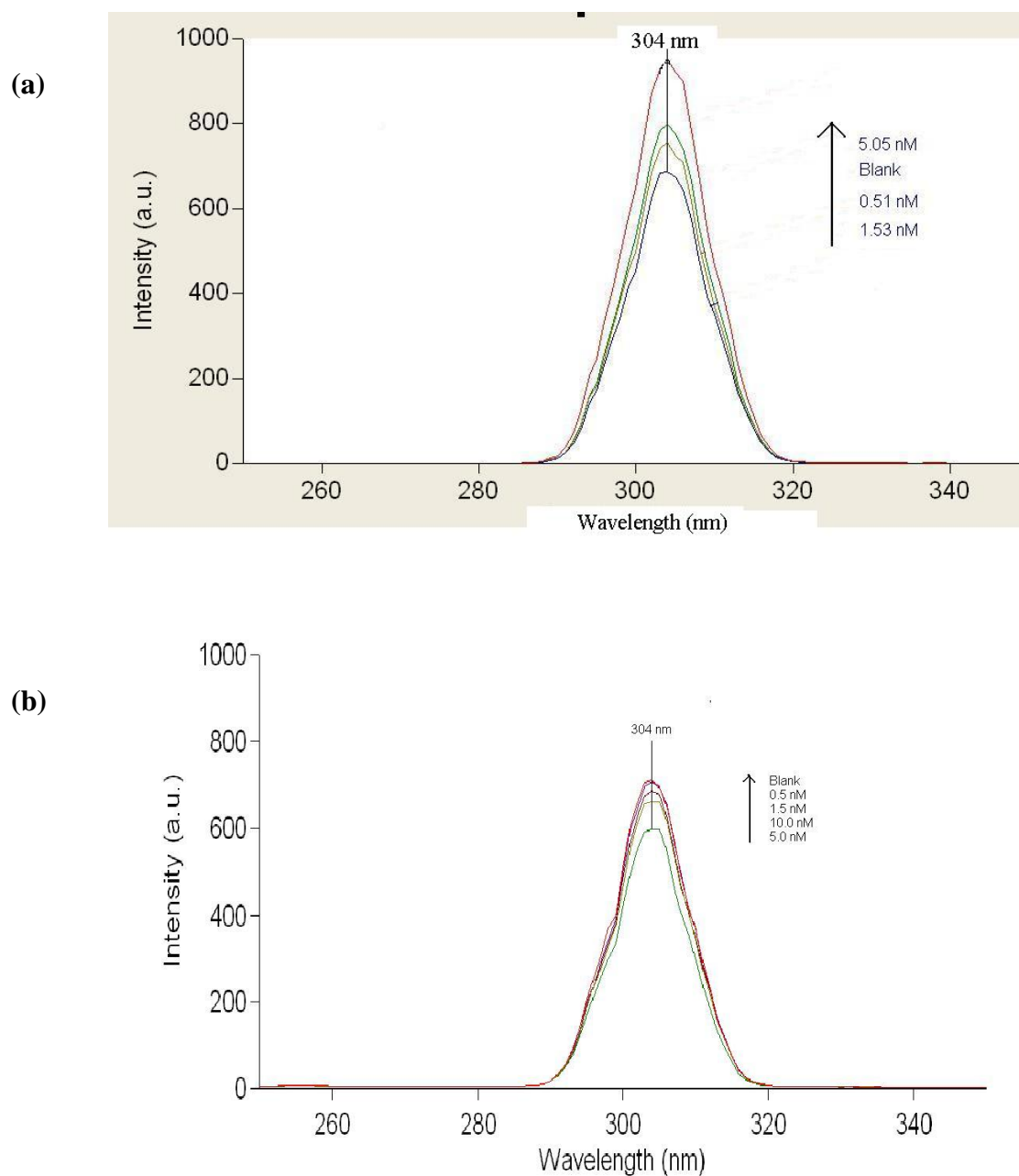


Figure 5: Synchronous fluorescence spectra for several Ag^+ standards.

All standards have a CdS concentration of approximately 2×10^{-4} M. $\Delta\lambda = 305$ nm; PMT = 600 V; slit widths = 5 nm (ex), 10 nm (em). (a) Using synthesized CdS QDs; (b) Using commercially-available CdS QDs.

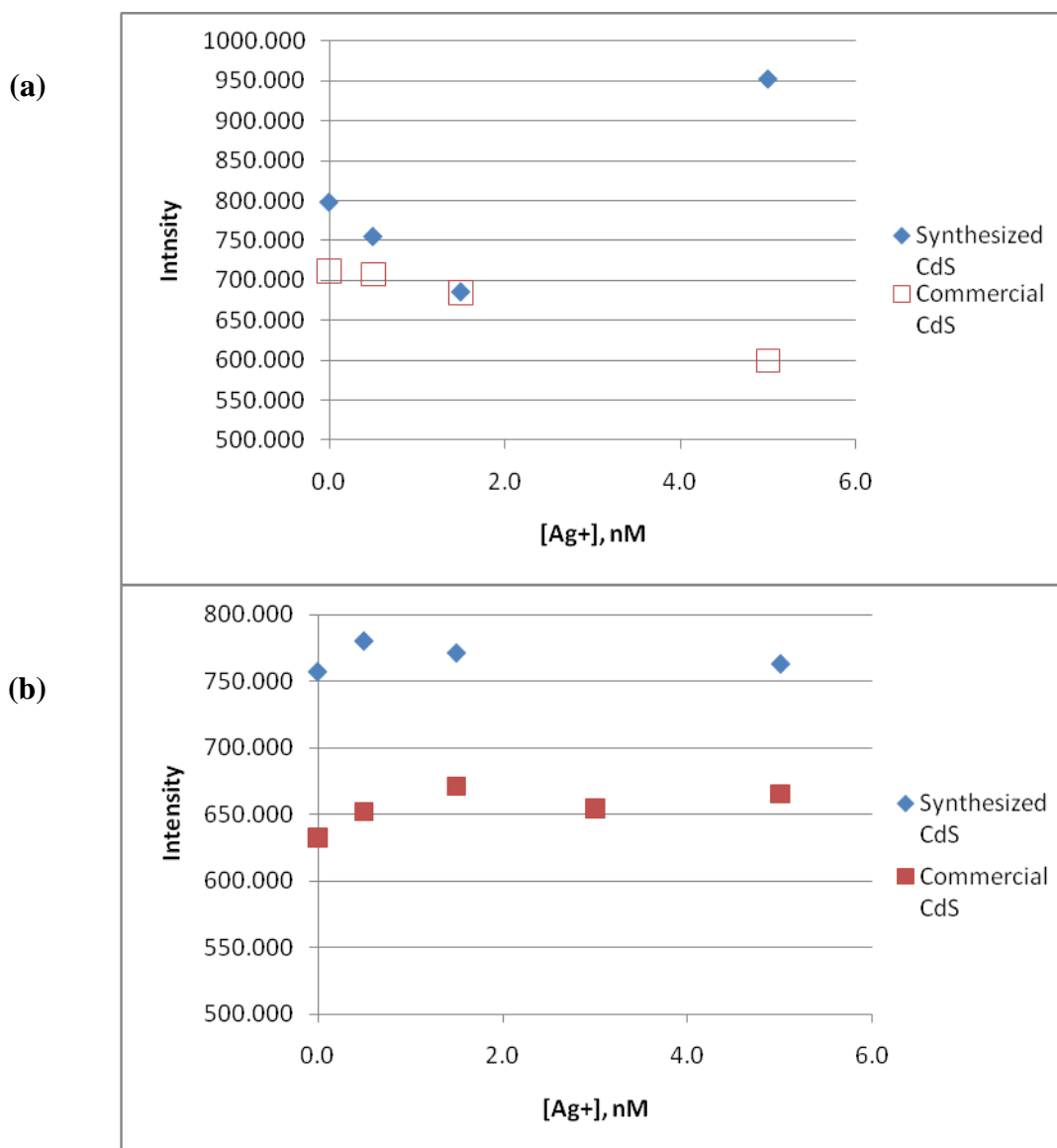


Figure 6: Selected synchronous fluorescence intensities at 304 nm when CdS exposed to solutions of Ag^+ ranging from 0.5-5 nM.

There appears to be no consistent, analytically-useful quenching or enhancement of the synchronous fluorescence due to increasing $[Ag^+]$. (a) Same points as shown in Figure 5 fluorescence spectra, suggesting quenching. (b) Suggestion of fluorescence enhancement at low end of concentrations. $\Delta\lambda = 305$ nm; PMT = 600 V; slit widths = 5 nm (ex), 10 nm (em) for all except (b) Commercial CdS: due to increased intensity near the upper limit of the detector, slit widths were 5 nm (ex), 5 nm (em).

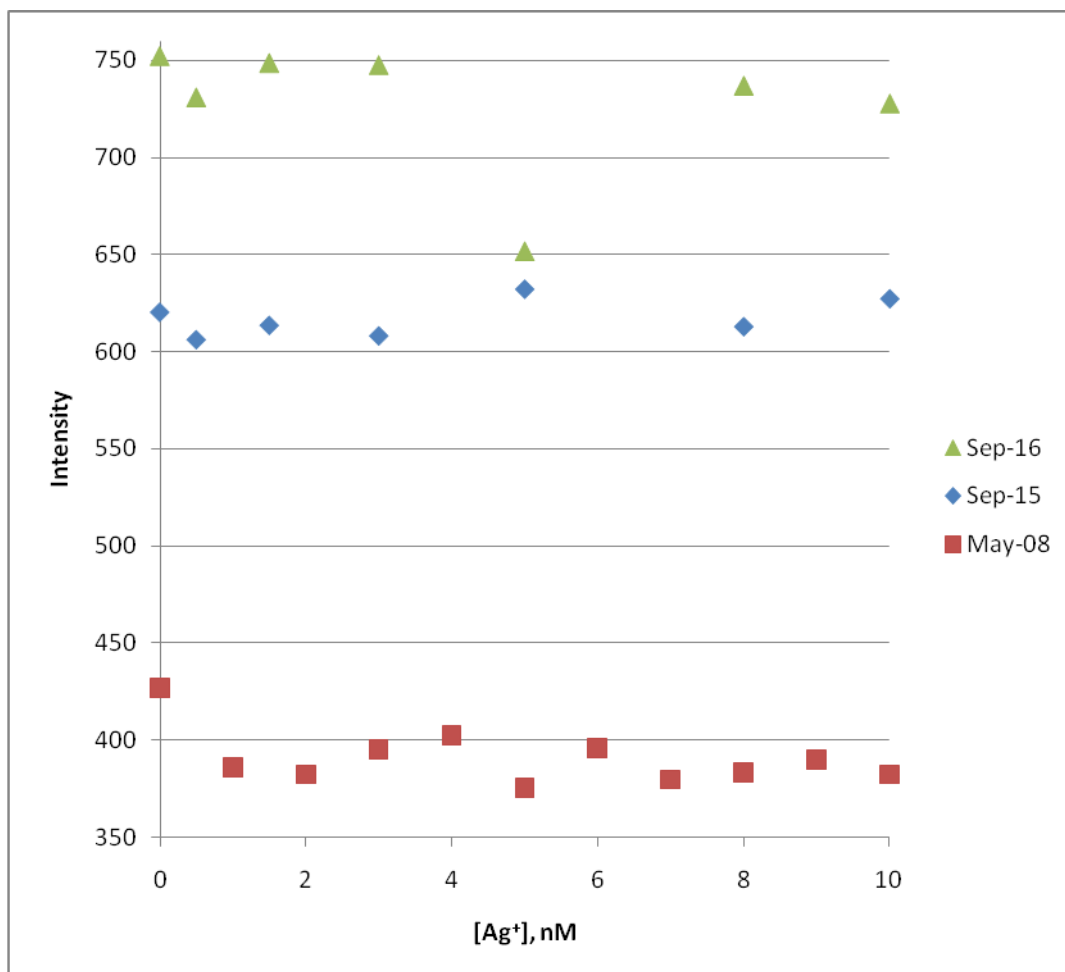


Figure 7: Effect of 0.5-10 nM Ag^+ on synchronous fluorescence of CdS QDs at 304 nm using $\Delta\lambda = 305$ nm.

Even over a larger concentration range, no consistent, analytically-useful pattern of quenching or enhancement is observed. PMT = 600 V; slit widths = 10 nm (ex), 10 nm (em) for May 8; 5 nm (ex), 5 nm (em) for Sept. 15; 5 nm (ex), 10 nm (em) for Sept. 16.

evaporated prior to functionalization with mercaptoacetic acid, and the results also suggested quenching (Figure 5b). No consistent pattern could be found, even when a larger range of standards was prepared (Figure 7). This led to a further investigation of pH and the effects of toluene in solution.

2.3.3 pH and toluene effects on quenching, enhancement of fluorescence

pH effects required further investigation because, after the first analysis using synthetic CdS QDs, Ag was prepared in 2% nitric acid solutions. These Ag stocks were used in such a way as to minimize the amount of acid added to the samples. However, as the concentration of Ag in the samples increased, the amount of 2% nitric acid being added to the samples also increased. This was found to affect the pH of samples prepared using synthetic QDs and 0.067 M PBS buffer: pH values typically ranged from 7.18 to 7.61 (Figure 8a). The pH effect on samples containing commercial QDs and 1 M HEPPS buffer was less severe: pH values ranged between 7.34 and 7.4 (Figure 8a). To minimize pH effects, HEPPS buffer was adopted for the remainder of the experiments.

To further tease apart pH and toluene effects, a buffered blank prepared with commercial CdS, without the toluene evaporated, was spiked with 5 nM Ag^+ in MQ water as it sat in the cuvette inside the fluorometer. This was done twice: once using an Ag^+ spike in 2% HNO_3 (Figure 9a), and once using an Ag^+ spike in milli-Q water (Figure 9b). The first test shows quenching: in the first 30 seconds, the fluorescence intensity dropped dramatically, then leveled off within the first ten minutes at a lower intensity than the buffered blank (Figure 9a). The second tests shows enhancement: in the first 30

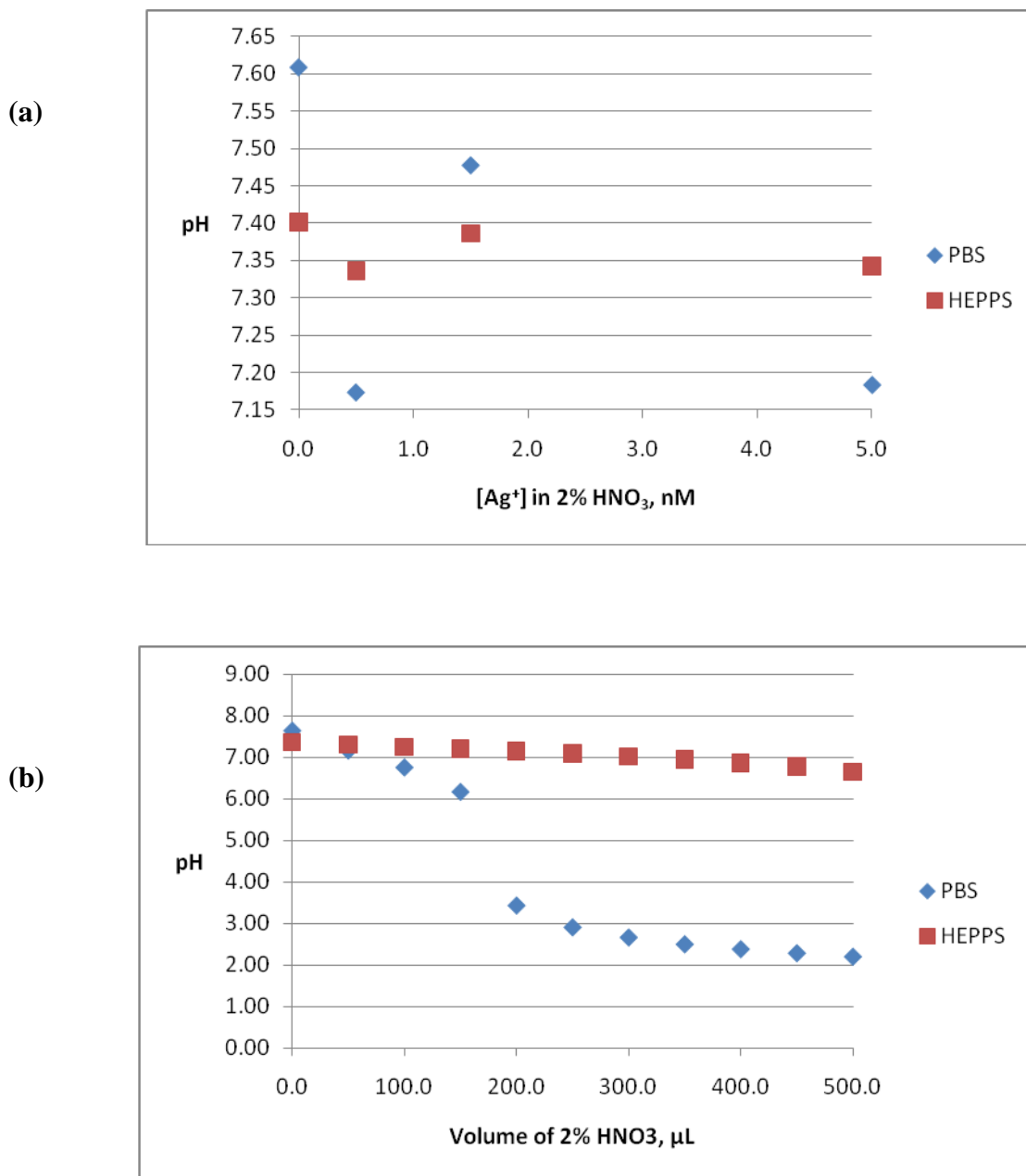


Figure 8: The effect of adding solutions containing 2% HNO₃ to buffered solutions containing 2×10^{-4} M CdS on pH.

In both cases, PBS buffered solutions responded more strongly to changes in pH than do HEPPS-buffered solutions. (a) Increasing Ag⁺ created by adding 50 μL of 100 nM Ag⁺ ([HNO₃] = 0.00158 M), 15 μL of 1000 nM Ag⁺ ([HNO₃] = 0.000474 M), and 50 μL of 1000 nM Ag⁺ ([HNO₃] = 0.00158 M). (b) Effect of adding only 2% HNO₃.

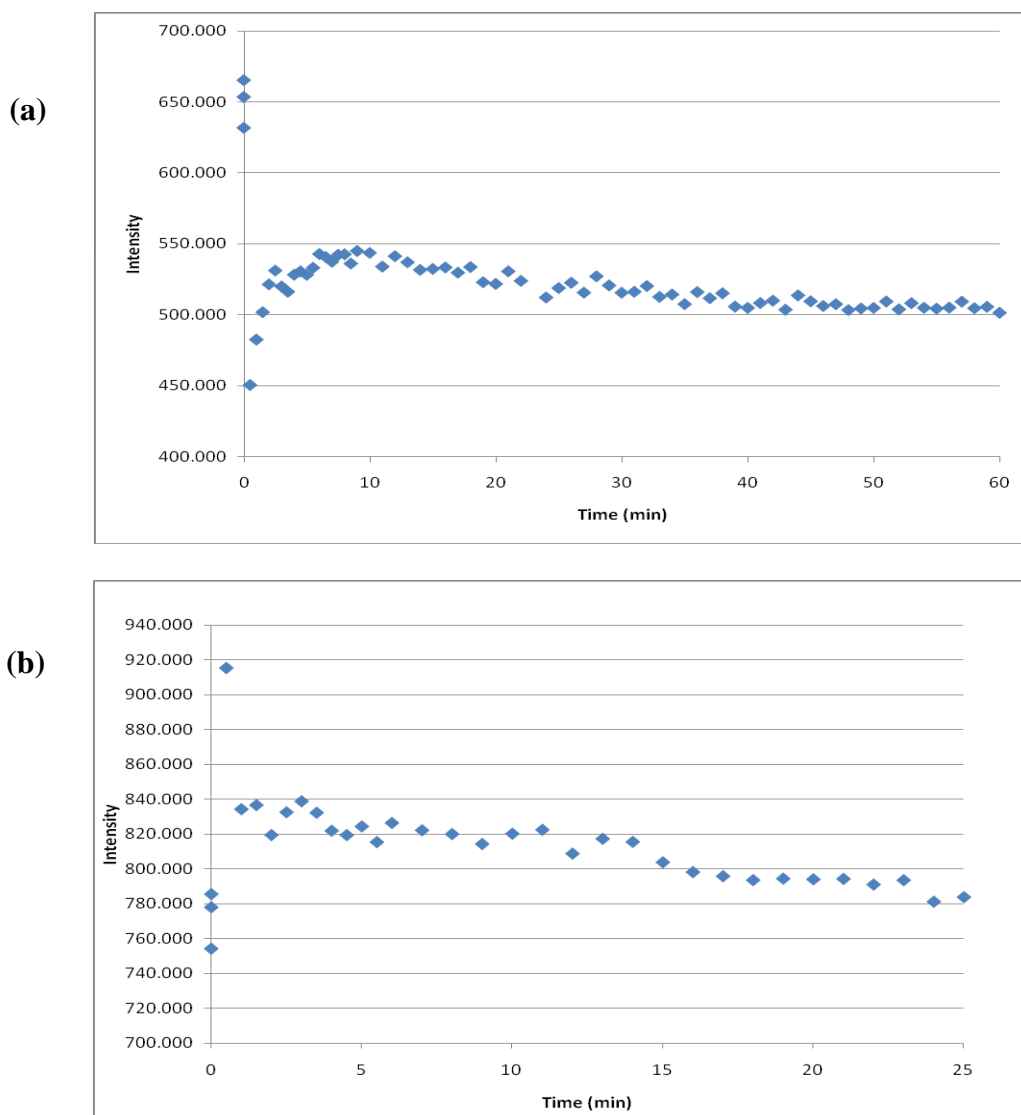


Figure 9: Synchronous fluorescence intensity at 304 nm over time with the addition of 5 nM Ag^+ to a blank solution containing 2×10^{-4} M commercial CdS QDs.

In both cases, toluene was not evaporated. $\Delta\lambda = 305$ nm; PMT = 600 V. (a) Ag^+ solution spike was made with 2% HNO_3 in a volume later shown to overwhelm the PBS buffer and drop the solution pH to 6.6. Slit widths = 10 nm (ex), 20 nm (em). (b) Ag^+ solution spike was made without HNO_3 ; no change in pH was observed as compared to blank. Slit widths = 10 nm (ex), 10 nm (em).

seconds, the fluorescence intensity spiked, then leveled off at a higher intensity than the buffered blank (Figure 9b). These results suggest that even small changes in pH may impact whether Ag^+ quenches or enhances CdS synchronous fluorescence. Following these two experiments, all further samples using commercial CdS and HEPPS buffer were made using Ag stocks made without or with reduced (0.04%) nitric acid.

Although toluene did not seem to affect whether or not quenching occurred, all further experiments involved evaporating off the toluene prior to functionalization in order to see if more consistent, linear changes to the peak at 304 nm could be observed. Evaporating off the toluene from the CdS had the effect of increasing the instrument sensitivity to fluorescence, but did not produce any more robust, reproducible, linear enhancement (Figure 6b). Similarly, providing an excess of mercaptoacetic acid during the functionalization/ligand equilibration stage of CdS preparation only served to support the adoption of the current concentration of 1×10^{-4} M MAA to maximize the signal enhancement seen when a 4 nM Ag^+ concentration was analyzed, relative to a blank (Figure 10).

2.4 Discussion

Both synthetic and commercial CdS QD's produced $\lambda_{\text{ex}}/\lambda_{\text{em}}$ more red-shifted than reported by Wang et al. (2008). This was probably the first indicator of large particle sizes, or clumps of QD's, in solution, as functionalized CdS QDs with larger diameters typically emit at longer wavelengths, since larger QDs have a smaller band gap energy

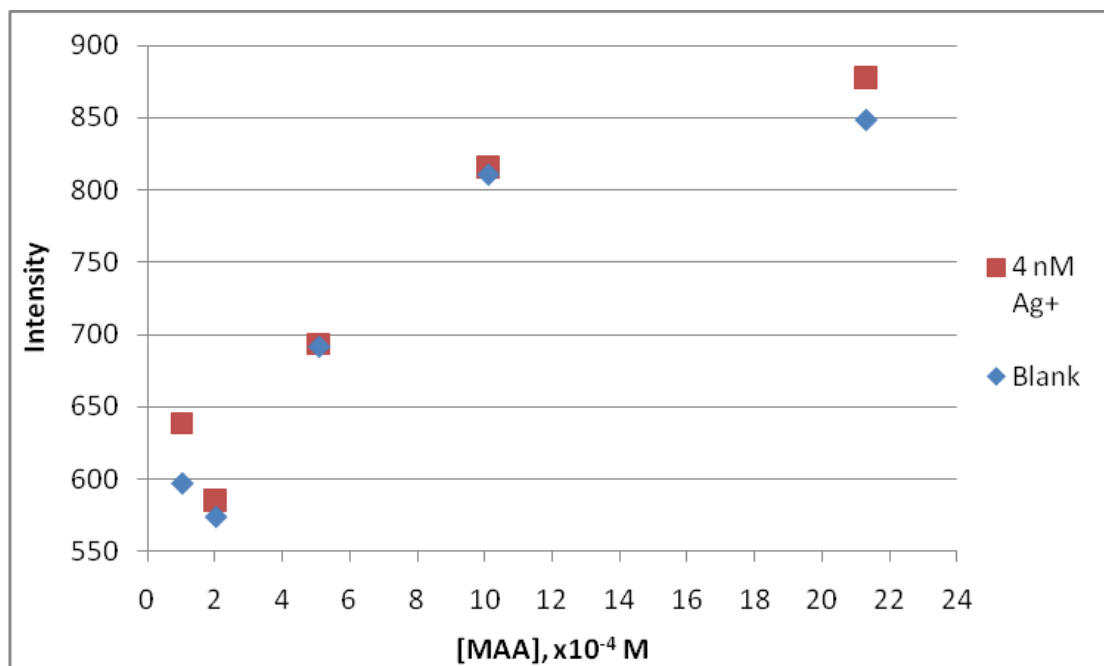


Figure 10: Effect of concentration of mercaptoacetic acid (MAA) on synchronous fluorescence intensity at 304 nm in blanks and 4 nM Ag⁺ made with commercial CdS.

The amount of MAA used to functionalize the CdS QDs varied from 1X to 20X the usual amount. In all cases, the intensity was slightly enhanced by the addition of 4 nM Ag⁺ to the blank. Although the greatest overall intensity was noted for samples containing approximately 20X the usual amount of MAA, the greatest signal enhancement by Ag⁺, and therefore the most effective [MAA] was noted in the normal (1X) MAA concentration. $\Delta\lambda = 305$ nm; PMT = 600 V; slit widths = 5 nm (ex), 10 nm (em).

(Y. Chen & Rosenzweig, 2002). The synchronous fluorescence peaks seen in the samples prepared using commercial CdS were even broader than those produced using synthesized CdS, and could be a reflection of an even larger heterogeneity of size of CdS particles, as seen in Figure 4b. Particle size of the QDs is important not only for controlling peak width and $\lambda_{\text{ex}}/\lambda_{\text{em}}$ (Murphy, 2002), but also for consistent uptake of Ag^+ from solution. This could be the main reason for the lack of analytical response of the fluorescence of the QD's to increasing concentrations of Ag^+ in solution.

Synthetic CdS, functionalized with a thiol-containing substance, should form a light yellow solution with no precipitate (Y. Chen & Rosenzweig, 2002). The original synthesis, as per Wang et al. (2008), produced a clear, nearly colourless solution which, under the transmission electron microscope, revealed no visible quantum dots. A comparison of the pale yellow seen in this solution did not match the much more intense yellow of the 2×10^{-3} M CdS solution produced from commercial QD's at the same concentration of CdS. Furthermore, a 2×10^{-3} M solution of commercial CdS QD's had clearly identifiable QDs (Figure 4). When synthesis employed a 10X excess of thioacetamide, a bright yellow solution of the same intensity seen in the commercial QD solution was produced, this time with an undesirable yellow precipitate. Distinct QD's in this solution were of the 20-25 nm size range (Figure 3), just as reported by Wang et al. (2008). However, significant amounts of other electron-dense material in the TEM images suggested smaller-sized QDs clumped together (Figure 3).

The presence of precipitate in the synthetic CdS mixture obtained in our experiments likely indicates the presence of by-products of synthesis, because no similar precipitate was observed in our functionalized CdS QD solution, or was mentioned in any of the literature involving synthesis of CdS QDs (H.-Q. Chen, Liang, Wang, Liu, & Qian, 2009; J.-L. Chen & Zhu, 2005; Y. Chen & Rosenzweig, 2002; Wang et al., 2008). The identity of these by-products was not investigated, though the deep yellow colour is suggestive of elemental sulfur or sulfur-containing compounds. Sulfide-containing by-products have the potential to serve as quenching material for Ag^+ , because Ag ions could be attracted to these non-fluorescent compounds instead of to the QDs. As a result, we could expect to see inconsistent quenching in the synchronous fluorescence peak as inconsistent quantities of Ag^+ are taken up by this material (Figures 4-6). The presence of this precipitate in the synthetic CdS samples could have been responsible for the non-ideal analytical response to Ag^+ , both in the presence of nitric acid and when nitric acid was not used.

Improvement of the synthetic CdS QDs would require an understanding of the mechanism of synthesis, and where variables could be manipulated. The type of reagents used, the order in which they are added, and their concentrations would all have an effect on the types of quantum dots produced in the end, as well as the quantity and type of by-products possible. Table 1 summarizes the roles of the different chemicals in the synthesis used here and by Wang et al. (2008). Here, thioacetamide was used as the source of sulfide ions, while other syntheses have directly utilized sulfide salts (Y. Chen & Rosenzweig, 2002) or elemental sulfur (Li et al., 2005). Studies carried out by Peeters

Chemical Name	Chemical Formula	Purpose
inert atmosphere (nitrogen gas)	$N_{2(g)}$	prevents $O_{2(g)}$ from being trapped in QDs; prevents oxidation of sulfide
cadmium chloride hemipentahydrate	$CdCl_2 \cdot 2.5H_2O_{(s)}$	source of Cd^{2+}
thioacetamide	$CH_3C(S)NH_{2(s)}$	source of S^{2-}
sodium hexametaphosphate	$(NaPO_3)_{6(s)}$	anti-aggregation; also helps keep QDs stable in presence of small amounts of $O_{2(g)}$
sodium hydroxide	NaOH	bring up pH to 8.5 to induce formation of CdS QD's
mercaptoacetic acid	$HSCH_2COOH_{(l)}$	QD capping agent which helps prevent QD aggregation while selectively attracting Ag^+

Table 1: Anticipated function of chemicals used in the synthesis of CdS quantum dots, in order of their addition to the reaction vessel.

Only the cadmium chloride, thioacetamide, and sodium hydroxide are believed to have a role in the reaction mechanism for producing CdS (Figure 11).

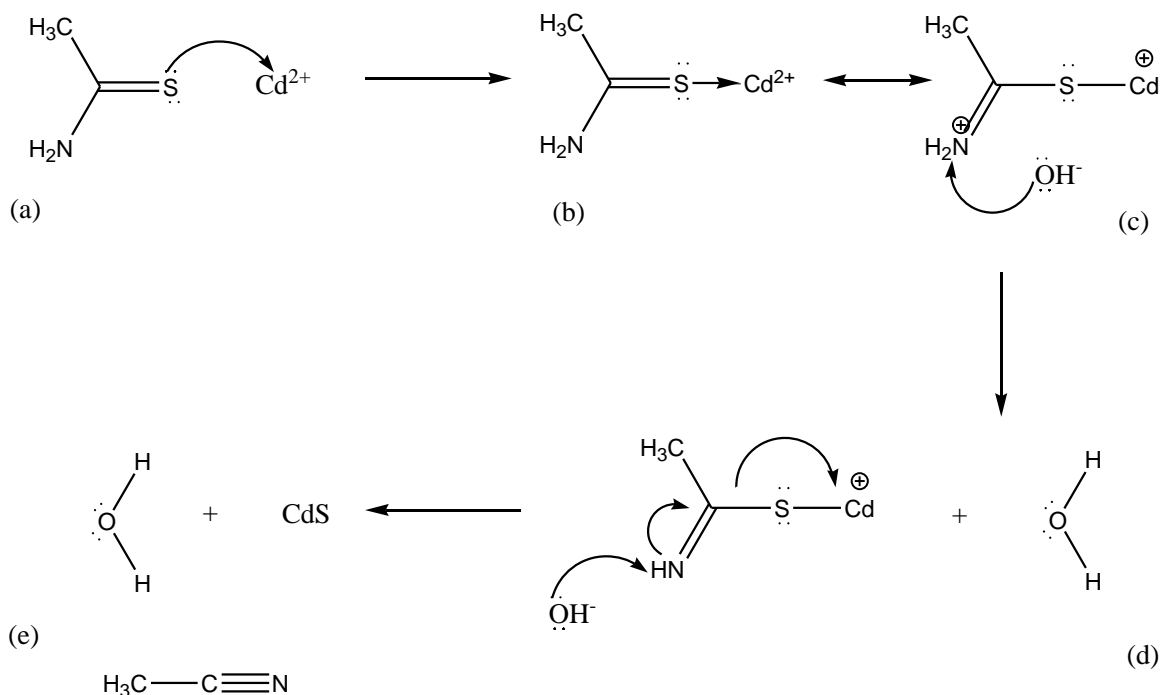


Figure 11: A possible mechanism for the formation of CdS from thioacetamide and cadmium chloride.

This mechanism is based on laboratory observations as well as studies carried out by Peeters et al. (1978) involving the interaction of thioacetamide and several soft metal ions, including cadmium. (a) Dissolved thioacetamide and cadmium ions interact. Cd^{2+} , being a soft cation, is more attracted to the sulfide portion of the molecule, since sulfur is a soft ligand. No visible changes are noted in the reaction vessel. (b) Keto-enol tautomerization of the thioacetamide as it remains coordinated with Cd^{2+} has been proposed based on infrared studies of CS and CN stretching frequencies (Peeters, Blaton, & Deranter, 1978). The “enol” form is believed to permit easier release of protons from the amino group (Peeters et al., 1978). (c), (d) The addition of NaOH is observed to promote the solution yellowing and eventually formation of CdS crystals within the reaction vessel; thus, hydroxide promotes the stepwise removal of amino protons. Without basic conditions, water molecules would facilitate this removal, though at a slower rate (Peeters et al., 1978). (e) Overall, two water molecules, one CdS unit, and one acetonitrile molecule are produced for each reaction between thioacetamide and Cd^{2+} .

et al. (1978) on the interaction of thioacetamide and several soft metal ions, including cadmium, suggested that no free sulfide is present in the starting stages of synthesis; instead, the cadmium directly interacts with the sulfur on the thioacetamide, a bond forms between the two, and then attack by a base (NaOH) allows cadmium sulfide to be released (Figure 11). The presence of a 10-fold excess of thioacetamide in the solution might have been responsible for the bright yellow precipitate which started to form during pH adjustment: once the thioacetamide had reacted with all of the cadmium ions, it would have been “free” to react with base, perhaps liberating elemental sulfur, or reacting with other thioacetamides to produce other sulfur compounds. Restricting the amount of thioacetamide to stoichiometric amounts produced no QDs, so future syntheses might try a lesser excess of thioacetamide (say, 2X stoichiometric), or trying the synthesis with a sulfide salt, to eliminate sulfur-containing by-products which might attract Ag^+ .

Added prior to the NaOH, the sodium hexametaphosphate plays no part in the synthesis mechanism; however, it is believed to have a role in limiting size of quantum dots produced by aggregation of newly-formed CdS units in solution (Murphy, 2002). Perhaps the amount of sodium hexametaphosphate needs to be investigated: in these experiments, not having enough in the matrix could have allowed for the clumping of smaller QDs as seen in Figure 3. This, in turn, may have affected the functionalization of our synthetic QDs. The mercaptoacetic acid (MAA), added after visible CdS QDs had formed, was meant to attach to the exterior of CdS QDs, thereby functionalizing them and later increasing their attraction to Ag^+ in solution (Wang et al., 2008). At a concentration of 1×10^{-4} M, there would have been ample MAA molecules to completely

cover the surface of the distinct QDs in solution; however, if QDs were clumping, then it is entirely possible that MAA was unable to evenly coat the surfaces of the QDs, thereby reducing their ability to attract Ag^+ evenly. Areas of the QDs not functionalized by MAA could have attracted Ag^+ directly to the surface of the QD, allowing for non-radiative energy transfer and therefore quenching the synchronous fluorescence, though not in any consistent way (Brolo et al., 2006).

Since refinement of synthesis and development of purification methods was not the goal of this research, the majority of our experiments focused upon using commercial QDs in place of synthetic ones. Functionalizing commercial CdS QDs, which were coated in oleic acid as a capping agent in order to be soluble in toluene, has not been reported before, so guidelines as provided by Sigma-Aldrich website (see 2.3.1, Results) were followed to attempt a surface-ligand exchange. Removing the toluene prior to exposing the QDs to mercaptoacetic acid (MAA) seemed to provide greater sensitivity and higher peaks at 304 nm; however, there was no linear quenching or enhancement response to increasing Ag^+ concentrations (Figures 5, 6). TEM images of functionalized CdS QDs in the matrix of sodium hexametaphosphate, at pH 8.6, showed a high degree of particle clumping (Figure 4b). It is unknown if the clumping was due to ineffective ligand exchange, causing particles still coated in oleic acid to stick together because they are hydrophobic in a hydrophilic environment, or if the clumping was due to an insufficient amount of anti-clumping chemical (sodium hexametaphosphate) in the matrix. In either case, just as before, clumps would create inconsistent particle sizes, and uneven surfaces of MAA-capped, oleic-capped, or uncapped CdS (Figure 12).

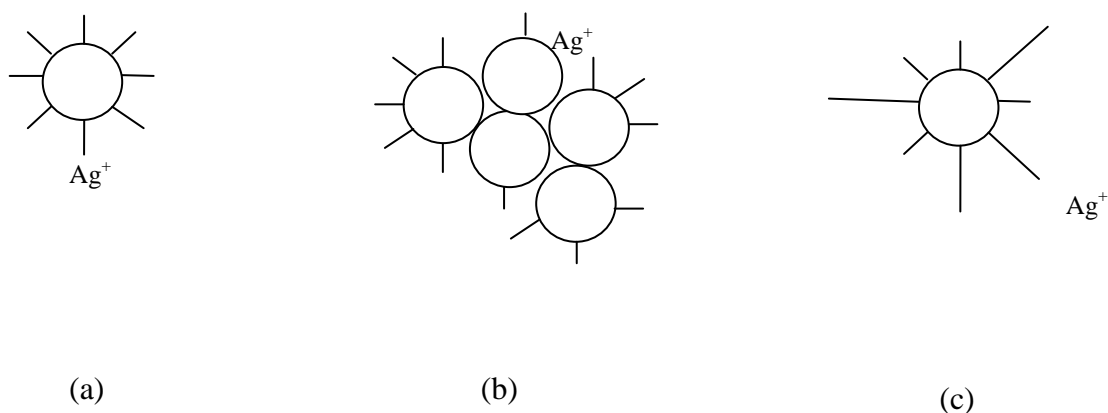


Figure 12: Diagram of functionalized commercial CdS QDs (circles) and some possible interactions with silver ions.

(a) Enhancement scenario: an isolated CdS QD, uniformly functionalized with mercaptoacetic acid (small lines) molecules, attracting Ag^+ to the correct distance for fluorescence enhancement. (b) Quenching scenario: a clump of QDs, partially functionalized with MAA molecules. Here, Ag^+ is attracted directly to a bare CdS surface, allowing for non-radiative energy transfer and a decrease in synchronous fluorescence. (c) No fluorescence effect: an isolated QD, partially functionalized with MAA but still with oleic acid (longer lines) molecules. The hydrophilic carboxyl group of oleic acid will be facing the CdS QD surface, leaving the hydrophobic fatty acid tail exposed. Ag^+ , being a charged species, would be repelled from the hydrophobic oleic acid tail and would not get close enough to the attractive MAA chains to affect synchronous fluorescence.

This is the first time that commercial CdS quantum dots have been investigated as probes for nanomolar quantities of Ag^+ in water. Commercial quantum dots were found to give just as inconsistent analytical responses as those produced by the synthesized quantum dots (Figures 4-6), most often appearing to somewhat be quenched with increasing Ag^+ concentration, and sometimes appearing to be somewhat enhanced. Before these CdS QDs can even be properly assessed for water samples in the picomolar range of Ag, the chemistry of either synthesis or functionalization of commercial QDs must be refined.

Due to the lack of analytical response in the low nanomolar range, synchronous fluorescence studies using picomolar levels of Ag^+ were not attempted, nor were total Ag analyses attempted for natural freshwater samples. However, the experiments described here have important implications for sample preparation, should the technique ever be refined to involve CdS QDs of a uniform size which would produce an analytical response to Ag^+ . Samples collected for total Ag analyses will have been acidified to below pH 2 in order to release any Ag^+ bound to organics. The results of our experiments showed that even microlitre quantities of 2% HNO_3 overwhelmed the buffers used in the experiments (Figure 8b), and even affected whether or not quenching or enhancement of synchronous fluorescence was observed (Figure 9). pH adjustment of samples to around 7 would be essential prior adding the CdS QDs for synchronous fluorescence analysis.

2.5 Conclusions

Low nanomolar quantities of Ag^+ do not appear to produce a robust, reliable quenching or enhancement of synchronous fluorescence of CdS quantum dots produced by the reaction of thioacetamide and cadmium chloride. This is most likely related to the variation in sizes of the CdS QDs, particles made of QD clusters, and sulfide-containing by-product which could all attenuate the interaction between Ag^+ and mercaptoacetic acid-capped CdS QDs. Following the synthesis method of Wang et al. (2008), CdS QDs were only produced when a 10-fold excess of thioacetamide was added to cadmium chloride. This process produced a significant amount of a yellow precipitate by-product which potentially contained attractive sulfide or sulfhydryl groups, where Ag could be absorbed instead of interacting with the CdS QDs to promote enhancement of synchronous fluorescence. Therefore, changes in synthesis, and possibly purification, may be necessary for this method to produce a reliable, robust, linear synchronous fluorescence enhancement.

Commercially-available CdS QDs were originally thought to be a time-saving, simplifying process that would provide better results. However, these experiments also failed to show any analytically-useful enhancement or quenching with increasing Ag^+ concentration. This is probably because the chemistry used to functionalize the toluene-soluble CdS QDs with mercaptoacetic acid (MAA) through exchange of surface ligands was not completely effective. TEM images of MAA-functionalized commercial CdS QDs show large clumps of QDs which may behave in a similar way to the by-product of

the synthetic QDs. Further ligand-exchange experiments are recommended before the utility of this type of commercial CdS QD can be assessed.

In each case, synchronous fluorescence signal output was very sensitive to pH, so any natural water samples which have been preserved for total Ag analysis by lowering the pH below 2 would require pH adjustment to 7 prior to addition of buffer and CdS quantum dots.

2.6 References

- Brolo, A. G., Kwok, S. C., Cooper, M. D., Moffitt, M. G., Wang, C.-W., Gordon, R., et al. (2006). Surface Plasmon-Quantum Dot Coupling from Arrays of Nanoholes. *Journal of Physical Chemistry*, *110*, 8307-8313.
- Bruland, K. W., Coale, K. H., & Mart, L. (1985). Analysis of seawater for dissolved cadmium, copper, and lead: an intercomparison of voltammetric and atomic absorption methods. *Marine Chemistry*, *17*, 285-300.
- Bruland, K. W., Franks, R. P., Knauer, G. A., & Martin, J. H. (1979). Sampling and analytical methods for the determination of copper, cadmium, zinc, and nickel at the nanogram per liter level in sea-water, *Analytica Chimica Acta* (Vol. 105, pp. 233-245).
- Chen, H.-Q., Liang, A.-N., Wang, L., Liu, Y., & Qian, B.-b. (2009). Ultrasensitive determination of Cu²⁺ by synchronous fluorescence spectroscopy with functional nanoparticles. *Microchimica Acta*, *164*, 453-458.

- Chen, J.-L., & Zhu, C.-Q. (2005). Functionalized cadmium sulfide quantum dots as fluorescence probe for silver ion determination. *Analytica Chimica Acta*, 546, 147-153.
- Chen, Y., & Rosenzweig, Z. (2002). Luminescent CdS Quantum Dots as Selective Ion Probes. *Analytical Chemistry*, 74, 5132-5138.
- Kinrade, J. D., & Van Loon, J. C. (1974). Solvent extraction for use with flame atomic absorption spectrometry. *Analytical Chemistry*, 46(13), 1894-1898.
- Kulakovich, O., Strekal, N., Yaroshevich, A., Maskevich, S., Gaponenko, S., Nabiev, I., et al. (2002). Enhanced Luminescence of CdSe Quantum Dots on Gold Colloids. *Nano Letters*, 2(12), 1449-1452.
- Li, Y., Liu, E. C. Y., Pickett, N., Skabara, P. J., Cummins, S. S., Ryley, S., et al. (2005). Synthesis and characterization of CdS quantum dots in polystyrene microbeads. *J. Mater. Chem.*, 15, 1238-1243.
- Miller, L. A., & Bruland, K. W. (1995). Organic Speciation of Silver in Marine Waters. *Environmental Science & Technology*, 29, 2616-2621.
- Murphy, C. J. (2002). Optical Sensing with Quantum Dots. *Analytical Chemistry*, 74, 520A-526A.
- Ndung'u, K., Ranville, M. A., Franks, R. P., & Flegal, A. R. (2006). On-line determination of silver in natural waters by inductively-coupled plasma mass spectrometry: influence of organic matter. *Marine Chemistry*, 98, 109-120.

- Peeters, O. M., Blaton, N. M., & Deranter, C. J. (1978). Kinetics and Mechanisms of Reaction between Thioacetamide and Lead(II), Cadmium(II), and Cobalt(II) Ions in Acetate Buffered Solution. *Journal of the Chemical Society-Perkin Transactions 2*(1), 23-26.
- Song, J.-H., Atay, T., Shi, S., Urabe, H., & Nurmikko, A. V. (2005). Large Enhancement of Fluorescence Efficiency from CdSe/ZnS Quantum Dots Induced by Resonant Coupling to Spatially Controlled Surface Plasmons. *Nano Letters*, 5(8), 1557-1561.
- Swamy, K. M. K., Kim, H. N., Soh, J. H., Kim, Y., Kim, S.-J., & Yoon, J. (2009). Manipulation of fluorescent and colorimetric changes of fluorescein derivatives and applications for sensing silver ions. *Chemical Communications*, 10, 1234-1236.
- Vo-Dinh, T. (1978). Multicomponent Analysis by Synchronous Luminescence Spectrometry. *Analytical Chemistry*, 50(3), 396-401.
- Wang, L., Liang, A.-N., Chen, H.-Q., Liu, Y., Qian, B.-b., & Fu, J. (2008). Ultrasensitive determination of silver ion based on synchronous fluorescence spectroscopy with nanoparticles. *Analytica Chimica Acta*, 616(2), 170-176.

Chapter 3: Using Competitive Ligand Exchange-Solvent Extraction to Examine Silver Interaction in Well Water Containing Triclosan and Thyroid Hormone T₃

3.1 Introduction

Total silver (Ag) is a measure of Ag in all its forms, while Ag speciation is a breakdown of the specific chemical forms of Ag present in a sample. For example, Ag can exist as a free (hydrated) ion (Ag^+), as soluble inorganic complexes (e.g. AgCl_x^-), as soluble organic complexes, or as a component of particulate matter (e.g. insoluble AgS species). Analytical methods designed to detect total Ag and Ag speciation have both evolved from initial investigations of organic extractions which compared the removal and pre-concentration of eight metals (including Ag) from water samples into organic solvents using a variety of complexing ligands (Kinrade & Van Loon, 1974). The sample preparation has been adjusted to include a back-extraction into nitric acid, so that the Ag is freed from these complexing ligands. Utilizing an aqueous medium with high concentrations of nitrate also keeps Ag more stable in the matrix over a longer time period (Bruland et al., 1985; Bruland et al., 1979; Miller & Bruland, 1995), and allows the analyst the option of using inductively-coupled plasma mass spectrometry (ICP-MS). The competitive ligand exchange-solvent extraction (CLE-SE) techniques for both total Ag and Ag speciation involve very similar sample preparation steps, thus utilizing the same equipment and many of the same reagents (Miller & Bruland, 1995).

To use CLE-SE for measurements of total Ag, the water sample is acidified to a pH below 1.6 to free Ag from natural ligands, and a strong Ag-binding ligand is added to the sample to complex available Ag and allow for its extraction to an organic solvent for sample pre-concentration. Therefore, the ligand chosen must (a) be present as an anion in aqueous solution, (b) be strongly attracted to Ag ion with minimal attraction to other major cations in natural water, and (c) form a neutral, hydrophobic complex once it binds with Ag^+ , so that it will move out of the aqueous solution and into a much-smaller volume of organic solvent (Kinrade & Van Loon, 1974). A blend of ammonium 1-pyrrolidine-dithiocarbamate (APDC) and diethylammonium diethyldithiocarbamate (DDDC) has proven the best combination for this purpose, allowing for pre-concentration and measurement of total Ag levels which would otherwise be below instrument detection limits (Bruland et al., 1979; Kinrade & Van Loon, 1974). The dithiocarbamate anions, PDC^- and DDC^- , have sulfur groups to serve as “soft” ligands which can attract Ag and other soft cations in the sample (Bruland et al., 1985). Since both ligands are present in large excess, side reactions with “soft” metals other than Ag present in the sample will be insignificant. Figure 13 illustrates how Ag likely coordinates with these ligands, as well as the structures of other ligands that are of interest to this study.

Ag speciation measurements, on the other hand, aim only to extract, and thus detect, Ag which is not strongly bound by natural ligands. Therefore, the ligand added to the system should establish a competition with these natural ligands instead of taking up all available Ag (Miller & Bruland, 1994). The experimental setup for measuring Ag speciation is quite similar to total Ag, except only one ligand is used (DDC^-) and it is

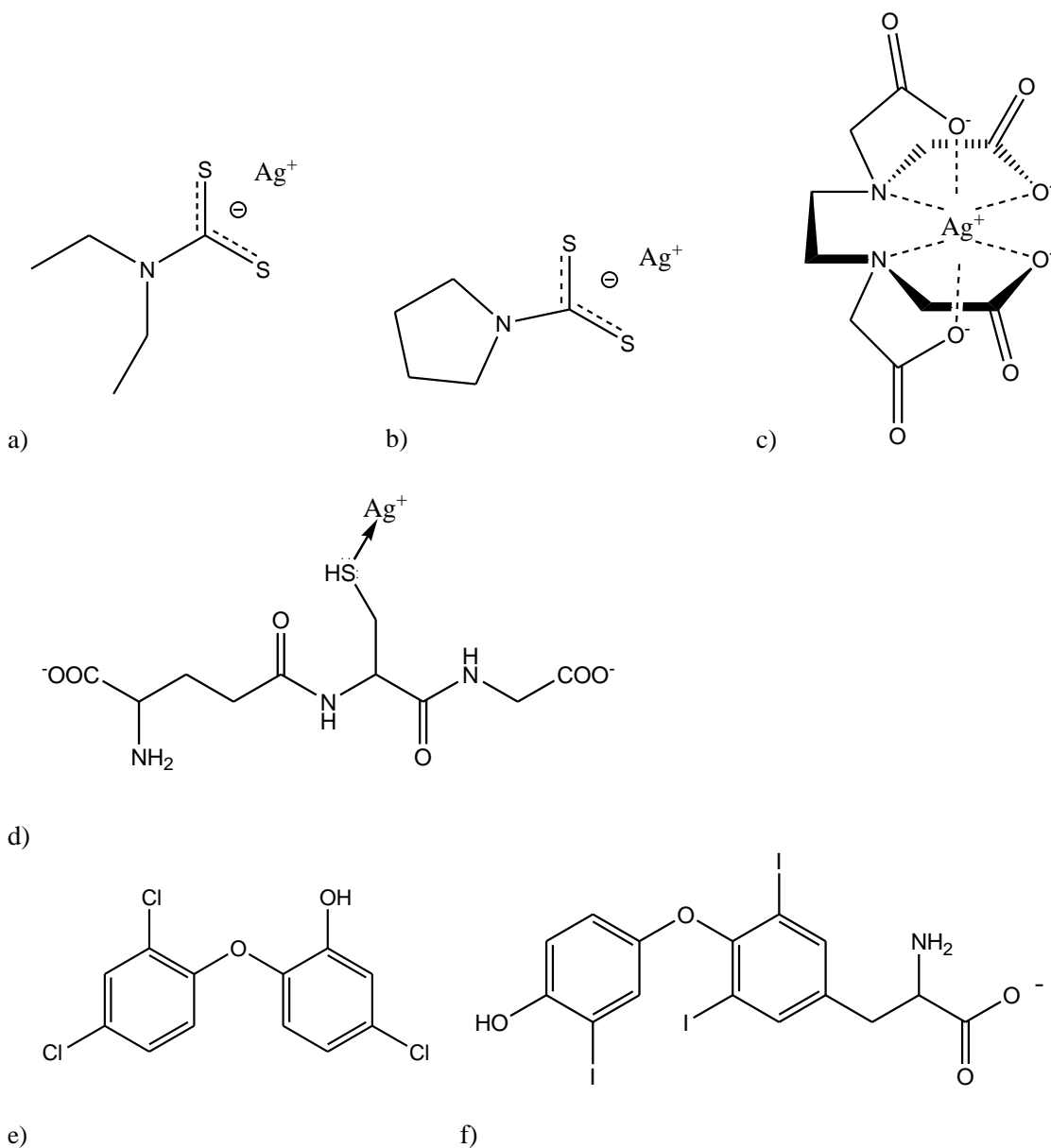


Figure 13: Appearance of ligands and Ag-ligand complexes formed in the experiments.

According to Hard-Soft Acid-Base (HSAB) theory, Ag, being a soft acid (cation) binds most strongly with soft bases (anions). Thiols (HS) and thiolates (RS), as well as iodine, being soft bases, would be the binding preference of Ag^+ in the above ligands. As a result, DDC^- (a), PDC^- (b), and glutathione (d) will bind Ag^+ through their sulfur groups. Being a chelating ligand, EDTA (c) could bind Ag^+ through N and O in an octahedral complex. Triclosan (e) may at first seem to have the least affinity for Ag^+ of all of the above ligands, since it only has hard bases (OH and Cl) with which to attract Ag^+ . 3,3',5-triiodothyronine, T_3 (f) may be able to bind up to three Ag^+ ions through the iodine atoms (binding not shown).

added in a much lower concentration. The water sample is kept at native pH, because acidification would break down any natural speciation by liberating Ag from organic complexes. As in the total method, the DDC^- ligand forms an uncharged, hydrophobic complex with Ag ($\log K'_{\text{AgDDC}} = 9.1$ in freshwater, (Adams & Kramer, 1999a)), and the complex moves into chloroform (CHCl_3) (Miller & Bruland, 1995) but this time, the DDC^- complexes only with free Ag and Ag bound in complexes weaker than Ag-DDC. For best quantitative results, DDC^- concentration ($[\text{DDC}^-]$) should be high enough so that the strength (as α_{AgDDC} : see Table 2) matches the strength of expected Ag complexes (as α_{AgL}) (Adams & Kramer, 1999a; Miller & Bruland, 1995). This can be difficult to gauge unless the ligands are well-known and well-characterized, so if time and sample volume permit, then it is preferred to conduct several titrations within certain “windows” of strength (α_{AgDDC}) (Miller & Bruland, 1994).

Titration of a sample with Ag^+ at a constant $[\text{DDC}^-]$ allows the analyst to establish whether or not any strong ligands exist in an aqueous sample that prevent Ag from forming the DDC^- complex (Adams & Kramer, 1999a; Miller & Bruland, 1994; Miller & Bruland, 1995). A first order interpretation of the data can be made from the appearance of the titration curve (Figure 14). If a plot of total Ag ($[\text{Ag}_T]$) versus extracted Ag ($[\text{Ag}^*]$) has a positive x-intercept or is curved, then the sample has some naturally-occurring strong Ag-binding ligands; if it forms a straight line, then the sample probably

<p>(1) $[Ag^*] = [Ag_{chl}]M_{ICPMS}/M_{aq}$</p> <p>(2) $[AgDDC] = [Ag_{chl}]/K_{d(Ag)}$</p> <p>(3) $\alpha_{AgY} = K'_{AgY}[Y] = [AgY]/[Ag^+]$</p> <p>(4) $K'_{AgY} = [AgY]/[Ag^+][Y]$</p> <p>(5) $\Sigma[AgL_i] = [Ag]_T - ([Ag^*] + [AgDDC] + [Ag^+] + [AgX_i])$</p>
--

Table 2: Equations used to take experimental data and quantify Ag species in freshwater using DDC⁻ as the added ligand.

In all cases, [DDC⁻] can be assumed to be equal to [DDC⁻]_T, since [Ag]_T ≪ [DDC⁻]_T and there are no significant side reactions between DDC⁻ and major cations in freshwater.

Notes:

$[Ag^*]$ = amount of Ag removed in the extraction, from the sample aqueous phase into CHCl₃

$[Ag_{chl}]$ = amount of Ag removed into CHCl₃, and ultimately detected by ICP-MS. Considered equivalent to $[AgDDC_{chl}]$, when no hydrophobic complexes with Ag extract.

M_{aq}/M_{ICPMS} is the sample pre-concentration factor. M_{aq} = mass of sample weighed out and treated with DDC⁻ and CHCl₃; M_{ICPMS} = final mass of sample analyzed by ICP-MS after extraction into CHCl₃, evaporation of CHCl₃, and dissolution in 2% HNO₃

$[AgDDC]$, $[Ag^+]$ = AgDDC complex, free Ag⁺ which are left behind in the aqueous layer

$K_{d(Ag)}$ = distribution coefficient of AgDDC between CHCl₃ and water; 10^{12.6} (Wytenbach & Bajo, 1975)

α_{AgY} = side reaction coefficient for an Ag-Y complex, where Y represents any Ag-binding ligand (including DDC⁻). α is a measure of the strength of that complex.

$[Y]$ = concentration of a ligand Y not bound to Ag⁺.

K'_{AgY} = stability constant for an Ag-Y complex, where Y represents any Ag-binding ligand. ($K'_{AgDDC} = 10^{9.1}$ (Adams & Kramer, 1999a))

$\Sigma[AgL_i]$ = sum of all Ag-ligand complexes remaining behind in the aqueous layer in the sample. Note that for freshwater samples, the contribution from inorganic complexes ($[AgX_i]$) is negligible. Total Ag ($[Ag]_T$) is determined by an independent analysis.

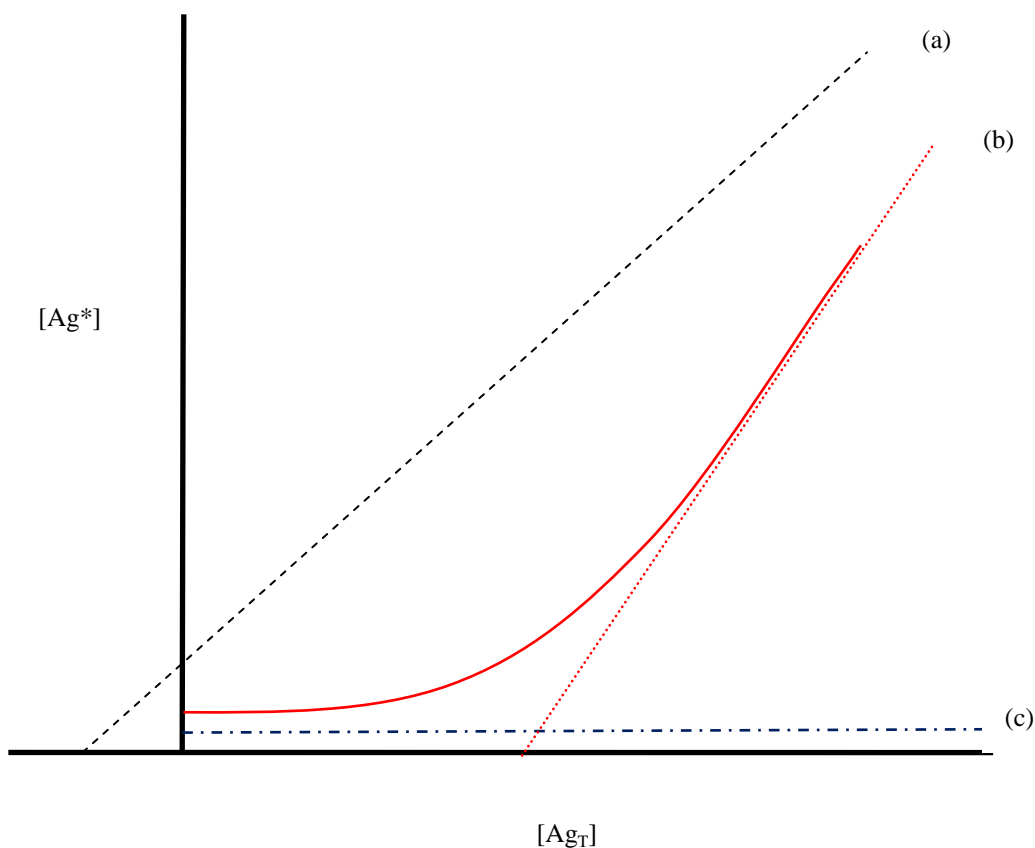


Figure 14: Schematic representation of titration curves for natural samples titrated with Ag^+ at a set concentration of DDC^- .

- (a) Natural ligand(s) in the sample are not competing with DDC^- . The titration curve looks like a standard additions curve.
- (b) Natural ligand(s) in the sample are competing with DDC^- . Carefully extrapolating from the highest concentrations of $[\text{Ag}_T]$, where the curve “straightens”, to the x-axis (dotted line) should give the total amount of ligand(s) in the sample ($[\text{L}_T]$).
- (c) Natural ligand(s) in the sample are out-competing DDC^- . The titration should be repeated at a higher $[\text{DDC}^-]$.

does not have appreciable strong Ag-binding ligands within that analytical window (Miller & Bruland, 1995). If the titration curve shows a horizontal line with no appreciable increase in Ag extraction, then the natural ligand in the sample must be strongly competitive, and the titration should be repeated using a different analytical window (i.e. a higher [DDC⁻]). If the slope of a titration of a sample without any strong Ag-binding ligands is compared to the slope of a titration of an unknown suspected of containing ligands, a significant difference can also serve as a sign of competitive ligands within that analytical window (Miller & Bruland, 1995).

A second order interpretation of the data requires linearization through a series of calculations. Using the following rationale, the total natural ligand concentration [$L'_{T,i}$] and a conditional stability constant (K'_{AgL_i}) for these natural ligands may be calculated from treatment of an unknown sample with increasing Ag^+ in the presence of constant [DDC⁻] (Adams & Kramer, 1999a). The mass balance for total Ag [Ag_T] in a system with no strong organic binding ligands is:

$$(1) [Ag_T] = [Ag^+] + [Ag^*] + [AgDDC] + [AgX_i]$$

where [Ag^*] represents the amount of Ag extracted into $CHCl_3$ and detected by ICP-MS; [$AgDDC$] represents the amount of $AgDDC$ left behind in the aqueous layer; [Ag^+] represents free Ag ion left behind in the aqueous layer, and [AgX_i] represents charged Ag-inorganic complexes also left behind in the aqueous layer. In freshwater samples, side reactions with inorganic ligands are insignificant, so [AgX_i] can be considered

negligible, simplifying Equation (1) (Adams & Kramer, 1999a). Dividing all terms by $[Ag^+]$ allows us to rewrite Equation (1) in terms of side reaction coefficients (α):

$$(2) [Ag_T]/[Ag^+] = 1 + \alpha_{Ag^*} + \alpha_{AgDDC}$$

Since by definition the side reaction coefficient $\alpha_{Ag^*} = [Ag^*]/[Ag^+]$, then it follows that $[Ag^+] = [Ag^*]/\alpha_{Ag^*}$. We can now write Equation (2) in terms of $[Ag^*]$, and we have an equation containing only side reaction coefficients and measured values.

$$(3) [Ag_T]/([Ag^*]/\alpha_{Ag^*}) = 1 + \alpha_{Ag^*} + \alpha_{AgDDC}$$

Rearranging equation (3) in terms of $[Ag^*]$ gives

$$(4) [Ag^*] = \alpha_{Ag^*}[Ag_T]/(1 + \alpha_{Ag^*} + \alpha_{AgDDC})$$

This equation is simply a straight line with a slope of $\alpha_{Ag^*}/(1 + \alpha_{Ag^*} + \alpha_{AgDDC})$ and a y-intercept of zero. The slope of this line can be interpreted as a measure of extraction sensitivity, S (Rue & Bruland, 1995):

$$(5) S = \alpha_{Ag^*}/(1 + \alpha_{Ag^*} + \alpha_{AgDDC})$$

The extraction sensitivity of a system without ligands can be compared qualitatively to a system suspected to have natural ligands. If the slope of the linear portion (at high metal concentrations) of the suspect system matches the slope of the representative system

without ligands, then one can say, with confidence, that the binding ligand in the system has been fully titrated out (Rue & Bruland, 1995), and the calculation of $[L_{T,i}]$, K'_{AgL_i} and Ag speciation within the sample (see Table 2) will be valid. If the slopes differ appreciably, then the binding ligand has not been completely titrated out, and these calculations will not be valid.

To finish the calculations of $[L'_{T,i}]$, K_{AgL_i} and Ag speciation, the sensitivity, S , in equation (5) of the linear portion of the titration curve is required. In a system containing natural ligands, the mass balance has an additional term:

$$(6) [Ag_T] = [Ag^+] + [Ag^*] + [AgDDC] + [AgX_i] + \Sigma[AgL_i]$$

where all other variables are the same as before, and $\Sigma[AgL_i]$ represents Ag bound to natural organic ligands present in the sample and thus left behind in the aqueous layer during extraction (Adams & Kramer, 1999a). Again assuming negligible $[AgX_i]$, rearranging equation (6) to solve for $\Sigma[AgL_i]$ gives

$$(7) \Sigma[AgL_i] = [Ag]_T - ([Ag^*] + [AgDDC] + [Ag^+])$$

and writing each term in brackets in terms of side reaction coefficients (α) we get

$$(8) \Sigma[AgL_i] = [Ag]_T - [Ag^*](1 + \alpha_{Ag^*} + \alpha_{AgDDC}) / \alpha_{Ag^*} = [Ag]_T - [Ag^*]/S$$

Once $\Sigma[\text{AgL}_i]$ for each titration point has been calculated using Equation (8), we can find $[\text{Ag}^+]$ for each point in the titration by using α_{Ag^*} (calculated from equation (5)) and $[\text{Ag}^*]$ ($[\text{Ag}^+] = [\text{Ag}^*]/\alpha_{\text{Ag}^*}$) (Adams & Kramer, 1999a). Knowing $\Sigma[\text{AgL}_i]$ and $[\text{Ag}^+]$ will allow us to linearize the data in one of two ways. A Langmuir (or van den Berg-Ružić) plot, $[\text{Ag}^+]/\Sigma[\text{AgL}_i]$ versus $[\text{Ag}^+]$, is a good starting point when there are only a few titration points, or in systems where one model ligand has been added to water without other natural Ag-binding ligands (Miller & Bruland, 1994; Rue & Bruland, 1995). With one competitive ligand binding in a 1:1 relationship with Ag^+ , a Langmuir plot will reveal a straight line with a slope of $1/[\text{L}_{\text{T},i}]$ and a y-intercept of $1/[\text{L}_{\text{T},i}]\text{K}'_{\text{AgL},i}$ (Croot & Johansson, 2000; Ruzic & Nikolic, 1982; van den Berg, 1984). However, a Langmuir linearization giving a negative intercept does not allow for determination of a stability constant (Miller & Bruland, 1994), and multiple ligands will show curvature in the plot at lower $[\text{Ag}^+]$, making individual $\text{K}'_{\text{AgL},i}$ values difficult to calculate (Rue & Bruland, 1995). An alternative is the Scatchard plot, $\Sigma[\text{AgL}_i]/[\text{Ag}^+]$ versus $\Sigma[\text{AgL}_i]$, which will produce a straight line with an x-intercept of $[\text{L}_{\text{T},i}]$ and a y-intercept of $\text{K}'_{\text{AgL},i}[\text{L}_{\text{T},i}]$ (Croot & Johansson, 2000). Given enough data, this plot can often resolve multiple linear regions that can be used to calculate separate $\text{K}'_{\text{AgL},i}$ and $[\text{L}_{\text{T},i}]$ for each ligand (Rue & Bruland, 1995).

There are many limitations in interpreting data gleaned from these linearizations. First, as previously mentioned, these quantitative calculations are most reliable when the strength of the added DDC⁻ is within one order of magnitude of the strength(s) of the natural ligand(s) present, as represented by the side reaction coefficients, α (Miller &

Bruland, 1995). Second, the values obtained from the plots will only be accurate at high Ag^+ concentrations, when it can be certain that all ligand has been titrated out (Adams & Kramer, 1999a; Croot & Johansson, 2000; Rue & Bruland, 1995). Furthermore, the plots cannot determine the identity of the ligand(s), nor can they always distinguish between more than one ligand with similar Ag-binding strengths. No matter which linearization is chosen, $K'_{\text{AgL},i}$ values for unknown natural samples more likely represent weighted averages of a mixture of several ligands (Miller & Bruland, 1995; Rue & Bruland, 1995).

Prior to taking the time to prepare titrations to evaluate organic ligands for their potential to bind Ag^+ , CLE-SE should be used qualitatively to test the effect on the extractability of Ag in solutions containing one suspected organic chemical. Adding increasing concentrations of DDC^- into a fixed concentration of Ag and suspected organic ligand should reveal how the two species interact. If the organic compound binds Ag to create a charged, hydrophilic complex which is stronger than DDC^- , then less Ag will be extracted into the CHCl_3 layer than with DDC^- alone. Miller and Bruland (1995) demonstrated this with glutathione, an amino which attracts Ag^+ with its thiol group (Figure 13). If the organic ligand binds Ag to create a neutral, hydrophobic ligand which is extractable, then more Ag will be extracted into CHCl_3 than with DDC^- alone.

The low chloride content and potential for high organic content in freshwater increases the probability that Ag will form complexes with organic ligands (Adams & Kramer, 1999a; Miller & Bruland, 1995). Man-made organic ligands which enter the environment through runoff, accidental spills, and after municipal sewage treatment seem

to be increasing in both quantity and variety, and their interactions with metals also found in these water sources are largely unknown. For example, EDTA, a chelating agent, has found widespread use in processed foods, cosmetics, and other household products, and is a moderately-strong Ag-binding ligand ($\log K'_{\text{AgEDTA}} = 8.2$ in freshwater (Morel & Hering, 1993)). In seawater, EDTA does not appreciably bind Ag, given side reactions with the more abundant cations (e.g. Ca^{2+} and Mg^{2+}) (Miller & Bruland, 1995); however, in freshwater, these cations are present in much diminished concentrations, so EDTA can interact more significantly with Ag (Miller & Bruland, 1995).

Another industrial chemical on the rise in effluents is triclosan, a germicidal agent used in antibacterial soaps, detergents, lotions, and toothpastes (Veldhoen et al., 2006). The structure of triclosan closely mimics thyroid hormone T_3 (Figure 13), and on its own has been shown to disrupt frog metamorphosis (Veldhoen et al., 2006) and have endocrine-disrupting effects in other organisms (Ahn et al., 2008; Zorrilla et al., 2009). Like EDTA, triclosan may have some interaction with Ag in freshwaters as it has recently been shown to disrupt bullfrog thyroid hormone-mediated metamorphosis more acutely when present in solutions containing low levels of nanoAg, another antibiotic agent released into effluents (C. C. Helbing, unpublished data). It is unknown whether nanoAg or the Ag^+ it releases over time are interacting with triclosan. Experiments with nanoAg and ionic Ag on tadpole tissues suggest Ag itself may be interacting with the active thyroid hormone 3,3',5-triiodothyronine (T_3), as T_3 seems to modify how the tissues respond to Ag (Hinter et al., in review). Competitive ligand exchange experiments should reveal if Ag^+ might be forming organic complexes with triclosan or

T₃, and provide some insight as to how this might modulate their respective bioavailability to frog cells. If the experiments outlined here suggest binding of either by Ag to create hydrophobic complexes, the bioavailability of Ag (and therefore toxicity) should increase, but if binding of either chemical by Ag creates hydrophilic complexes, then the bioavailability of Ag⁺ (and therefore toxicity) should decrease (Phinney & Bruland, 1997). Conversely, by binding Ag⁺, the bioavailability of triclosan or T₃ compounds might be altered.

The goals of the work presented in this chapter are twofold. First, the chapter discusses the characterization of well water used as a medium for tadpole growth in the frogSCOPE Ag exposure studies. Well water will be assessed for total Ag using the method developed for pre-concentration and extraction of picomolar metals by Bruland et al. (1979, 1985), and will be titrated as per Miller and Bruland's (1995) Ag speciation approach to determine if natural ligands are present. This part of the work also will help answer some questions related to the methodology of total Ag and Ag speciation using competitive ligand exchange. Second, the chapter discusses the experiments used to explore the interaction between Ag and EDTA, triclosan and T₃, which have not yet been characterized for interaction with Ag in freshwater. Miller and Bruland's (1995) CLE-SE technique will be used to determine if triclosan or T₃ might act as coordinating ligands comparable to EDTA, which should allow us to shed some light on possible mechanisms for the endocrine disruption effects observed by Hinthner et al. (in review) and C. C. Helbing (unpublished data).

3.2 Methods

Preparation of samples and reagents took place in a Class 1000 or 100 clean space at the University of Victoria. All chemicals used were reagent ACS grade or higher; all acids and bases were ultra-high purity. All bottles used to store reagents and samples were trace metal-clean Teflon and LDPE (see Appendix I). All solutions were made with Milli-Q (MQ) water (Millipore ELEMENT/Elix purification system). pH measurements were made on a Thermo ORION 720A+ pH meter, with a Ross Sure-Flow Combination Electrode calibrated using pH 4, 7, and 10 buffers from VWR. Batches of samples were run on a Thermo X Series II ICP-MS using Thermo PlasmaLab software.

Well water collection took place at the Pacific Environmental Science Centre (PESC) in North Vancouver, B. C., on May 10, 2010. Approximately 10 L of well water was run through a 0.2 μm filter (Pall AcroPak 500) in 1- and 2-L Teflon bottles and stored in a room temperature, dark cabinet. Two-1L portions of water were acidified to pH <1.6 using concentrated ultra-pure (Seastar) hydrochloric acid for 28 days prior to total Ag analysis; the remaining volume was kept at native pH.

Both methods can be summarized in the following steps: (a) bring a measured volume of the sample to a suitable pH (4.5 for total Ag, 7.4 for speciation); (b) expose the sample to complexing ligands to bind Ag and then extract the resulting neutral species into CHCl_3 ; (c) digest (break down) the ligands using nitric acid, releasing Ag^+ for analysis by ICP-MS. For full details on chemical and sample preparation, please refer to Appendix III.

3.2.1 Total Ag using PDC⁻/DDC⁻

Approximately 250 mL of sample on its own or, in the case of a titration, containing an added concentration of Ag⁺ (from 10-100 pM) were transferred into a clean 500 mL Teflon-FEP separatory funnel. The sample bottle was weighed before and after collection to determine the exact mass of water. To adjust pH to about 4.5, 2.00 mL of 3M ammonium acetate buffer and 450 µL of concentrated ultra-pure ammonium hydroxide (Seastar, Baseline) were added to each sample. 1.00 mL of APDC/DDC⁻ (as NaDDC or DDDC) solution (1% w/w) was then added, and the funnel was shaken again to thoroughly mix the ligands into the sample. The mixture was allowed to stand 1 hour.

The sample was then treated with 7.00 mL pre-cleaned CHCl₃, shaken vigorously for 2 minutes, and allowed to separate for five minutes. This separation time was varied (5-240 minutes) in one set of experiments. The CHCl₃ layer was then collected into a cleaned 125 mL Teflon-FEP separatory funnel. The process was repeated with a second 7.00 mL fraction of CHCl₃. The aqueous layer remaining in the 500 mL funnel was checked for post-extraction pH using a pH meter and was then discarded, as all Ag⁺ would have been taken up by the ligands and moved into the organic layer.

4.00 mL of 8 M ultra-pure HNO₃ (Seastar, Baseline) was added to the 125 mL separatory funnel containing the CHCl₃ extractions. The funnel was shaken for 2 minutes and allowed to separate for at least 5 minutes. Brown NO₂ gas formed in the funnel

during this extraction. The CHCl_3 layer was collected and discarded; the aqueous (nitric acid) layer was collected into an acid-cleaned 15 mL Teflon-FEP vial. The 15-mL vials containing samples were placed on a pancake griddle (Hamilton Beach StepSavor) pre-heated to 350 °F and allowed to evaporate to dryness over a period of approximately 1.5 hours. Small, brown pellets remained in each vial after evaporation. Three aliquots of 200 μL of concentrated ultra-pure HNO_3 were added to each vial, and evaporated down to dryness each time. After cooling, vials were weighed, then 25 μL of concentrated ultra-pure HNO_3 were added to each vial, followed by 25 μL of internal standard (containing 40 ppb Rh) to monitor instrument drift, and then 1.20 mL of MQ water, all gravimetrically, creating a total volume of 1.25 mL of sample suspended in 2% ultra-pure nitric acid. Vials were gently swirled to thoroughly mix contents, then contents were transferred to acid-cleaned 1.5 mL polypropylene snap-top vials and analyzed manually by ICP-MS using a combination of internal and external standardization (Table 3).

3.2.2 Qualitative competitive ligand exchange experiments

Model ligand experiments using glutathione and EDTA were done using a modified Fraquil medium, using the major salts (see <http://www-cyanosite.bio.purdue.edu/media/nontable/fraquilnt/html>). Competitive ligand exchange

Instrument	Thermo X-Series II
Software	Thermo PlasmaLab
Nebulizer type	quartz
Cone types	nickel (both skimmer and sample cones)
Sample uptake setting	25 rpm. Using narrow-bore sample tubing, this consumed about 0.25 mL sample per minute.
Analytes	^{91}Zr , ^{93}Nb , ^{101}Bkg (background), ^{103}Rh (internal standard), ^{107}Ag , ^{109}Ag
Uptake time	50-80 s, depending on run
Acquisition time	13 s per cycle; 3 cycles, with 100 replicates per cycle
Rinse	30 s with 2% HCl; 50 s with 2% HNO ₃
Internal Standard	0.8 ppb ^{103}Rh

Table 3: ICP-MS instrument parameters for total Ag and Ag speciation methods.

Each extraction contained 0.8 ppb (7.8 nM) ^{103}Rh in order to monitor instrument sensitivity during the run. A series of external standards (varying Ag^+ in 2% HNO₃, and 0.8 ppb ^{103}Rh) were made for each sample run, and used to set up a calibration curve based on ^{107}Ag signal. Sample ^{107}Ag signals were then matched to this calibration curve to determine a sample Ag concentration. In spite of any matrix differences between external standards and samples, this analysis procedure was considered valid, as no samples required adjustment based on changes in ^{103}Rh sensitivity.

experiments with triclosan and 3,3',5-triiodothyronine were done using well water collected from PESC. Approximately 100 mL of the water sample was transferred into a clean 500 mL Teflon-FEP separatory funnel. The sample bottle was weighed before and after removal to determine the exact mass of water. pH adjustment to 7.4 was accomplished by adding 1 mL of 1M HEPPS buffer and 30 μL of concentrated ultra-pure ammonium hydroxide. For samples with a competing ligand, the competing ligand was added next (100 μL of 1 mM glutathione, 100 or 1000 μL of 100 mM EDTA, 1000 μL of 3.0 mg/L (10.4 μM) triclosan, or 100 μL of 10 μM T_3). 100 μL of 100 nM Ag^+ solution were added gravimetrically to give a solution of 100 pM Ag^+ . Finally, 1.00 mL of DDC^- solution (either NaDDC or DDDC) of varying concentrations (from 10^{-5} M to 10^{-2} M), were added, and the funnel was shaken for 2 minutes to thoroughly mix all ligand(s) into the sample. The treated sample was then allowed to equilibrate for 1 hour.

After one hour, 5.00 mL of pre-cleaned CHCl_3 were added, and the mixture shaken for 2 minutes, and allowed to separate for 20 minutes. The CHCl_3 layer was then collected into a cleaned 125 mL Teflon-FEP separatory funnel. The process was repeated with a second 5.00 mL fraction of CHCl_3 , collected into the same 125 mL separatory funnel. All Ag^+ should have been taken up by the ligands and moved into the organic layer. The CHCl_3 layers were washed once with 5.00 mL of MQ water, then collected into an acid-cleaned 15 mL Teflon-FEP vial.

CHCl_3 fractions were covered with 2.00 mL of ultra-pure nitric acid, placed on a pancake griddle pre-heated to 200 °F, and allowed to slowly evaporate. Once the CHCl_3

had evaporated (after about 1.5 hours), the temperature was increased to 350 °F to facilitate digestion and then evaporation of the HNO₃ (another 30 minutes). Tiny amber-brown pellets remained in each vial after evaporation. Three sequential 100 µL aliquots of concentrated ultra-pure HNO₃ were added to each vial, and evaporated down to dryness each time. Once cooled, sample vials were weighed, vials were then re-warmed, and 20 µL of concentrated ultra-pure HNO₃ were added to each vial to dissolve the brown pellets. 20 µL of internal standard (containing 40 ppb Rh), and then 0.96 mL of MQ water were added gravimetrically, creating a total volume of 1.00 mL of sample suspended in 2% ultra-pure nitric acid. Vials were gently swirled to thoroughly mix contents, then contents were transferred to a 1.5 mL capped polypropylene vial and analyzed by ICP-MS as in 3.2.1.

3.2.3 Titrations of Ag into well water used in frogSCOPE

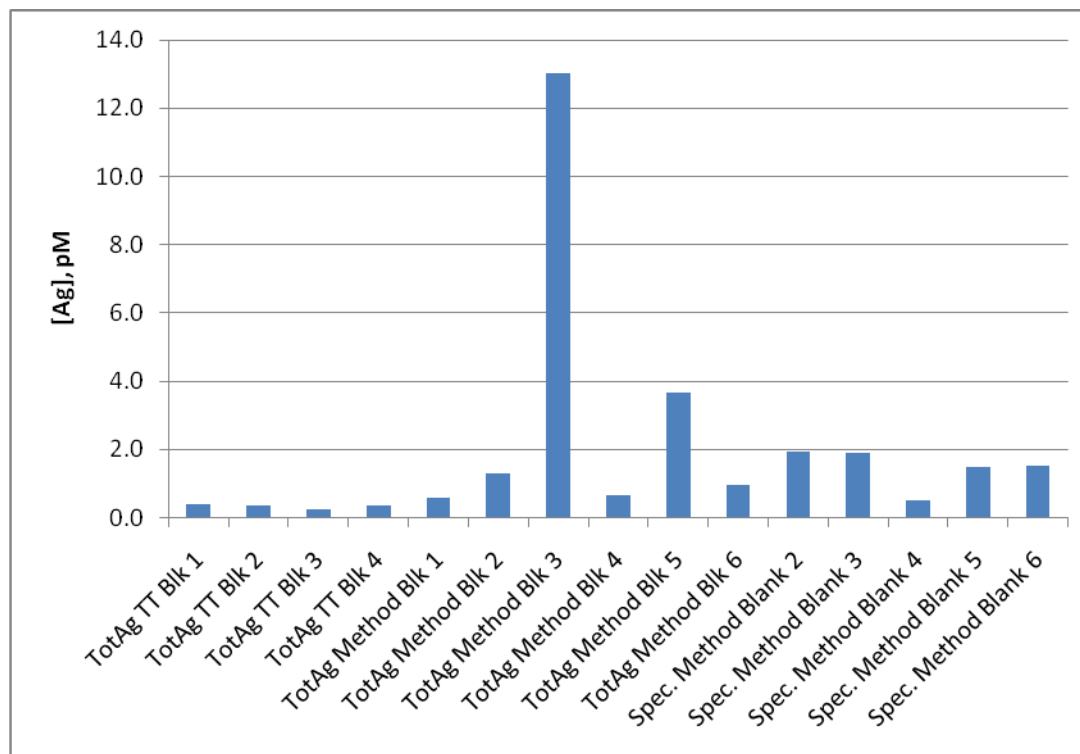
Well water used as a basis for frogSCOPE toxicity studies and for our own sample titrations was collected as described in the opening paragraphs of section 3.2. The method described in 3.2.2, without the addition of 100 pM Ag⁺ and using enough DDC⁻ stock to create 10⁻⁶ M DDC⁻ in the final sample, was followed for titrations with added Ag on well water. The following scenarios were used: (a) without DDC⁻, to check for the presence of natural ligands capable of creating hydrophobic, extractable Ag complexes; (b) with 10⁻⁶ M DDC⁻ only, to check for naturally-occurring competitive ligands; (c) with 10⁻⁶ M DDC⁻ and a competing ligand (one of 100 µM EDTA, 30 µg/L triclosan, or 10 nM T₃).

Several samples in the nanomolar Ag range, used for amphibian Ag exposure studies, were also collected and titrated with increasing Ag^+ . Full details of sample collection and titration procedures can be found in Appendix III.

3.3 Results

3.3.1 Total Ag using $\text{PDC}^-/\text{DDC}^-$

Experiments with various forms of blanks, as 2% ultra-pure HNO_3 in polypropylene test tubes and as method blanks (acidified Milli-Q water treated with APDC/NaDDC , then extracted into CHCl_3) showed that the ultra-pure acids and the test tubes used to house the samples for ICP-MS analysis contributed little to the ^{107}Ag or ^{109}Ag ICP-MS signal intensity (Figure 15). As expected, method blanks contributed more signal (Figure 15). The largest of these blanks, corresponding to about 13 pM Ag^+ in the original sample, is evidence of just how easily the method can concentrate even small amounts of contaminants. Based on the test tube blanks, the instrument detection limit was 0.2 pM, while the method detection limit (MDL), excluding the contaminated method blank #3, was calculated to be 4.8 pM (Figure 15). If the limit of quantification (LOQ) is 3-5X the MDL, then the total Ag method should allow for reasonable distinction between Ag concentrations of about 15-25 pM and higher.



	TotAg test tube blanks	TotAg method blanks	Speciation method blanks
Number of replicates	4	5	5
Average [Ag], pM	0.33	1.4	1.5
Standard Deviation	0.067	1.3	0.58
Detection Limit ¹	0.20	4.8	2.2

¹based on 3 standard deviations for instrument (test tube) blanks; based on 3.747 standard deviations for method blanks (3.747 = Student's *t* at 99% confidence interval for 5 replicates).

Figure 15: Comparison of blanks using the total Ag method involving APDC/NaDDC, and the Ag speciation method involving 10^{-6} M DDDC.

Note that Speciation Method Blank 1 was spilled during the evaporative step, and therefore does not appear here.

A set of titrations of 50, 75, 100, and 200 pM Ag^+ into acidified MQ water reflected only 30-49% recovery (Figure 16), which does not match the nearly 100% quantitative recoveries of Cu, Cd, and Zn using this method (Bruland et al., 1979). Experiments using varying equilibration times (time to allow for AgDDC and AgPDC complexes to move into the organic layer) revealed between 30 and 105% recoveries (Figure 17). It seems that the best recoveries with the highest precision were for the 5 minute equilibration time (Figure 17).

Using the method of standard additions, total Ag for the well water collected at PESC for speciation studies was analyzed using a six-point titration plot (Figure 18). From the absolute value of the x-intercept of the plot, the sample is estimated to contain about 4 pM, which is below the MDL. Percent recoveries of added Ag for the points included in this plot ranged between 64-94%.

3.3.2 Qualitative competitive ligand exchange experiments

Six sets of competitive ligand exchange experiments were set up using either Fraquil medium (<http://www-cyanosite.bio.purdue.edu/media/nontable/fraquilnt/html>) or well water from the Pacific Environmental Science Centre (PESC) containing 100 pM Ag^+ . Figure 19 illustrates how percent Ag recovered varied with concentration over these six experiments, and suggests that identity of the DDC^- salt may be important when studying freshwater samples. The sodium salt seems to have significantly lower recovery at low concentration than the diethylammonium salt. There was also quite a lot of

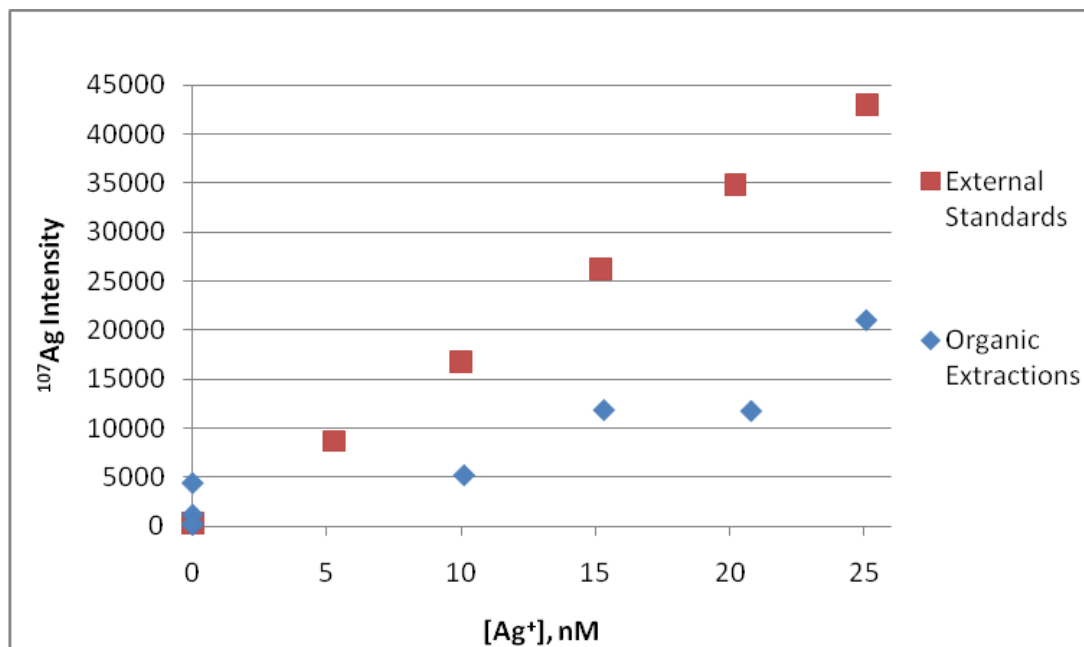


Figure 16: Comparison of ICP-MS counts from a series of external standards and a series of APDC/NaDDC extractions on acidified water.

ICP-MS gives a linear calibration curve over the nanomolar range of study. However, the organic extractions in this titration suggested that only 30-50% of the Ag in the prepared samples was being extracted by the APDC/NaDDC ligand mixture. This could be due to method limitations or due to organic residue in the matrix interfering with Ag^+ analysis. Based on the organic content of the samples alone, we did not expect suppression of Ag^+ signal, so lower extraction efficiency more likely reflects method limitations. Furthermore, there was no suppression of internal standard (^{103}Rh) in samples as compared to external standards. As ^{103}Rh has a similar in charge-size ratio as ^{107}Ag , we can assume similar behaviour with respect to organic material.

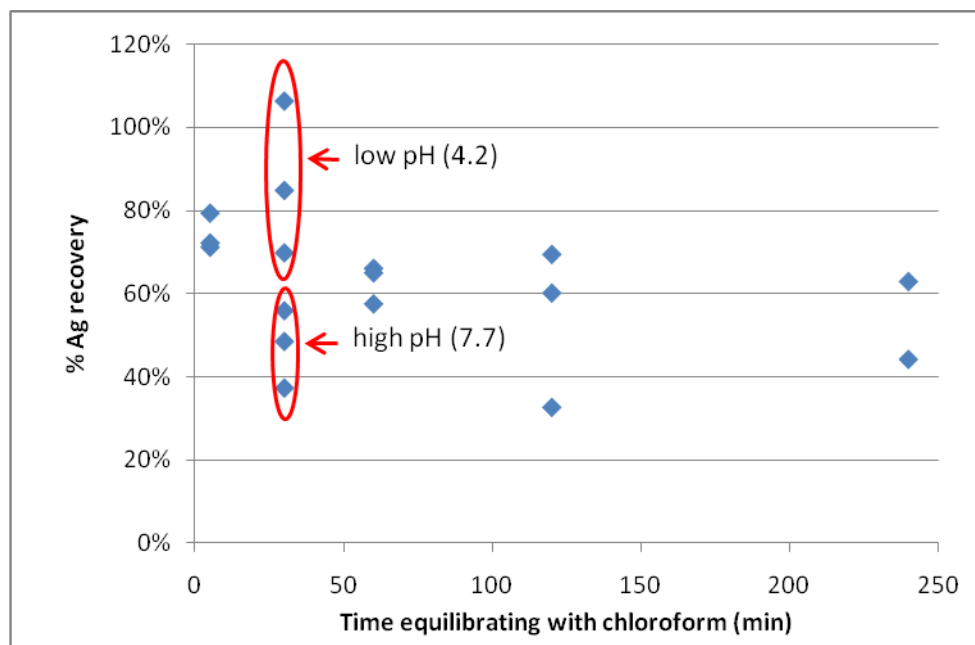
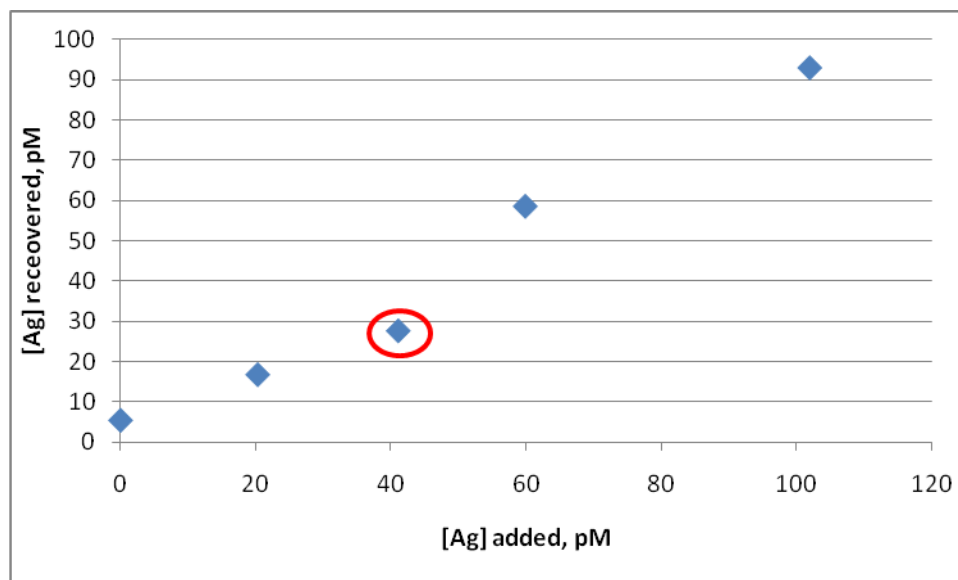


Figure 17: Effect of equilibration time with CHCl_3 on percent recovery of Ag ion using an APDC/NaDDC ligand mixture.

Each time period reflects three sample replicates. For the 30 minute set, two pH values were used (3 replicates each), to illustrate the effect of pH on the samples. Overall, the 5 minute equilibration time produced the highest recovery (average: 74%) with the least amount of variation between replicates (RSD = 6%).



[Ag] added, pM	[Ag], pM	Slope	y-intercept	x-intercept	r ²
0	5.356133				
20.3	16.69599				
41.1	27.60442	0.87914	3.712093	-3.8296202	0.996046
59.9	58.58169				
102	93.05478				

Figure 18: Standard additions curve for total Ag on well water collected from PESC on May 10, 2010.

Water had been acidified 28 days prior to treatment with APDC/DDDC and organic extraction. The highlighted (red-circled) point was excluded from the analysis due to uncharacteristically-low recovery, as compared with the other data points.

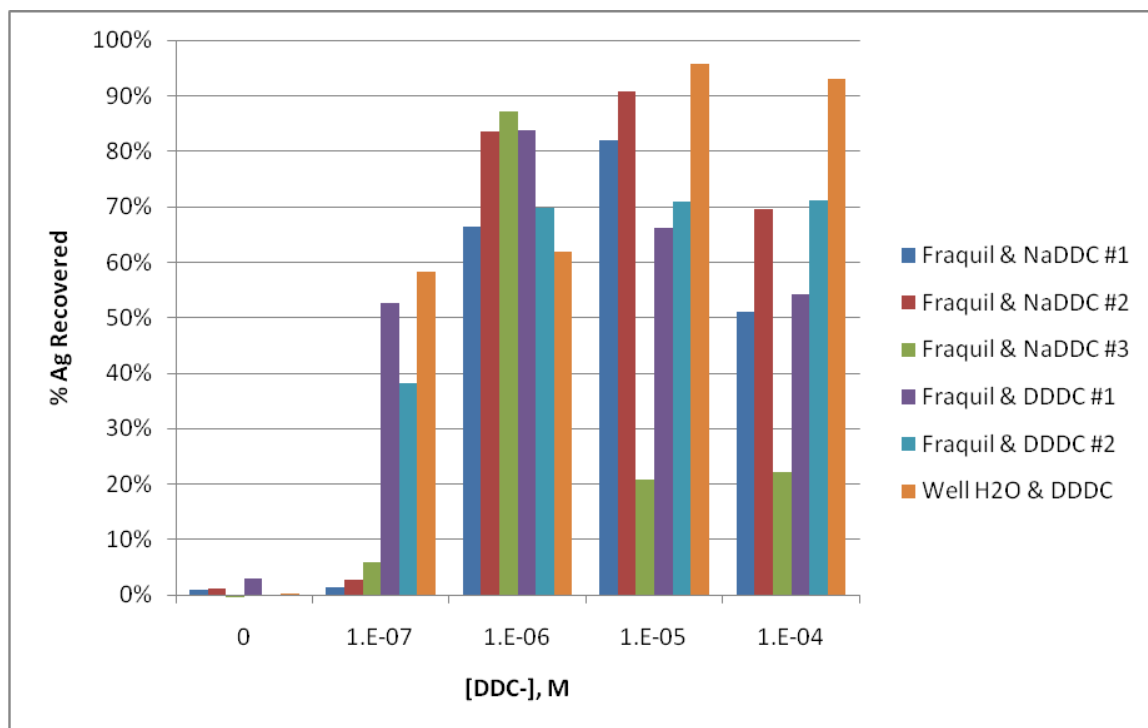
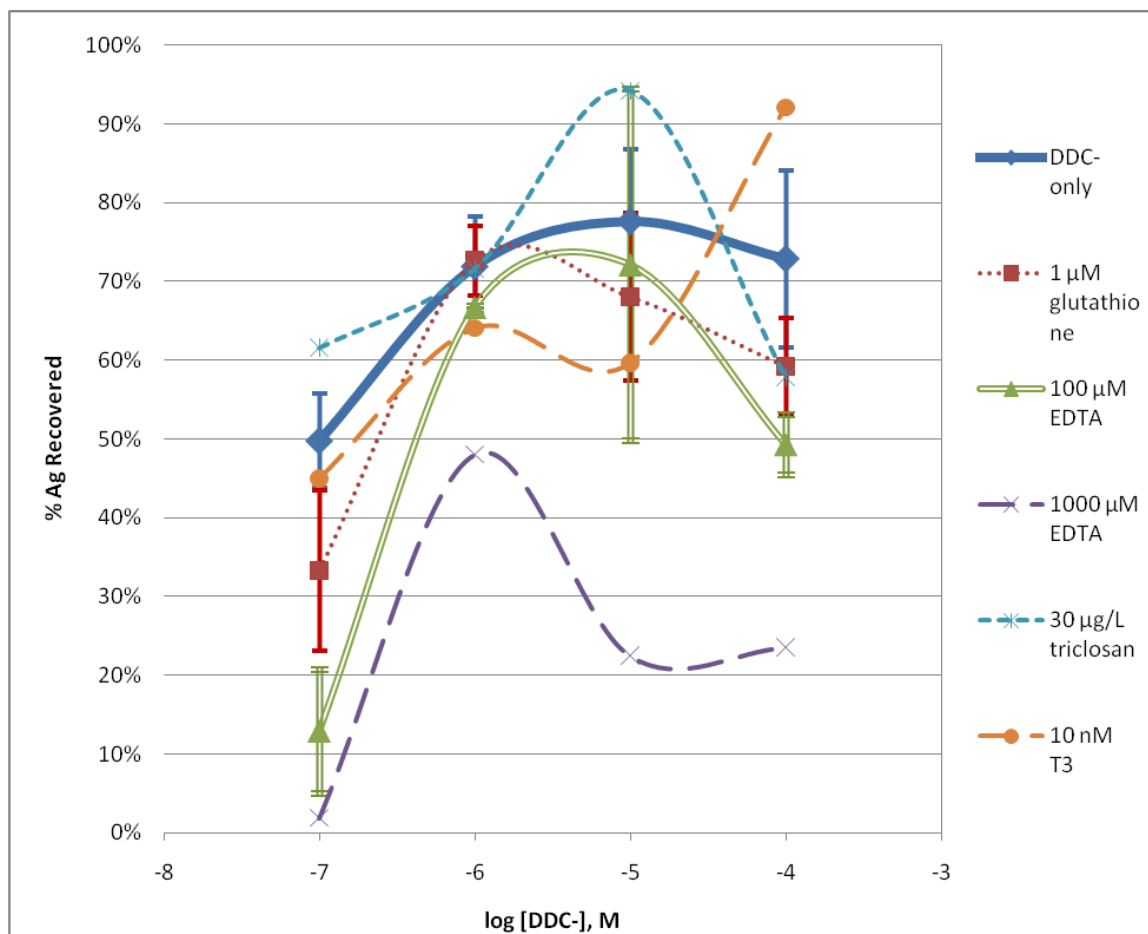


Figure 19: Comparison of effect of [DDC⁻] on Ag⁺ recovery.

Six replicates, under different experimental conditions (see legend), are shown to illustrate variability in percent recovery of 100 pM Ag⁺ during the ligand competition experiments. 10⁻⁶ M DDC⁻ seemed to give the most consistent recovery of Ag, regardless of salt (NaDDC or DDDC) or water medium (Fraquil or well water).

variation at the 10^{-5} and 10^{-4} M concentrations for both salts. 10^{-6} M DDC^- showed the least amount of variation. It was chosen as the concentration for examining speciation in the well water samples through titration with added Ag^+ . Figure 20 illustrates the results of ligand competition experiments with DDC^- and either 1 μM glutathione, 100 or 1000 μM of EDTA, 30 $\mu\text{g/L}$ (=104 nM) triclosan, and 10 nM T_3 . Both EDTA and glutathione were expected to form charged, hydrophilic complexes with Ag, as shown in Figure 13, so their behavior was expected to model what to expect from other ligands which might be complexing Ag and forming similar charged complexes. Glutathione, expected to be the strongest ligand ($\log K' = 33.15$ in seawater (Miller & Bruland, 1995)), does prevent Ag from being extracted, though in these samples, it appears to be less effective than either concentration of EDTA ($\log K' = 8.2$ in freshwater (Morel & Hering, 1993)). Ten nanomolar T_3 seems to behave with Ag in a similar fashion as EDTA and glutathione, reducing the recovery of Ag at all $[\text{DDC}^-]$ except the highest. Samples prepared with 30 $\mu\text{g/L}$ triclosan, on the other hand, seem to match or exceed Ag recovery seen in DDC^- only samples in all but the highest $[\text{DDC}^-]$, suggesting that hydrophobic complexes may be formed. The variability in percent Ag recovery using this method, as illustrated by the variability of DDC^- alone (Figure 19), highlights the need for further replicates containing T_3 or triclosan.

3.3.3 Titrations of Ag into well water used in frogSCOPE



[DDC ⁻], M	DDC ⁻ only	1 μM glutathione	100 μM EDTA	1000 μM EDTA	30 μg/L (104 nM) triclosan	10 nM T ₃
# of replicates	3	3	2	1	1	1
0	2%	2%	1%	0%	0%	0%
10 ⁻⁷	50%	33%	13%	2%	62%	45%
10 ⁻⁶	72%	73%	67%	48%	72%	64%
10 ⁻⁵	78%	68%	72%	22%	94%	60%
10 ⁻⁴	73%	59%	49%	24%	58%	92%

Figure 20: A comparison of percentage recoveries of 100 pM Ag⁺ in freshwater (Fraquil and well water) containing DDC⁻ and other competitive ligands.

Error bars represent standard error between replicate samples. 1000 μM EDTA, 30 μg/L triclosan, and 10 nM T₃ are represented by one sample replicate each.

Based on method blanks created by treating Fraquil water with 10^{-6} M DDC⁻ (see Figure 15), the MDL was 2.2 pM. If the limit of quantification (LOQ) is 3-5X the MDL, then the Ag speciation method employing 10^{-6} M DDC⁻ should allow for reasonable distinction between Ag concentrations of about 7-11 pM and higher.

Titration of Ag into well water suggests that the well water used as a basis for all frogSCOPE exposure studies contains no ligands capable of binding Ag in the experimental timeframe (about 2 hours). Without DDC⁻, there was no measurable Ag extracting from the well water, indicating that there are no ligands that would bind to Ag to form hydrophobic complexes within this analytical window (Figure 21). The titration of Ag into well water containing 10^{-6} M DDC⁻ can be interpreted as linear with a negative x-intercept, suggesting no measurable competing ligands which would bind Ag to create hydrophilic complexes in this analytical window (Figure 21).

Titration of Ag into well water containing 10^{-6} M DDC⁻ and 100 μ M EDTA shows data that can be interpreted as a straight line with a slope significantly different than that of the water without EDTA, and an x-intercept that is positive, inclusive of added and subtracted uncertainty (Figure 21, Table 4). It could also be interpreted as a concave-upwards curve, where the last four points can be fitted to a line (Figure 22). Either way it is interpreted, the titration curve for water with 100 μ M EDTA suggests the presence of a strong ligand capable of competing with DDC⁻ to create a hydrophilic complex with Ag within this analytical window. Langmuir linearization of the data based

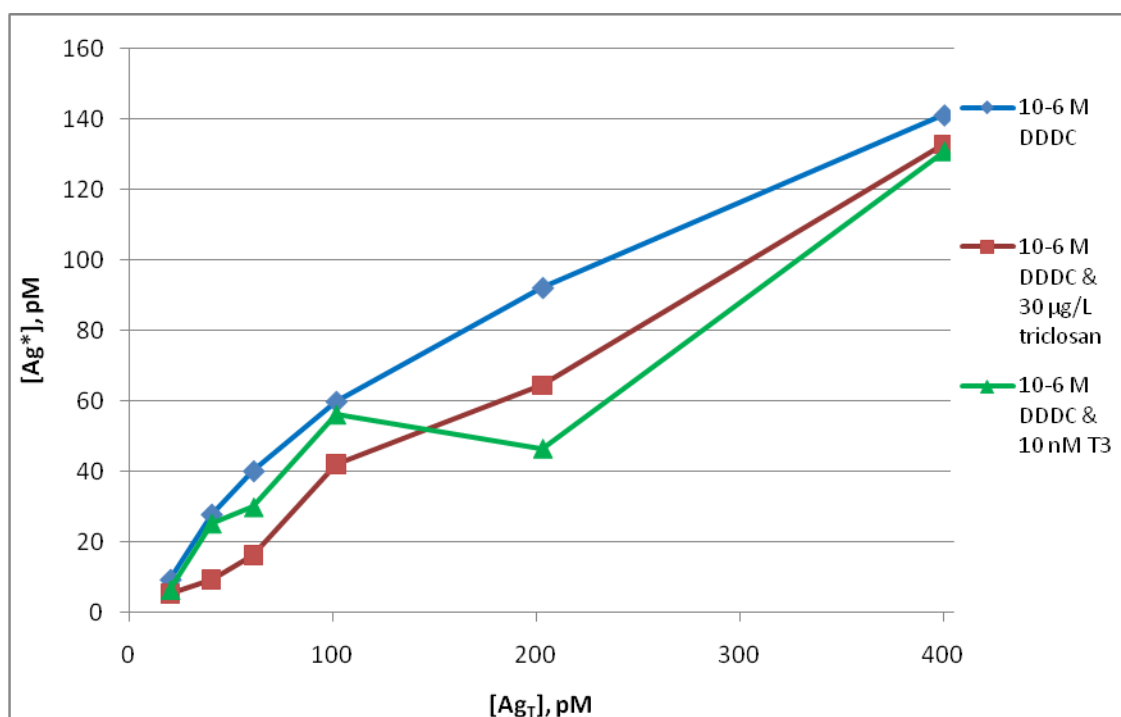
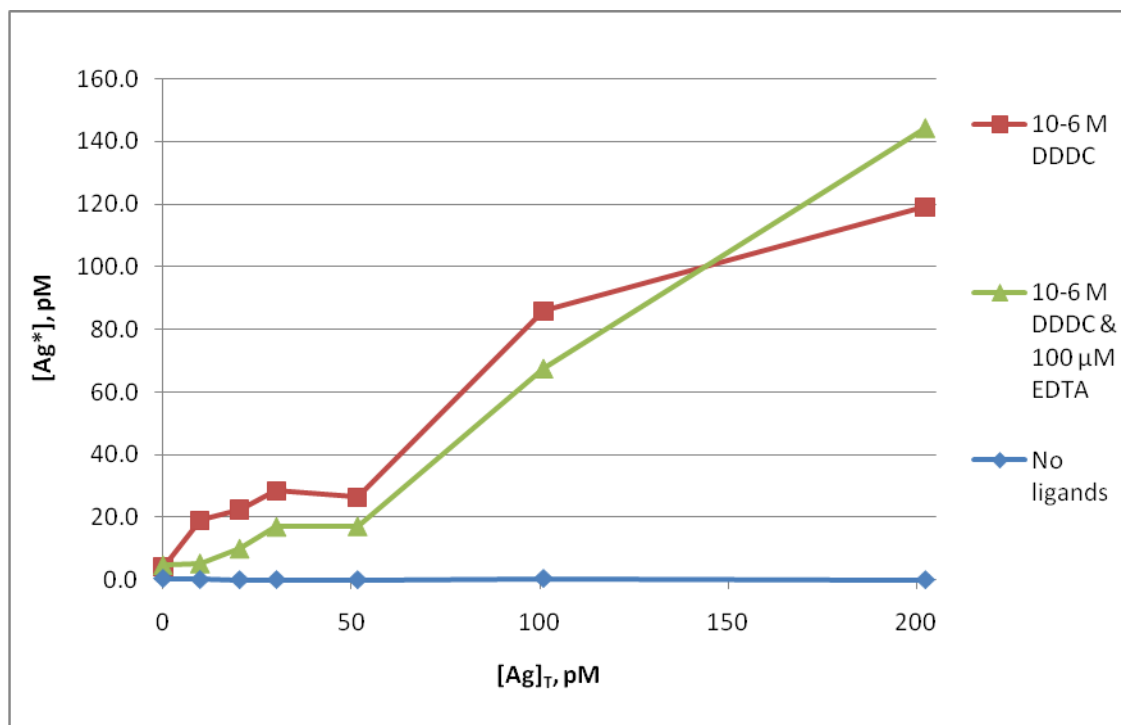


Figure 21: Titration curves for PESC well water used as a medium in frogSCOPE toxicity studies.

All titration points are represented by one sample replicate. Points are joined for clarity.

Sample	Slope	y-intercept	x-intercept	r²
Well water (1)	0.57 ± 0.06	9.7 ± 5.6	-13 ± 10	0.94
Well water & 100 μ M EDTA	0.72 ± 0.05	-4.4 ± 4.2	7.3 ± 5.5	0.98
Well water (2)	0.33 ± 0.03	17 ± 6	-43 ± 22	0.96
Well water & 30 μ g/L triclosan	0.34 ± 0.02	-1.1 ± 3.1	4.4 ± 9.0	0.99
Well water & 10 nM T ₃	0.29 ± 0.05	9.7 ± 8.9	-17 ± 32	0.91

Table 4: Regression analysis of well water titrations.

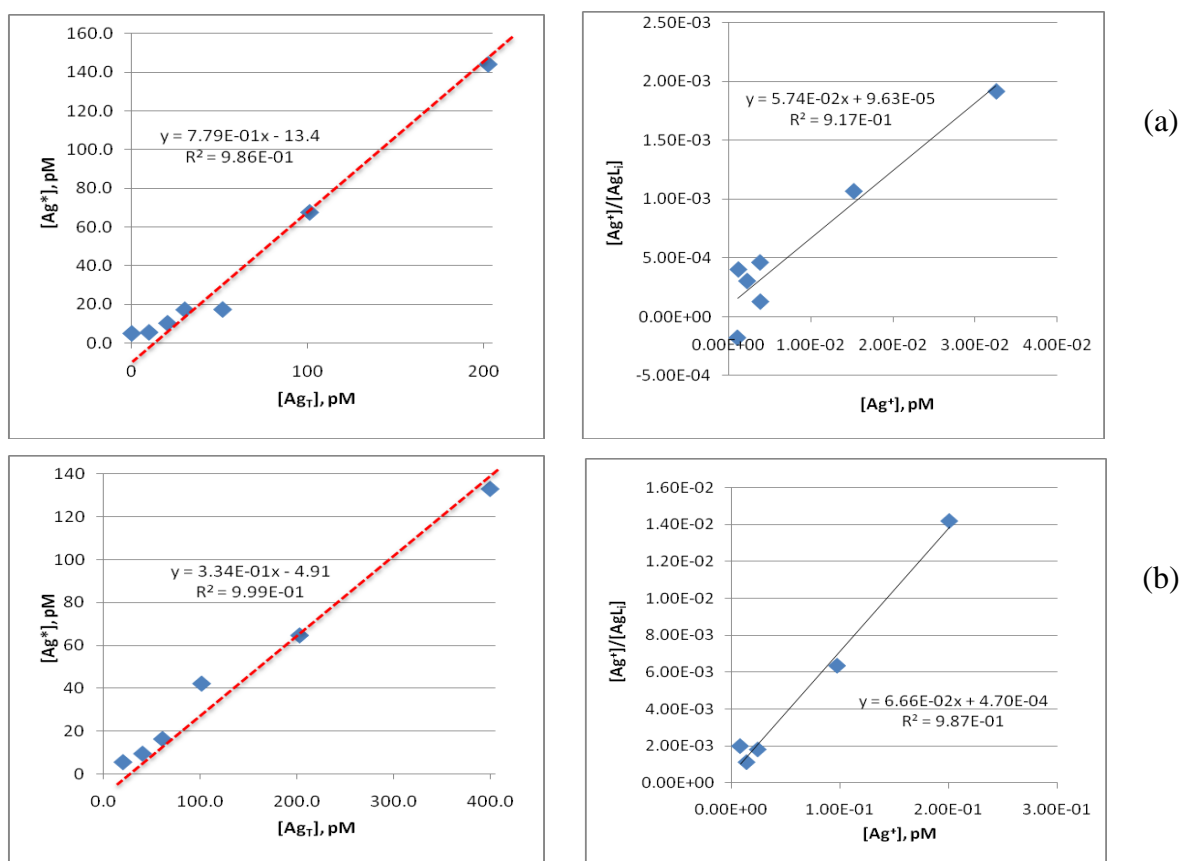


Figure 22: Titration plots (left) and Langmuir linearizations (right) for well water containing 100 μM EDTA (a) and 30 μg/L triclosan (b).

The dotted red line in each titration plot represents the slope of the line (S) used to calculate α_{Ag^*} , $[Ag^+]$, and $\Sigma[AgL_i]$ (see Appendix IV).

Sample	[Ag _T], pM	α_{AgDDC}	from Langmuir plot		Calculated α_{AgLi}^1	Comments
			[L _{T,i}], pM	log K' _{AgLi,i}		
Well H ₂ O & 100 μ M EDTA	<5	1.26×10^{-3}	17	14.8	1.04×10^{-4}	α_{AgL} is within one order of magnitude as α_{AgDDC} . An Ag-binding ligand is clearly present, but has not been fully titrated. $\alpha_{AgEDTA} = 1.58 \times 10^{-4}$ using log K = 8.2 and [EDTA] = 100 μ M.
Well H ₂ O & 30 μ g/L triclosan	<5	1.26×10^{-3}	15	14.2	2.13×10^{-3}	α_{AgL} is same order of magnitude as α_{AgDDC} . An Ag-binding ligand may be present, but this interpretation is subjective.

¹ $\alpha_{AgLi} = K'_{AgLi,i} * [L_{T,i}]$ where $[L_{T,i}] = 1/(\text{slope of Langmuir plot})$ and $K'_{AgLi,i} = 1/([L_{T,i}] * \text{y-intercept of Langmuir plot})$. α_{AgLi} cannot be calculated as defined here if $[Ag_T] > [L_{T,i}]$ (Miller&Bruland, 1994).

Table 5: Summary of information attained from Langmuir linearizations shown in Figure 22.

on the slope of the last four titration points gave a total ligand concentration $[L_{T,i}]$ of 17 pM, and a $\log K'_{AgL,i}$ of 14.8 (Figure 22, Table 5).

Titration of Ag into well water containing 10^{-6} M DDC^- and 30 $\mu\text{g/L}$ (104 nM) triclosan shows data that can be interpreted as a straight line with a slope similar to that of the water without ligand. Its x-intercept is slightly positive, inclusive of added uncertainty (Figure 21, Table 4). These attributes suggest that triclosan is not strongly competing with DDC^- within this analytical window. If it is interpreted as a concave-upwards curve, where the last four points are fitted to a line, it does not appear as curved as does the EDTA example (Figure 22). A Langmuir linearization of the data also suggests that $\log K'_{AgL,i}$ is 14.2, lower than that calculated for EDTA (Figure 22, Table 5).

Titration of Ag into well water containing 10^{-6} M DDC^- and 10 nM T_3 shows data that appears to create a straight line with a slope similar to that of the water without ligand, and an x-intercept which is only positive when the uncertainty value is added (Figure 21, Table 4). These results suggest that T_3 may not be competing with DDC^- within this analytical window.

Samples used in the medium (0.6 $\mu\text{g/L}$) and high (6.0 $\mu\text{g/L}$) Ag exposures for frogSCOPE were titrated with increasing Ag in order to observe how titration curves would appear in samples containing nanomolar ionic Ag and nanomolar nanoAg (Figure 23). Only five titration points were used for each sample and only one replicate was performed at each titration point, and several of the points needed to be excluded,

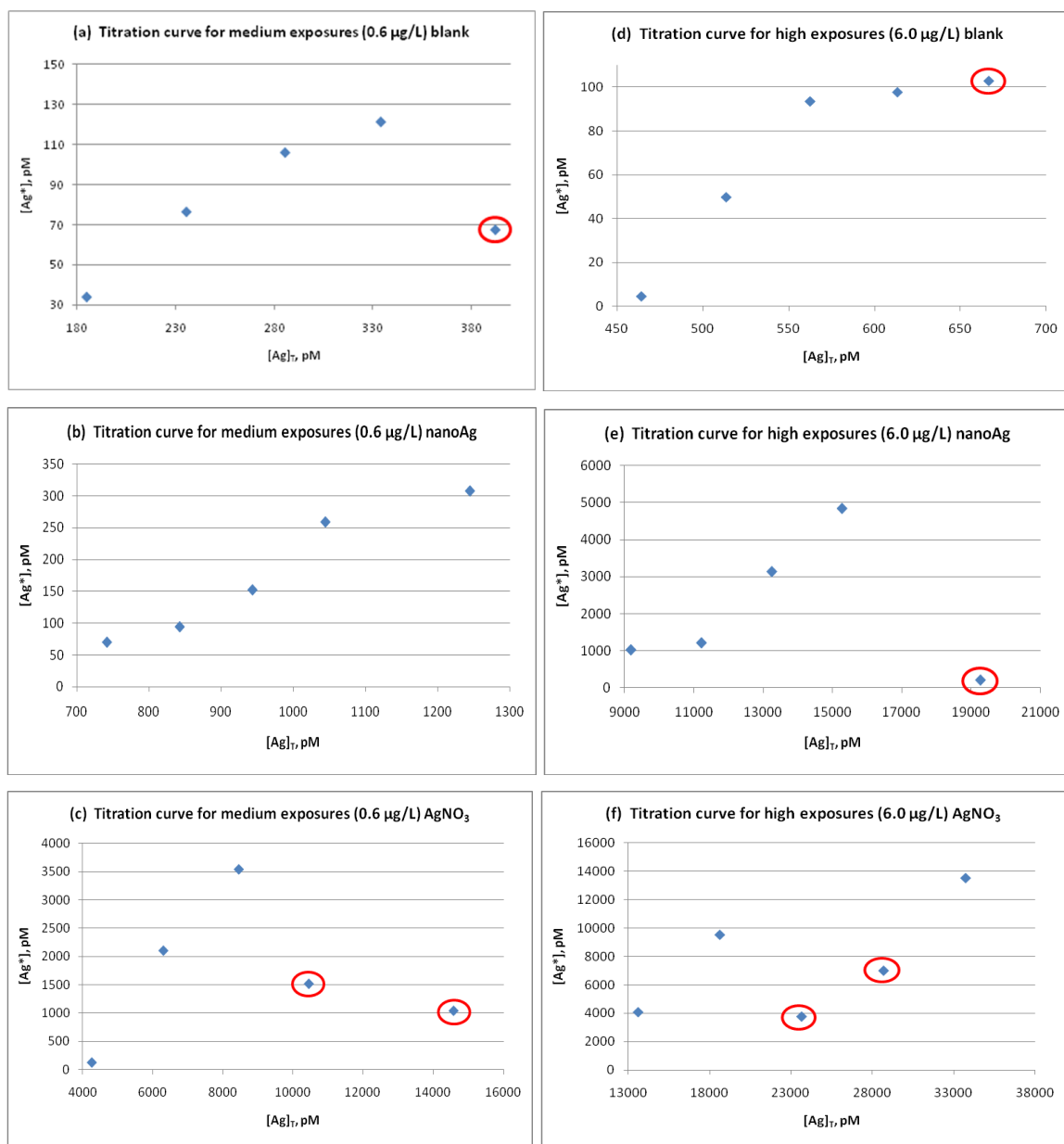


Figure 23: Titrations of frogSCOPE samples.

Waters used during medium Ag exposures (0.6 $\mu\text{g/L}$ Ag) are shown on the left; waters used during high Ag exposures (6.0 $\mu\text{g/L}$ Ag) are shown on the right. In all titrations, points circled in red were not included in regression analysis.

increasing the uncertainty in quantitative interpretation of the curves (Figure 23). Excluding data points circled in Figure 23, the data were analyzed via linear regression (Table 6). The plots for the blanks and the 0.6 $\mu\text{g/L}$ AgNO_3 do not suggest any binding ligands, and the scatter in the data points in the 6.0 $\mu\text{g/L}$ AgNO_3 curve make it difficult to make even a qualitative assessment. The shapes of the titration curves seen in both concentrations of nanoAg suggest that there might be an interaction between the added Ag^+ and nanoAg itself (Figure 23).

3.4 Discussion

3.4.1 Characterization of well water used collected from PESC

The well water collected from the Pacific Environmental Science Centre (PESC) in North Vancouver, B. C., was used as the medium for frogSCOPE tadpole Ag exposures, so full knowledge of Ag concentration and speciation was required. The well water had total dissolved (<0.2 micron filtered) Ag below the MDL for the total Ag method (Figure 18). To check for the presence of naturally-occurring ligands which could form hydrophobic complexes with Ag, well water was titrated with increasing Ag^+ but without DDC^- (Figure 21). The below-MDL response to increasing Ag^+ is solid evidence that no such ligands existed in the sample which were capable of forming hydrophobic complexes within a short time frame (the time it takes to prepare and equilibrate a sample prior to extraction, which was usually about 2 hours). To check for the presence of naturally-occurring ligands which could form hydrophilic complexes with

Sample	Slope	y-intercept	x-intercept	r²
Medium Ag Blank	0.72 ± 0.07	-97 ± 17	120 ± 21	0.99
0.6 µg/L nAg	0.52 ± 0.07	-320 ± 73	640 ± 52	0.94
0.6 µg/L AgNO ₃	0.81 ± 0.09	-3200 ± 570	4000 ± 310	0.99
High Ag Blank	0.65 ± 0.14	-290 ± 78	450 ± 23	0.91
6 µg/L nAg	0.66 ± 0.14	-5500 ± 1700	8700 ± 870	0.92
6 µg/L AgNO ₃	0.42 ± 0.16	-260 ± 3900	3400 ± 7800	0.87

Table 6: Regression analysis of frogSCOPE Ag exposure sample titrations.

Ag, well water was titrated with increasing Ag and 10^{-6} M DDC^- . The lack of concave-upwards curvature in both titrations (Figure 21), as well as the negative x-intercepts, suggest that no ligands were able to compete with DDC^- in this analytical window within a short time frame (about 2 hours). Thus, the well water used as a basis for all exposure experiments in frogSCOPE was not contributing any of its own Ag or potentially Ag-binding ligands which might skew the results.

3.4.2 Qualitative interaction of model ligands, triclosan, and T_3 with Ag

Glutathione (1 μM) and 100 μM EDTA were used as model Ag-binding ligands in qualitative experiments used to test whether or not triclosan or T_3 affected the recovery of Ag^+ by DDC^- . The EDTA concentration was selected to match α_{AgEDTA} to α_{AgDDC} within one order of magnitude; the glutathione concentration was identical to that used in seawater by Miller and Bruland (1995). To make best use of a limited timeframe, it was decided that replicate analysis should be done for these model ligands, to establish how formation of hydrophilic complexes with Ag appears analytically. Glutathione, expected to be the most strongly competitive ligand of those tested due to its highly attractive thiol (-SH) functional group and large conditional stability constant ($\log K' = 33.15$ in seawater (Miller & Bruland, 1995)), appears to keep Ag^+ in solution less effectively than it did in seawater (Miller & Bruland, 1995) or in our experiments with EDTA (Figure 20). In freshwater, glutathione would be expected to be even more competitive, so this result may reflect the age of the chemical used here rather than the different medium.

Glutathione oxidizes over time to create a dimer with a cystine linkage (S-S) through the former thiol groups. The cystine linkage formed as a result of oxidation is not as attractive to Ag^+ as a thiol, and access of the ion to the sulfur would be sterically hindered by the rest of the complex. Our glutathione was not just freshly opened, nor was it stored under nitrogen; therefore, it would have been susceptible to oxidation. EDTA, a more robust ligand in terms of stability in oxygenated solutions, is expected to be only a mildly-competitive ligand for Ag^+ based on its conditional stability constant ($\log K'_{\text{AgEDTA}} = 8.2$ in freshwater (Morel & Hering, 1993)), but it appears to keep Ag^+ from extracting into CHCl_3 at both concentrations studied (Figure 20). As predicted by Miller and Bruland (1995), EDTA seems more available for binding Ag^+ in freshwater than it would normally be in seawater, as there was less competition from major “hard” cations which bind EDTA more strongly than Ag^+ (e.g. Ca^{2+} , Mg^{2+}). These experiments suggest that wastewater effluents containing EDTA may actually bind free Ag^+ to create a charged species which remains in solution, reducing its bioavailability and therefore its potential toxicity to aquatic organisms.

The experiment involving one replicate of 10 nM T_3 at each [DDC⁻] suggests that T_3 is forming a non-extractable, hydrophilic complex with Ag, as it appears to decrease Ag^+ recovery just as do glutathione and EDTA (Figure 20). This could also mean that, by binding Ag^+ , T_3 itself becomes less bioavailable. The T_3 concentration used here was chosen on the basis of T_3 exposure concentrations used in a number of amphibian studies both before and during frogSCOPE (Hinther, Domanski, Vawda, & Helbing, 2010; Hinther et al., in review; Veldhoen et al., 2006). If it has formed a charged complex with

Ag^+ , as the experiment suggests, then T_3 would be unable to diffuse through the lipophilic plasma membrane, yet would be too large to be taken up by protein channels which would normally allow free ions into the cell (Phinney & Bruland, 1997). Less bioavailability of T_3 could be one mechanism explaining the disruption of T_3 -mediated metamorphosis observed in the presence of nanoAg and ionic Ag (Hinther et al., in review).

Like T_3 , one replicate at each $[\text{DDC}^-]$ was performed for 30 $\mu\text{g/L}$ (104 nM) triclosan. Unlike T_3 and the model ligands, triclosan appears to be forming an extractable, hydrophobic complex with Ag at certain $[\text{DDC}^-]$, creating the enhancement in recovery as compared to DDC^- alone (Figure 20). The triclosan concentration used here was chosen on the basis of the highest triclosan concentration used in prior amphibian studies to represent concentrations seen in some sewage effluents (Veldhoen et al., 2006). However, triclosan in the presence of 100 nM Ag^+ in the absence of DDC^- did not produce any extractable complexes (Figure 20). This could mean that there is an interaction among triclosan, Ag^+ , and DDC^- which create an uncharged, extractable complex. Miller and Bruland (1994) discussed the possibility of mixed-ligand complexes forming when Cu^{2+} and acetoacetate (“acac”, used in the same way as DDC^- is for Ag) interact with natural ligands, so mixed-ligand complexes containing Ag, triclosan, and DDC^- might also be a possibility. This type of interaction would only occur in natural waters if there were another ligand which could bind Ag and triclosan in a similar manner.

Being a lipophilic molecule on its own, T₃ would normally be able to diffuse through the cell membrane, but if it is coordinating with Ag⁺ to produce a charged complex, as suggested by one set of experiments, then it is possible that Ag⁺ might be reducing its bioavailability. As nanoAg releases Ag⁺ over time, this mechanism could explain the increased endocrine disruption reported by Hinthner et al. (in review). If triclosan is interacting with Ag⁺ and a third, negatively-charged species to create a hydrophobic complex, then triclosan may instead act as a vehicle to bring Ag⁺ across the cell membrane. If this type of complexation is happening in real aquatic systems between triclosan, Ag⁺, and other small organic ligands found in natural waters or in effluents, then it could possibly be a mechanism allowing more Ag⁺ to enter the cells, perhaps resulting in more toxic effects than seen with ionic Ag or nanoAg alone.

3.4.3 Interpretation of titrations of Ag into well water

Because it was not practical or desired (in terms of contamination of labware and instrument) to titrate samples out to very high concentrations of Ag⁺, all calculations performed for well water with added ligands can only be used qualitatively determine the relative strengths of the binding ligands. Based solely on the positivity of x-intercepts in the original titration plots (Table 4 and Figure 21), EDTA is the strongest of the Ag-binding ligands, having the most positive x-intercept, followed by triclosan, then followed by T₃.

The behavior of 100 μM EDTA in the titrations agrees well with what was initially seen in the ligand competition experiments (Figure 20). In the titrations, it

appeared to be behaving as a ligand which would create a hydrophilic complex with Ag, thereby keeping it from being extracted into the CHCl_3 and reducing the Ag detected by ICP-MS (Figure 21). With the exception of the highest $[\text{Ag}^+]$, each titration point experienced a lower Ag recovery than the corresponding DDC^- -alone scenario. The great difference between the slope of the EDTA curve and the no-ligands curve, along with the low total ligand concentration $[\text{L}_{\text{T},i}]$ and the higher-than-literature conditional stability constant (K'_{AgEDTA}) calculated in the Langmuir plot both show that the EDTA has not been fully titrated by the added Ag^+ . Fortunately, full titration of EDTA and accurate quantification of these parameters was not the goal of the experiment: instead, the titration with EDTA was meant to serve as a model of a strong Ag-binding ligand to which the behavior of triclosan and T_3 could be compared.

Initially, the behavior of 10 nM T_3 in the titrations also seems to support what was seen in the ligand competition experiments (Figure 20). Each titration point experienced a lower Ag recovery than the corresponding DDC^- -alone scenario. However, the slope of all data points in this titration is not significantly different from that of well water without added ligands (Figure 21, Table 4), suggesting that there is no significant interaction within this analytical window. To better establish the complexing behavior of T_3 and Ag^+ , the titration with 10 nM T_3 should be repeated at a different analytical window, using a lower $[\text{DDC}^-]$.

The behavior of 30 $\mu\text{g/L}$ triclosan in the titrations seems to contradict what was initially seen in the ligand competition experiments (Figure 20). In the titrations, it

seemed to reduce the extraction efficiency, compared to well water alone (Figure 21). Although there might be slight curvature at the low end of the titration curve, the slope of all data points in this titration is not significantly different from that of well water without added ligands (Figure 21, Table 4), suggesting that there is no significant interaction within this analytical window. Furthermore, the initial ligand competition results suggest no significant difference in extractability between 10^{-6} M DDC^- alone and DDC^- with triclosan (Figure 20). Because of the small curvature, a Langmuir linearization was carried out on this titration to compare triclosan to EDTA (Figure 22, Table 5). Even with incomplete titration of both ligands, the Langmuir plots give us a rough estimate of relative strength of the ligands using the K' values. K'_{AgEDTA} is greater than $K'_{\text{AgTriclosan}}$, indicating that the Ag-EDTA complex is more stable than that which may be forming with triclosan. The only way to be certain of the interaction between Ag and triclosan would be to repeat the titration with two different analytical windows, at lower and higher $[\text{DDC}^-]$. Using both a higher and a lower analytical window might reveal if there is any interaction to form hydrophilic complexes at lower $[\text{DDC}^-]$, or if there is any interaction to form hydrophobic Ag-triclosan complexes at higher $[\text{DDC}^-]$.

In order to titrate samples used in the medium ($0.6 \mu\text{g/L}$) and high ($6.0 \mu\text{g/L}$) Ag exposures for frogSCOPE, the method scaled down both sample and reagent volumes (see Appendix III, Tables 8-10). These samples were collected from the aquariums used to house tadpoles for exposure studies at PESC, with well water containing either zero, $0.6 \mu\text{g/L}$, or $6.0 \mu\text{g/L}$ AgNO_3 or nanoAg. As the samples were taken from the aquariums at “Day Zero” in the exposure studies, there should not have been time for the tadpoles or

algae to contribute organic ligands to the well water; therefore, the results seen should entirely reflect the well water and the added Ag species. In both blank samples, there was no evidence of strong Ag-binding ligands (Figure 23). In both AgNO₃ samples, two data points had to be disregarded, making it difficult to make any definitive conclusions about speciation; however, because the blanks are the same as the well water we titrated in Figure 21 and neither suggested any measurable Ag-binding ligands, it is likely that Ag⁺ is the dominant species in these samples. In both nanoAg samples, there was a curvature in the titration data which might illustrate an interaction between the nanoAg already present and the Ag⁺ being added (Figure 23). As the nanoAg used was capped by a proprietary carboxyl-rich coating to make the particles water-soluble, there may be interaction of Ag⁺ with the coating. Because the samples were “Day Zero”, with no other Ag-binding ligands present, nanoAg was likely the dominant Ag species in these particular samples. To confirm this assumption and explore the potential of capped nanoAg particles interacting with Ag⁺, a ligand competition experiment similar to that carried out for triclosan and T₃ (Figure 20) could be carried out, using nanoAg as the potential ligand.

3.5 Conclusions

Using CLE-SE and the method of standard additions, well water collected at PESC and used as a medium for frogSCOPE toxicity studies was found to have near-quantification limits Ag levels; therefore, the contribution of Ag from the well water was negligible in all Ag exposure studies. The well water also contained no Ag-binding

ligands capable of reacting with Ag^+ in a short time frame; therefore, the major species in those exposure solutions containing AgNO_3 will be ionic Ag. The variation in recoveries seen in both the total Ag and Ag speciation methods highlight the need for replicate analysis in order to make accurate conclusions from the data. In our experiments, timelines dictated that replicates be performed only in cases where we believed them essential (e.g. method detection limits; establishing behaviour of model ligands).

The Ag speciation method developed by Miller and Bruland (1995) can be applied to mixtures of Ag and suspected binding ligands in order to better understand the possible interactions of species which might be present in complex wastewater streams, and to help predict the possible effects of these interactions on aquatic organisms. The free ion model of toxicity states that the most toxic species to organisms is the free ion, but ions bound to ligands which produce hydrophobic complexes may also increase toxicity by allowing the metals to directly cross the cell membrane into the cells (Hudson, 2005; Phinney & Bruland, 1997). In the ligand competition experiments involving adding varying DDC^- concentrations to a system containing Ag and either glutathione or EDTA, both chemicals reduced Ag extraction efficiency in freshwater, producing charged complexes which could not be extracted into CHCl_3 . If formed in natural aquatic systems, this type of complex would be unable to pass into the cells through either passive diffusion through the lipophilic cell membrane, or through the tiny protein channels through the cell membrane which provide access to small ions (Phinney & Bruland, 1997; Ratte, 1999). The presence of either thiol-containing amino acids or

EDTA in wastewater effluents may therefore have a protective effect on aquatic organisms, reducing the toxicity of Ag.

In similar ligand competition experiments with systems containing Ag and either triclosan or thyroid hormone 3,3',5-triiodothyronine (T_3), T_3 also reduced extraction efficiency, suggesting the creation of charged complexes. Triclosan, on the other hand, increased extraction efficiency relative to DDC^- alone, suggesting that perhaps there is an interaction between triclosan, Ag^+ , and DDC^- . In titrations with Ag, EDTA visibly behaved as a strong binding ligand within the analytical window, while T_3 and triclosan did not show detectable coordination with Ag. To better constrain these interactions, the titrations with T_3 and triclosan should be repeated using different analytical windows, and the results compared to the initial ligand competition experiments.

This is the first time that CLE-SE has been reported for samples containing nanoAg. The most interesting result from these titrations is a potential interaction between nanoAg and added Ag^+ , which should be investigated further by conducting ligand competition experiments.

3.6 References

Adams, N. W. H., & Kramer, J. (1999a). Determination of silver speciation in wastewater and receiving waters by competitive ligand equilibration/solvent extraction. *Environmental Toxicology and Chemistry*, 18(12), 2674.

- Ahn, K. C., Zhao, B., Chen, J., Cherednichenko, G., Sanmarti, E., Denison, M. S., et al. (2008). In vitro Biologic Activities of the Antimicrobials Triclocarban, Its Analogs, and Triclosan in Bioassay Screens: Receptor-Based Bioassay Screens. *Environmental Health Perspectives*, *116*(9), 1203-1210.
- Bruland, K. W., Coale, K. H., & Mart, L. (1985). Analysis of seawater for dissolved cadmium, copper, and lead: an intercomparison of voltammetric and atomic absorption methods. *Marine Chemistry*, *17*, 285-300.
- Bruland, K. W., Franks, R. P., Knauer, G. A., & Martin, J. H. (1979). Sampling and analytical methods for the determination of copper, cadmium, zinc, and nickel at the nanogram per liter level in sea-water. *Analytica Chimica Acta*, *105*(1), 233-245.
- Croot, P. L., & Johansson, M. (2000). Determination of Iron Speciation by Cathodic Stripping Voltammetry in Seawater Using the Competing Ligand 2-(2-Thiazolylazo)-p-cresol (TAC). *Electroanalysis*, *12*(8), 565-576.
- Hinther, A., Domanski, D., Vawda, S., & Helbing, C. C. (2010). C-fin: A cultured frog tadpole tail fin biopsy approach for detection of thyroid hormone-disrupting chemicals, *Environmental Toxicology and Chemistry* (Vol. 29, pp. 380-388).
- Hinther, A., Vawda, S., Skirrow, R. C., Veldhoen, N., Collins, P., Cullen, J. T., et al. (in review). Nanometals induce stress and alter thyroid hormone action in amphibia at or below North American water quality guidelines.
- Hudson, R. J. M. (2005). Trace metal uptake, natural organic matter, and the free-ion model. *J. Phycol.*, *41*, 1-6.

- Kinrade, J. D., & Van Loon, J. C. (1974). Solvent extraction for use with flame atomic absorption spectrometry. *Analytical Chemistry*, 46(13), 1894-1898.
- Miller, L. A., & Bruland, K. W. (1994). Determination of copper speciation in marine waters by competitive ligand equilibration/liquid-liquid extraction: an evaluation of the technique. *Analytica Chimica Acta*, 284, 573-586.
- Miller, L. A., & Bruland, K. W. (1995). Organic Speciation of Silver in Marine Waters. *Environmental Science & Technology*, 29, 2616-2621.
- Morel, F. M. M., & Hering, J. G. (1993). *Principles and Applications of Aquatic Chemistry*. New York, NY: John Wiley & Sons, Inc.
- Phinney, J. T., & Bruland, K. W. (1997). Trace metal exchange in solution by the fungicides Ziram and Maneb (dithiocarbamates) and subsequent uptake of lipophilic organic zinc, copper, and lead complexes into phytoplankton cells. *Environmental Toxicology and Chemistry*, 16(10), 2046-2053.
- Ratte, H. T. (1999). Bioaccumulation and toxicity of silver compounds: a review. *Environmental Toxicology and Chemistry*, 18(1), 89-108.
- Rue, E. L., & Bruland, K. W. (1995). Complexation of iron(III) by natural organic ligands in the Central North Pacific as determined by a new competitive ligand equilibration/adsorptive cathodic stripping voltammetric method. *Marine Chemistry*, 50, 117-138.
- Ruzic, I., & Nikolic, S. (1982). The influence of kinetics on the direct titration curves of natural water systems -- theoretical considerations. *Analytica Chimica Acta*, 140(1), 331-334.

- van den Berg, C. M. G. (1984). Determination of copper in sea water by cathodic stripping voltammetry of complexes with catechol. *Analytica Chimica Acta*, *164*, 195-207.
- Veldhoen, N., Skirrow, R. C., Osachoff, H., Wigmore, H., Clapson, D. J., Gunderson, M. P., et al. (2006). The bactericidal agent triclosan modulates thyroid hormone-associated gene expression and disrupts postembryonic anuran development. *Aquatic Toxicology*, *80*(3), 217-227.
- Wytenbach, A., & Bajo, S. (1975). Substoichiometric extraction of 14 metals from sulfuric, hydrochloric, and perchloric acids with zinc diethyldithiocarbamate by radiometric extractive titration. *Analytical Chemistry*, *47*(1), 2-7.
- Zorrilla, L. M., Gibson, E. K., Jeffay, S. C., Crofton, K. M., Setzer, W. R., Cooper, R. L., et al. (2009). The Effects of Triclosan on Puberty and Thyroid Hormones in Male Wistar Rats. *Toxicol. Sci.*, *107*(1), 56-64.

Chapter 4: Conclusions

The new method for total silver (Ag) in natural water samples, which employs cadmium sulfide quantum dots (CdS QDs) as probes for Ag, did not appear analytically useful over the range reported in the literature (Wang et al., 2008). Whether the QDs were synthesized from starting materials, or were purchased commercially and then functionalized with mercaptoacetic acid, the results were the same: no consistent, analytical enhancement, or quenching, of CdS synchronous fluorescence at 304 nm with increasing Ag ion (Ag^+) concentration. It seemed likely that inconsistent sizes of particles in the CdS solutions prepared could be a factor in the inconsistent enhancement and quenching observed. As a result, well water samples collected from the frogSCOPE Ag exposures were not analyzed for total Ag using this method, nor could they be compared to the total Ag results obtained by ICP-MS at the Pacific Environmental Science Centre (PESC) in North Vancouver, B.C. Having shown little promise in distinguishing $[\text{Ag}^+]$ in the nanomolar range, the method was not further tested for analytical application in the pM Ag^+ range. To better evaluate the method's analytical response, it is recommended that either the synthesis or functionalization of commercial CdS QDs be investigated and modified in ways which will obtain uniform QD sizes. With the ongoing expansion of commercially-available CdS QDs with different capping agents, it is recommended that further studies select commercial QDs functionalized with water-soluble chemicals, especially those containing thiols which may allow for selective sensing of Ag^+ .

On the other hand, competitive ligand exchange-solvent extraction (CLE-SE) appeared to be a useful tool for assessing total dissolved Ag content and speciation in water samples. Developed by Bruland et al. (1979) for pre-concentration and extraction of low-level Cu, Cd, and Zn from seawater, the method appears to have variable recoveries well below 100% of picomolar Ag in solution; however, quantitative Ag data can still be obtained by coupling it to the method of standard additions (Flegal, Sañudo-Wilhelmy, & Scelfo, 1995; Rivera-Duarte, Flegal, Sañudo-Wilhelmy, & Véron, 1999) or isotope dilution (Kramer, 2006). Well water obtained at the Pacific Environmental Science Centre (PESC) and used as a basis for the toxicity studies involving ionic and nanoAg on bullfrog tadpoles for the frogSCOPE program was characterized for total Ag (employing standard additions) and the presence of natural Ag-binding ligands through CLE-SE. The water was found to have near-quantitative limits Ag levels and no appreciable binding ligands capable of creating an organic-extractable (and therefore bioavailable) hydrophobic complex or a non-extractable hydrophilic complex in a short time frame. Therefore, the water itself should not have made any contribution to the results seen in the frogSCOPE toxicity studies.

It appears that CLE-SE can be applied not only to examine Ag speciation in natural waters, but also to qualitatively evaluate the binding potential of organic ligands. CLE-SE could find a wider application in helping understand the interaction between low-level Ag⁺ and suspected metal-binding ligands which could mitigate or enhance its toxicity. In both ligand exchange experiments and titrations, EDTA, a powerful metal chelator, exhibited strong Ag-binding behavior in freshwater that would not be possible

in seawater due to the presence of other metal cations. This suggest that the presence of EDTA in freshwaters containing Ag^+ could create hydrophilic species which would help reduce the amount of free Ag^+ , thereby reducing its toxicity to aquatic species, as per the free ion model of toxicity (Hudson, 2005; Phinney & Bruland, 1997).

CLE-SE revealed that both 30 $\mu\text{g/L}$ triclosan and 10 nM thyroid hormone 3,3',5-triiodothyronine (T_3) may be having some weak Ag-binding interactions. In ligand equilibration experiments, T_3 behaved as EDTA and glutathione, suggesting that there is a binding interaction between Ag^+ and T_3 which may create a hydrophilic complex incapable of crossing the cell membrane. Triclosan, on the other hand, seemed to enhance Ag recovery over these same concentrations of competing ligand (DDC^-), suggesting the possibility of a hydrophobic triclosan-Ag- DDC^- complex. If this behavior happens in aquatic samples with another naturally-occurring (or man-made, in the case of effluents) small, negatively-charged ligand, then it could be a mechanism for allowing Ag to cross the cell membrane and exert increased toxic effects on the cell.

Titration increasing Ag^+ into samples containing a fixed DDC^- concentration ($[\text{DDC}^-]$) and either 30 $\mu\text{g/L}$ triclosan or 10 nM T_3 provided a second way to explore the interaction within a fixed analytical window. Both samples suggested no visible complexation with Ag^+ , although extraction efficiency was somewhat reduced compared to DDC^- alone. Further studies should be done at different analytical windows to better evaluate this effect, because for triclosan, the reduced extraction efficiency seem to contradict those initially observed in the ligand competition experiments with varying

[DDC⁻]. What can be said qualitatively from these titrations is that both triclosan and T₃ demonstrated less binding affinity for Ag⁺ than EDTA within this analytical window.

With frog metamorphosis dependent on the presence of T₃, the weak interaction between Ag⁺ and T₃ observed in the ligand competition experiments could be a reason for the observation that both ionic Ag and the highest-concentration nanoAg disrupted T₃-mediated cell signaling in tadpoles (Hinther et al., in review). The presence of thyroid hormone T₃ induces the expression of one of its receptors, TR β , which then produces transcripts (m-RNA) to express proteins signaling the onset of metamorphosis in amphibians (Veldhoen et al., 2006). T₃ can actually increase expression of TR β 10-fold (C. C. Helbing, personal communication), and it is this increase in expression of TR β which triggers metamorphosis from tadpole to frog (Veldhoen et al., 2006). Preliminary data from frogSCOPE suggests that the presence of T₃ may modulate how Ag⁺ and nanoAg are affecting the organism (Hinther et al., in review). Low concentrations of nanoAg, in the presence of T₃, seemed to increase TR β transcripts (Hinther et al., in review), which is consistent with the observation that low nanoAg concentrations seem to accelerate tail and leg development in tadpoles (C. C. Helbing, personal communication). However, higher concentrations of nanoAg, in the presence of T₃, seemed to decrease TR β transcripts, as did ionic Ag (Hinther et al., in review). The similarity in behavior of the high-concentration nanoAg (which releases more Ag⁺) and ionic Ag in the presence of T₃ suggest that this particular response is due to Ag⁺, rather than a distinct effect of nanoAg. The decrease in TR β transcripts suggests an interaction between Ag⁺ and T₃ which is preventing T₃ from reaching the amphibian cell; our experiments seem to

corroborate this conclusion. As less Ag^+ was extractable in the presence of 10 nM T_3 , it was likely forming a charged complex with T_3 , thus turning the lipophilic T_3 molecule into a hydrophilic complex which would no longer be capable of diffusing across the lipophilic cell membrane. So, in this case, perhaps it is not Ag^+ entering the cells to create a toxic effect; instead, it may be Ag^+ binding T_3 to prevent it from reaching the cell nucleus and inducing expression of its receptor, $\text{TR}\beta$.

At the moment, all that can be said with certainty about triclosan is that it seems to have the potential to bind Ag^+ , but the type of complex formed by this association needs further investigation. Further titration experiments employing different analytical windows are required in order to better examine whether or not it is more likely to create hydrophobic or hydrophilic complexes with Ag^+ . If hydrophobic complexes involving triclosan, Ag^+ , and a third small ligand are happening in-situ, then this might serve as a mechanism for delivering more Ag^+ into the cells, thus increasing the ion's bioavailability and therefore its toxicity. If hydrophilic complexes involving triclosan and Ag^+ are forming, this should reduce Ag^+ bioavailability and toxicity, while at the same time reducing the bioavailability of triclosan, since it would have been transformed from a hydrophobic compound capable of passive diffusion through the lipophilic cell membrane into a hydrophilic complex. If ionic Ag is involved in a synergistic thyroid hormone disruption effect when both triclosan and nano Ag are present, then only the former case of forming hydrophilic complexes supports this effect. Clearly, more experiments with triclosan and Ag^+ are needed.

CLE-SE could become an important tool in aquatic toxicology studies involving low-level Ag^+ and organic molecules found in nature and in wastewater effluents. Understanding Ag toxicity in freshwater is linked to understanding Ag speciation, because without high chloride levels Ag^+ has much more potential to be influenced by the presence of organic ligands in freshwater than it has in seawater (Adams & Kramer, 1999a; Miller & Bruland, 1995). The free ion model of toxicity states that the proportion of free metals ions available to cells influences toxicity (Hudson, 2005; Phinney & Bruland, 1997), and in freshwater, there is much less opportunity for free Ag^+ to bind with chloride to form the low-toxicity AgCl_x^- species (Ratte, 1999). As a result, a picture of ligands present in freshwater as well as an understanding of how they bind Ag^+ is very important to understanding toxicity. Complexation of metal ions with organic ligands to create hydrophilic complexes which remain in solution reduces metal toxicity (Choi et al., 2008; Ratte, 1999), while complexation to form hydrophobic complexes capable of passive diffusion across cell membranes increases metal toxicity (Phinney & Bruland, 1997). The types of experiments carried out in Chapter 3 can be extended to other types of freshwater with higher natural dissolved or particulate organic matter, first to assess the “baseline” presence of Ag-binding ligands and then to observe the “true” effect of the addition of any chemicals of concern. The apparent utility of CLE-SE in studying interactions between Ag^+ and organic ligands might be extended to mixtures including low-levels of additional metal ions and ligands typical in wastewater effluents, helping scientists gain important insight on the potential impact of these mixtures on aquatic organisms.

4.1 References

- Adams, N. W. H., & Kramer, J. (1999a). Determination of silver speciation in wastewater and receiving waters by competitive ligand equilibration/solvent extraction. *Environmental Toxicology and Chemistry*, 18(12), 2674.
- Choi, O., Deng, K. K., Kim, N.-J., Ross Jr., L., Surampalli, R. Y., & Hu, Z. (2008). The inhibitory effects of silver nanoparticles, silver ions, and silver chloride colloids on microbial growth. *Water Research*, 42, 3066-3074.
- Flegal, A. R., Sañudo-Wilhelmy, S. A., & Scelfo, G. M. (1995). Silver in the Eastern Atlantic Ocean. *Marine Chemistry*, 49(4), 315-320.
- Hinther, A., Vawda, S., Skirrow, R. C., Veldhoen, N., Collins, P., Cullen, J. T., et al. (in review). Nanometals induce stress and alter thyroid hormone action in amphibia at or below North American water quality guidelines.
- Hudson, R. J. M. (2005). Trace metal uptake, natural organic matter, and the free-ion model. *J. Phycol.*, 41, 1-6.
- Kramer, D. (2006). *An Exploration of the Marine Silver Cycle in Coastal and Open Ocean Environments of the North Pacific*. M.Sc. Thesis, University of Victoria, Victoria, B.C.
- Miller, L. A., & Bruland, K. W. (1995). Organic Speciation of Silver in Marine Waters. *Environmental Science & Technology*, 29, 2616-2621.
- Phinney, J. T., & Bruland, K. W. (1997). Trace metal exchange in solution by the fungicides Ziram and Maneb (dithiocarbamates) and subsequent uptake of

lipophilic organic zinc, copper, and lead complexes into phytoplankton cells.

Environmental Toxicology and Chemistry, 16(10), 2046-2053.

Ratte, H. T. (1999). Bioaccumulation and toxicity of silver compounds: a review.

Environmental Toxicology and Chemistry, 18(1), 89-108.

Rivera-Duarte, I., Flegal, A. R., Sañudo-Wilhelmy, S. A., & Véron, A. J. (1999). Silver

in the far North Atlantic Ocean. *Deep Sea Research Part II: Topical Studies in*

Oceanography, 46(5), 979-990.

Veldhoen, N., Skirrow, R. C., Osachoff, H., Wigmore, H., Clapson, D. J., Gunderson, M.

P., et al. (2006). The bactericidal agent triclosan modulates thyroid hormone-associated gene expression and disrupts postembryonic anuran development.

Aquatic Toxicology, 80(3), 217-227.

Wang, L., Liang, A.-N., Chen, H.-Q., Liu, Y., Qian, B.-b., & Fu, J. (2008). Ultrasensitive

determination of silver ion based on synchronous fluorescence spectroscopy with

nanoparticles. *Analytica Chimica Acta*, 616(2), 170-176.

Appendix I: Cleaning protocols for equipment used in trace silver analysis

AI.i Definition of “clean”

The terms “trace-metal clean” and “acid-cleaned” have been used interchangeably throughout this thesis to indicate that the cleaning methods used for LDPE bottles and caps, all PP volumetric ware, PP snap-top vials, Teflon-FEP equipment, and glassware were based on the GEOTRACES protocols (Cutter et al., 2007). These cleaning protocols were employed for equipment used in both fluorometric and organic extraction methods.

All cleaning was carried out in a designated laminar flow hood inside a Class 100 lab space. Note that cleaning protocols described here are powerful and thus NOT appropriate for materials which have painted-on labels, such as the outsides of glass beakers or the label spots on some plastic volumetric tubes. Such equipment may be acid-cleaned internally only, not fully submerged.

AI.ii Glassware, low-density polyethylene (LDPE), and polypropylene (PP)

Glassware, LDPE, and PP used in all analyses were treated as follows before use. First, they were rinsed in reverse osmosis (RO) water 4X before submerging in a detergent bath (FisherBrand Versa-Clean Concentrate) for 1 week (or 1 day at 60 °C). Labware removed from the detergent were rinsed 4X with RO water before being rinsed

3X with milli-Q (MQ) water and then submerged into a bath containing 6M reagent-grade HCl (Anachemia). Labware were left in this bath for 1 month at room temperature or 1 week at 60 °C. Once removed from HCl, labware were rinsed 3X with MQ, submerged in MQ overnight, and then rinsed 3X more before being dried in a designated laminar flow hood. Plastic bottles and labware were either individually double-bagged or stored together in a designated acid-cleaned, Rubbermaid-type sealed storage tote; glassware was stored together in a separate tote.

AI.iii Teflon-FEP bottles, sample vials, and separatory funnels

Teflon-FEP bottles used in organic extraction analyses were rinsed in RO water 4X before submerging in a detergent bath for 1 week, or 1 day at 60 °C. Bottles removed from the detergent were rinsed 4X with RO water before being rinsed 3X with MQ and then submerged into a bath containing 6M reagent-grade HCl. Bottles were left in this bath for 1 month at room temperature or 1 week at 60 °C. Once removed from HCl, bottles were rinsed 3X with MQ and filled with about 100 mL concentrated trace-metal grade HCl (Anachemia). Bottles were “polished” with this HCl by swirling at least once per day over the course of one month; funnels were completely filled with HCl and stored like this for two weeks. Upon completion of polishing step, bottles were rinsed 4X with MQ, submerged in MQ overnight, and then rinsed 4X more before being filled with MQ and bagged.

15-mL Teflon-FEP sample vials used in the organic extractions were initially treated as above; however, early in the work a serious silver contamination issue arose following a series of high samples. In subsequent analyses, it was determined that a more powerful acid bath was required to fully remove silver from the Teflon. Instead of the 6M HCl bath and conc HCl polishing prescribed by GEOTRACES, Teflon-FEP vials received 2 weeks (or 2 days on heat) in a 50% aqua regia bath made from 4 parts MQ water, 3 parts reagent-grade HCl, and 1 part reagent-grade HNO₃ (Anachemia). Following this bath, vials were rinsed 3X with MQ, submerged in MQ overnight, and then rinsed 3X more before being filled with MQ water and stored double-bagged.

In between experiments, Teflon-FEP separatory funnels followed the cleaning protocol of the 15-mL Teflon FEP vials described above. In between samples and standards within one particular experiment (i.e. with similar [Ag⁺]), Teflon-FEP funnels were rinsed 4X with MQ, “polished” overnight using about 10 mL of 1% ultra-pure HNO₃ (made from Seastar Baseline concentrated HNO₃), rinsed 4X with MQ again, and then filled with MQ for at least 1 hour prior to the next batch of extractions. This is referred to as a “clean funnel”, so as to distinguish it from “acid-cleaned”.

AI.iv References

Cutter, G., Andersson, P., Codispoti, L., Croot, P., Francois, R., Lohan, M. C., et al. (2007). *Sampling and Sample-handling Protocols for GEOTRACES-related IPY Cruises, 2007-2008*. Retrieved January 22, 2010, from http://www.geotraces.org/documents/GEOTRACESIPYProtocols-Final_000.pdf

Appendix II: Fluorometric Method for Total Silver using CdS Quantum Dots

AII.i Experiments involving synthesized quantum dots (QDs)

All solutions were stored in acid-cleaned LDPE bottles, unless otherwise noted. Volumetric solution preparation involved the use of polypropylene (PP) volumetric ware. Small volumes were administered by various Eppendorf pipettes. Following Wang et al. (2008), to make each silver sample would require a recipe of 500 microlitres of CdS solution, as prepared, plus 1.00 mL of PBS buffer, and 8.50 mL of silver sample, for a total volume of 10.00 mL.

AII.i.i Synthesis of CdS QDs via controlled colloidal precipitation

Successful production of CdS QDs followed the Wang et al. (2008) procedure with one change: the thioacetamide concentration was increased 10X. In a 250 mL glass beaker, 0.4567 g cadmium chloride hemipentahydrate (Fisher) was dissolved in approximately 200 mL of milli-Q (MQ) water to create a 0.01 M solution. This solution was poured into a 500 mL three-neck, round-bottom flask attached to a nitrogen line, under which a magnetic stirrer was placed. In another 250 mL beaker, 1.5030 g thioacetamide (Acros Organics) was dissolved in approximately 200 mL of MQ water and stirred to dissolve, creating a 0.1 M solution, then added to the round bottom flask. After adding an acid-cleaned 1-inch Teflon-coated stirring bean, the flask's necks were

sealed with rubber septa, and the mixture was purged with nitrogen under vigorous stirring for 20 minutes.

In a 50 mL beaker, 1.2235 g sodium hexametaphosphate (Anachemia) was dissolved in approximately 20 mL of MQ water and stirred to dissolve, creating a 0.1 M solution. To minimize the introduction of oxygen to the system, a 20 mL glass syringe with a stainless steel needle was used to remove nitrogen from the round-bottom flask atmosphere and bubble through the sodium hexametaphosphate solution. This solution was then added to the system by syringe, and the speed of stirring increased. The pH of the system was adjusted to pH 8.5 by adding approximately 45 mL of approximately 0.1 M NaOH, prepared by dissolving 0.4 g NaOH pellets (ACP) in 100 mL MQ water. During pH adjustment, the solution turned yellow and upon reaching the desired pH, yellow precipitate was visible. The pH was checked by removing a drop via syringe and placing on pH paper (EMD ColourpHast pH 6.5-10.0). The pH-adjusted mixture was then stirred vigorously for 75 minutes.

To give a final mercaptoacetic acid concentration of 1×10^{-4} M in the samples (later), 67.9 μ L of mercaptoacetic acid (Acros Organics, 98%) were added via Eppendorf pipette, and the total volume adjusted to approximately 500 mL using MQ water. Assuming the reaction had gone to completion, this final step would create a mixture with a CdS concentration of 4×10^{-3} M. The mixture was stirred for another 30 minutes. Following synthesis, the reaction vessel was capped to preserve the nitrogen atmosphere, and covered in aluminum foil to avoid exposure to light.

All.i.ii Preparation of other reagents

Silver stock solutions

All silver stocks were refrigerated and stored in LDPE bottles covered in nitrile gloves to keep out the light. A primary silver stock solution was created gravimetrically by taking 542 microlitres of an ICP standard (SPEX Certi-Prep, 996 mg/mL Ag⁰ in 2% HNO₃) and diluting it to 50 mL with MQ water and 2 mL of ultra-pure nitric acid (Seastar, Baseline) to create a 100 micromolar silver stock in 2% nitric acid. 1000 and 100 nanomolar silver stocks were created gravimetrically by taking 1000 and 100 µL of the 100 µM stock, respectively, and diluting each to 100 mL with MQ water. The 100 µM solution was remade monthly; the 100 nM and 1000 nM stocks were remade each time a sample set was to be created. For approximately half of the analyses, the 100 nM and 1000 nM stocks were prepared in 2% HNO₃ by adding 2 mL of concentrated HNO₃ prior to dilution to 100 mL.

PBS buffer solution

PBS buffer solution was prepared volumetrically by making 100.00 mL each of 0.067 M potassium phosphate monobasic (ACP; 0.9118 g required) and 0.067 M sodium phosphate dibasic (ACP; 0.9511 g required). As per Wang et al., the potassium phosphate monobasic solution was adjusted to pH 7.4 using the sodium phosphate dibasic, a process that required approximately 4 parts KH₂PO₄ to 1 part Na₂HPO₄ (ie. 100

mL KH_2PO_4 to 25 mL Na_2HPO_4). A Thermo ORION 720A+ pH meter with Ross Sure-Flow Combination Electrode were used to measure pH.

Silver “Samples”

All samples were prepared gravimetrically in LDPE bottles. The blank was just MQ water; the 0.5 nM silver solution was prepared by taking 50 μL of 100 nM stock and diluting to 10 mL using MQ water; the 1.5 and 5.0 nM solutions were prepared by taking 15 and 50 μL of 1000 nM stock, respectively, and diluting each to 10 mL.

AII.i.iii Sample preparation and fluorometric analysis

Prior to each analysis, a 10 mL aliquot of CdS was removed from the sealed round-bottom flask via syringe. Samples were prepared gravimetrically by measuring 500 microlitres CdS, 1.00 mL PBS buffer, a suitable volume of either 100 or 1000 μM Ag^+ (see AII.i.ii above) and the remainder MQ water, all via Eppendorf pipette, into an acid-cleaned, 30-mL LDPE bottle. Samples were swirled by hand and allowed to equilibrate approximately 15 minutes before running on the fluorometer.

For each sample run, the blank was checked for emission and excitation maxima, as well as for synchronous fluorescence maxima. Each time a new sample was ready to analyze, a small portion was used to rinse out the quartz cuvette. The quartz cuvette was then filled within 0.5 cm of the top (about 3 mL), placed into the instrument, and analyzed for synchronous fluorescence with $\Delta\lambda = 305$ nm. Peak height was adjusted to

between 500 and 1000 counts by manipulating emission and excitation slit widths. Each sample was scanned just once.

AII.ii Experiments involving commercial CdS quantum dots (QDs)

All reagents were prepared in a Class 100 clean space. Reagents were stored in acid-cleaned LDPE bottles, unless otherwise noted. Volumetric solution preparation involved the use of polypropylene volumetric ware. Small volumes were administered by various Eppendorf pipettes. To make each silver sample would require a recipe of 500 microlitres of functionalized CdS solution, as prepared, plus 1.00 mL of PBS or HEPPS buffer, and 8.50 mL of silver sample, for a total volume of 10.00 mL.

AII.ii.i Functionalization of commercial CdS QDs with mercaptoacetic acid (MAA)

Commercial Lumidot™ CdS QDs (Sigma-Aldrich) arrived functionalized with an oleic acid coating to make them soluble in toluene. As these QDs were not soluble in our mercaptoacetic acid-sodium hexametaphosphate matrix, even after agitation and sonication, we sought a way to exchange the surface oleic acid ligands with mercaptoacetic acid (MAA). Using guidelines from Sigma-Aldrich (http://www.sigmaaldrich.com/etc/medialib/docs/Sigma-Aldrich/General_Information/lumidot_faqs.Par.0001.File.tmp/lumidot_faqs.pdf), we sought to treat the CdS QDs with MAA. In a nitrogen-filled glove bag, 1.16 mL of 5 mg/mL CdS in toluene (Sigma-Aldrich) were pipetted into a 50 mL round-bottom flask and capped. Initially, this entire

aliquot, including the toluene, was treated with the chemicals described below; in later experiments, we subjected the aliquot to a flow of nitrogen gas to evaporate off the toluene.

The yellow film left on the inside of the flask was then treated with 141 μL of 0.98% mercaptoacetic acid (prepared by taking 100 μL into 10.00 mL of 98% MAA from Acros Organics) to loosen it from the flask. This amount of MAA would, in the final 10.00 mL Ag^+ samples, give $[\text{MAA}] = 1 \times 10^{-4}$ M, matching that used by Wang et al. Once all yellow material had been loosened (about 15 minutes), 9.86 mL of 4×10^{-3} M sodium hexametaphosphate, adjusted to pH 10.5, was added to match the matrix and pH employed in the earlier CdS QD synthesis. This $(\text{NaPO}_3)_6$ solution was created by adding 0.2447 g of $(\text{NaPO}_3)_6$ (Anachemia) to approximately 90 mL of MQ water, adding about 250 μL of 1 M NaOH (prepared by dissolving approximately 1 g NaOH pellets in 50 mL of MQ water) to reach pH 10.5, and diluting volumetrically to 100.00 mL. Following addition of the pH 10.5 sodium hexametaphosphate, the flask was capped and placed on a shaker table and shaken for at least 24 hours to allow for ligand exchange between the oleic acid coating on the commercial QDs and the MAA in the solution. This resulting functionalized CdS would be approximately 4×10^{-3} M and would have a matrix matching that achieved in the synthesis outlined in AII.i.

The functionalized CdS solution was a bright yellow, appearing to match the intensity of the yellow exhibited by the synthesized CdS QD mixture. However, when left to settle, each night a visible white film appeared on the top of the mixture. This film

would easily mix into the matrix, creating soap-like bubbles, and was most likely the result of oleic acid freed during ligand exchange with MAA. The flask was capped and stored in a dark place, under nitrogen. The contents were used up to a month.

AII.ii.ii Preparation of other reagents

Silver stock solutions

Please refer to Section AII.i.ii for the details.

1.0 M HEPPS Buffer Solution

Approximately 25.23 g of HEPPS buffer (Sigma Ultra, >99.5%) were weighed and added to about 90 mL of MQ water. The pH was adjusted to approximately 7.4 by dissolving in 3-4 NaOH pellets (ACP) and checking with a pH meter. Once pH-adjusted, the solution was brought up to 100.00 mL volumetrically.

Silver “Samples”

All samples were prepared gravimetrically in LDPE bottles. The blank was just MQ water; the 0.5 nM silver solution was prepared by taking 50 μ L of 100 nM stock and diluting to 10 mL using MQ water; the 1.5 and 5.0 nM solutions were prepared by taking 15 and 50 μ L of 1000 nM stock, respectively, and diluting each to 10 mL. Other concentrations ranging from 1-15 nM were also created for different experiments; most of these involved dilution of the 1000 nM stock to 10 mL.

AII.ii.iii Sample preparation and fluorometric analysis

Prior to each analysis, a 1 mL aliquot of functionalized CdS was removed from the sealed round-bottom flask via syringe and delivered to an acid-cleaned 30 mL LDPE bottle. Approximately half of the samples were prepared as in AII.i.iii, using functionalized commercial CdS in place of synthetic CdS; in the remainder of experiments, samples were prepared volumetrically, fluorometer-side, by measuring 500 μL of this functionalized CdS solution, followed by 1.00 mL HEPPS buffer and 8.50 mL of “silver sample”, all delivered via Eppendorf pipette into separate acid-cleaned, 30-mL LDPE bottles. Samples were swirled for 30 seconds by hand and allowed to equilibrate at least 10 minutes before running on the fluorometer.

For each sample run, the blank was checked for emission and excitation maxima, as well as for synchronous fluorescence maxima. Each time a new sample was ready to analyze, a small portion was used to rinse out the quartz cuvette. The quartz cuvette was then filled with 3.00 mL of solution, placed into the instrument, and analyzed for synchronous fluorescence with $\Delta\lambda = 305$ nm. Peak height was adjusted to between 500 and 1000 counts by manipulating emission and excitation slit widths. Each sample was scanned at least 3 times, and the peak heights recorded and averaged.

Appendix III: Organic Extraction Method for Total Silver and Silver Speciation

All reagents were prepared in a Class 1000 or Class 100 clean space. Reagents were stored in acid-cleaned Teflon-FEP bottles, unless otherwise noted. Volumetric solution preparation involved the use of polypropylene volumetric ware. Small volumes were administered by various Eppendorf pipettes. Three-500 mL and three-125 mL Teflon separatory funnels were available for extraction of three samples at a time.

AIII.i Total silver experiments

AIII.i.i Sample preparation

Samples assessed for total silver included a number of method blanks made from acidified Milli-Q (MQ) water, a series of titrations of Ag^+ into acidified MQ, and well water quantified through the method of standard additions, obtained from the Pacific Environmental Science Centre (PESC), 2545 Dollarton Highway, North Vancouver, B.C., Canada, V7H 1V2. The sample to be analyzed was initially weighed in its bottle, then approximately 250 mL of the water sample was transferred into a clean 500 mL Teflon-FEP separatory funnel. The sample bottle was then reweighed to determine the exact mass of water removed, for later calculation of concentration factor (approximately 200X). 2.00 mL of 3M ammonium acetate buffer and approximately 450 μL of concentrated ultra-pure ammonium hydroxide (Seastar, Baseline or Fisher, Optima) were then added to each sample. The buffered sample was then shaken well and checked for

pH by withdrawing 20 μL of buffered sample onto a pH strip (EM-Reagents, ColorpHast pH 2.5-4.5). The desired pH was 4-4.5. 1.00 mL of APDC/NaDDC (or DDDC) solution (1% w/w) was then added, and the funnel was shaken again to thoroughly mix the ligands into the sample. The mixture was allowed to stand 1 hour.

For the first extraction and pre-concentration step, the sample was then treated with 7.00 mL pre-cleaned chloroform (CHCl_3), mixed vigorously for 2 minutes, and allowed to settle and separate for five minutes. In one experiment, this time of separation was varied from 5 to 240 minutes in order to compare percent recoveries of 100 μM Ag^+ . The CHCl_3 layer was then collected into a cleaned 125 mL Teflon-FEP separatory funnel. Following this main extraction, a second 7.00 mL fraction of CHCl_3 was added to the same sample in the 500 mL separatory funnel, shaken for 2 minutes, and allowed to separate for at least 5 minutes. This second CHCl_3 layer was then collected into the same 125 mL separatory funnel. The aqueous layer remaining in the 500 mL funnel was checked for post-extraction pH using a pH meter and was then discarded, as all Ag^+ could be assumed to have been taken up by the ligands and moved into the organic layer.

For the second extraction and pre-concentration step, 4.00 mL of 8 M ultra-pure HNO_3 (Seastar, Baseline) was added to the 125 mL separatory funnel containing the CHCl_3 extractions. The funnel was shaken for 2 minutes and allowed to separate for at least 5 minutes. Brown NO_2 gas formed in the funnel during this extraction. The CHCl_3 layer, significantly more yellow-brown than the upper aqueous layer, was collected and discarded; the aqueous (nitric acid) layer was collected into an acid-cleaned 15 mL

Teflon-FEP vial, capped, and stored refrigerated until a suitable time for evaporation and bulking-up. Depending on the equilibration time used (5-240 minutes), three samples could be prepared and stored away in 2-5 hours with the equipment available.

Samples were evaporated and bulked-up on the same day as ICP-MS analysis. The 15-mL vials containing samples were uncapped, placed on a pancake griddle (Hamilton Beach StepSavor) which had been pre-heated to 350 °F, and allowed to evaporate to dryness over a period of approximately 1.5 hours. Small, brown “pellets” remained in each vial after evaporation. After removing from heat but without substantial cooling, 200 µL of concentrated ultra-pure HNO₃ were added to each vial being careful to cover the pellet, and evaporated down to dryness. This was repeated two more times. Each time, the sample pellet remaining became a little lighter, eventually being yellowish-white in colour. After cooling, vials were weighed, then 25 µL of concentrated ultra-pure HNO₃ were added to each vial. Vials were given about 10 minutes to allow for dissolution of the sample pellet before 25 µL of internal standard (containing about 40 ppb Rh), and then 1.20 mL of milli-Q (MQ) water were added. These volumes created a 1.25 mL sample suspended in 2% ultra-pure nitric acid. All of these additions were done gravimetrically. Vials were gently swirled to thoroughly mix contents.

Samples were poured into to acid-cleaned 1.5 mL polypropylene snap-top vials (Sarstedt) and analyzed manually on a Thermo X Series II ICP-MS spectrophotometer, with a 30s rinse of 2% ultra-pure hydrochloric acid followed by a 50s rinse of 2% ultra-

pure nitric acid in between each sample. With the settings used and manual handling, approximately 0.5 mL of sample was consumed with each analysis.

AIII.i.ii Preparation of other reagents

Saturated (19.2 M) ammonium acetate solution

Ammonia gas was bubbled through approximately 600 mL of three-times distilled glacial acetic acid (reagent grade, ACP) in an acid-cleaned 1-L Teflon-FEP bottle. Over time, ammonium acetate crystals could be seen forming near the gas outlet, and the solution started to heat up and become more viscous. As the reaction progressed, the solution was placed in a cold water bath. The solution was saturated once no more crystals were produced. The bottle appeared to contain half solid, white crystals and half viscous, clear, colourless liquid.

3M ammonium acetate buffer

The saturated (19.2) M ammonium acetate solution above was gently rolled to mix the stratified layers of viscous saturated solution without disturbing the ammonium acetate crystals. 80.00 mL of saturated solution were pipetted into an acid-cleaned 500 mL polypropylene volumetric flask containing about 100 mL MQ water, then made up to volume using MQ water and shaken. The solution was then transferred to an acid-cleaned Teflon-FEP bottle and stored in the dark.

APDC/NaDDC(DDDC) solution, 1% w/w

Approximately 1 g of APDC (1-pyrrolidinecarbodithioic acid, ammonium salt, Acros Organics) and 1g of NaDDC (diethyldithiocarbamic acid, sodium salt trihydrate, Acros Organics) were weighed and quantitatively transferred using 24.00 mL MQ water into a clean 125 mL Teflon-FEP separatory funnel which already contained 75.00 mL MQ water. The NaDDC crystals dissolved on contact; the APDC crystals dissolved easily, and with a little shaking. 1.00 mL of concentrated, ultra-pure ammonium hydroxide was added, then the funnel was shaken thoroughly until homogeneous. The solution was extracted with five aliquots of 4.00 mL of cleaned CHCl_3 to remove any organic silver complexes which might be present in the powders. The resulting solution would contain approximately 0.06 M APDC and 0.04 M NaDDC. This solution was stored in the refrigerator and made fresh weekly. In well water analysis, 1 g of DDDC (diethyldithiocarbamic acid, diethylammonium salt) was used in place of NaDDC.

Clean CHCl_3

Approximately 250 mL of HPLC-grade or spectro-grade CHCl_3 (Caledon) were added to an acid-cleaned Teflon-FEP separatory funnel. 100 mL of MQ water were added, and the contents were shaken for 1 minute, allowing at least 2 minutes for settling and separation. CHCl_3 was collected into an acid-cleaned glass beaker; water was discarded, and the process repeated four more times for a total of 5X. Cleaned CHCl_3 was stored in an acid-cleaned amber glass bottle in a vented cabinet.

An interesting aside: many sources indicate that Teflon-FEP is suitable for long-term storage of CHCl_3 . In the early stages of experimentation, an initial batch of cleaned CHCl_3 was stored in Teflon-FEP. It was used for a month without problems, but after a second month of storage, it was yellow. When it was opened, the acrid smell of chlorine was present. To confirm the presence of chlorine (a strong oxidizing agent), a reducing agent (30% hydrogen peroxide) was added and the mixture shaken in a separatory funnel. The result: both the yellow colour and chlorine odour disappeared, suggesting that free chlorine was produced over time. This solution was returned to its Teflon-FEP bottle; after only 2 more weeks of storage, it was yellow again. There was some chemical process occurring between the CHCl_3 and either the Teflon-FEP itself (exchange with fluorine?) or a plastic additive that released free chlorine over time. It is thus recommended that CHCl_3 not be stored Teflon-FEP bottles.

Silver stock solutions and working standards

All silver stocks and working standards were refrigerated and stored in LDPE bottles covered in nitrile gloves to keep out the light. A primary silver stock solution was created gravimetrically by taking 542 microlitres of an ICP standard (SPEX Certi-Prep, 996 mg/mL Ag^0 in 2% HNO_3) and diluting it to 50 mL with MQ water and 2 mL of nitric acid (Seastar, Baseline) to create a 100 μM silver stock in 2% nitric acid. A 100 nanomolar silver working standard was created gravimetrically by taking 100 microlitres of 100 μM stock, adding 2 mL of ultra-pure concentrated nitric acid, and diluting to 100 mL with MQ water. A 1000 nanomolar (1 micromolar) silver working standard was

similarly created, instead using 1.00 mL of 100 μM stock. All of these solutions were stable over the four-month testing period.

Samples

“Acidified water”, made with MQ water acidified to below pH 2 with ultra-pure HCl (approx. 2.4 mL conc HCl per litre of water), was used as a model of a natural water sample collected then acidified for storage. 2 L of acidified water could be created by adding 4.8 mL ultra-pure HCl (Seastar, Baseline, or Fisher, Optima) to some MQ water in a 2L polypropylene volumetric flask and then making up to volume with MQ. This acidified water, without Ag^+ , served as a method blank for extractions, and was used as a base for adding Ag^+ spikes to all proof-of-concept and titrations (see Table 7 for titration setup). All such silver “samples” were prepared and stored in acid-cleaned 1-2 L Teflon-FEP bottles, and were used within two days.

Well water was collected from PESC on May 10, 2010. Prior to collection, about 10L of well water was filtered through a Pall AcroPak 500 filter with a 0.2 μm pore size. This wash water was discarded, then fresh well water was filtered through this and collected in acid-cleaned 2L Teflon bottles and 1L LDPE bottles. Bottles containing well water were stored at room temperature in a darkened cabinet during the month of analysis. For total Ag analysis, two-1L bottles of well water were acidified to pH 1.6 for 28 days by adding 2.4 mL ultra-pure HCl to each; the rest of the bottles were maintained at native pH for speciation studies.

Internal standard

An internal standard used by the ICP-MS lab in the School of Earth and Ocean Sciences at the University of Victoria, Victoria, B.C., contains approximately 400 ppb Rh in 2% nitric acid. This standard was diluted 10X, gravimetrically, in 2% HNO₃, giving a stock of approximately 40 ppb Rh. When 25 µL of this stock were added to each sample and external standard, this created approximately 0.8 ppb (7.8 nM) Rh in each sample, a Rh value which would have counts in the same range as our mid-range Ag⁺ external standard (75 pM, or 15 nM in “real” terms). This internal standard allowed for monitoring the instrument’s performance over time: if the instrument drifted, the ¹⁰³Rh signal would change; similarly, if there was a significant matrix effect between samples and external standards, the ¹⁰³Rh signal would change.

External standards (calibration standards)

When a batch of extractions was ready to be run by ICP-MS, a series of external standards were prepared, gravimetrically, in acid-cleaned 15 mL Teflon-FEP vials. A curve representing 0, 25, 50, 75, 100, and 125 pM standards concentrated 200X thus required preparing standards of 0, 5, 10, 15, 20, and 25 nM, respectively. To each vial, 25 µL of internal standard were weighed, followed by the desired volume of 100 nM Ag⁺ working standard (0, 65, 125, 187.5, 250, and 312.5 µL, respectively), followed by the remainder of 2% ultra-pure HNO₃ for a final volume of 1.25 mL. Vials were swirled to combine contents, and then transferred into acid-cleaned 1.5 mL polypropylene snap-top vials for ICP-MS analysis. External standards were prepared each time a series of extractions were ready for analysis.

[Ag⁺], pM	Water volume, L	Moles Ag⁺ required	Moles Ag⁺ already	Moles Ag⁺ to add	Volume of 100 nM Ag⁺ required, μL
50	1	5×10^{-11}	0	5×10^{-11}	500
75	0.75	5.625×10^{-11}	3.75×10^{-11}	1.875×10^{-12}	187.5
100	0.5	5×10^{-11}	3.75×10^{-11}	1.25×10^{-12}	125
125	0.25	3.125×10^{-11}	2.5×10^{-11}	6.25×10^{-12}	62.5

Table 7: Titration set-up for total silver in milli-Q water.

This setup was created as a first comparison of percent recovery of Ag⁺ from acidified milli-Q water. One 250-mL replicate was created at each concentration point.

AIII.ii Silver speciation experiments

AIII.ii.i Sample preparation

These experiments generally fell into one of two categories: (a) ligand competition experiments with fixed $[\text{Ag}^+]$, $[\text{ligand}]$, and varying $[\text{DDC}^-]$, and (b) titration experiments with varying $[\text{Ag}^+]$ and fixed $[\text{DDC}^-]$. Proof-of-concept ligand competition experiments involving glutathione and EDTA as strong binding ligands involved the use of Fraquil as the water base. In titration experiments, as well as ligand equilibration experiments testing the binding ability of triclosan and 3,3',5-triiodothyronine (T_3), well water collected from PESC was used as the water base.

The water sample to be analyzed (with or without Ag^+ already added) was initially weighed in its bottle, then approximately 100 mL of the water sample was transferred into a clean 500 mL Teflon-FEP separatory funnel. The sample bottle was then reweighed to determine the exact mass of water removed, for later calculation of concentration factor (approximately 100X). 1.00 mL of 1M HEPPS buffer and approximately 30 μL of concentrated ultra-pure ammonium hydroxide (Seastar, Baseline or Fisher, Optima) were then added to each sample. The buffered sample was then shaken well and checked for pH by withdrawing 15 μL of buffered sample onto a pH strip (EM-Reagents, ColorpHast pH 6.5-10.0). The desired pH was 7.4-7.7.

For samples with a competing ligand, the competing ligand was added next (100 μL of 1 mM glutathione; 100 or 1000 μL of 100 mM EDTA; 1000 μL of 3.0 mg/L

triclosan; or 100 μL of 10 μM T_3). In ligand competition experiments, 100 μL of 100 nM Ag^+ solution were added gravimetrically to each pH-adjusted water sample prior to addition of any ligands. The Ag^+ solution was weighed in a Teflon vial, then added to the separatory funnel, then the vial was re-weighed: the difference was the amount of silver ion added. In titration experiments, the silver was already in the water sample (Table 8, Table 11) and additional silver was not required. The final step in sample treatment involved the addition DDC^- : in ligand competition experiments, this involved adding 1.00 mL of DDC^- solution (either NaDDC or DDDC) of varying concentrations (from 10^{-5} M to 10^{-2} M). In titration experiments, this involved adding 100 μL of 10^{-3} M DDC^- to give a final $[\text{DDC}^-]$ of 10^{-6} M in the sample. The funnel was shaken for 2 minutes to mix all ligand(s) into the sample, and the mixture was allowed to stand 1 hour.

For the extraction and pre-concentration step, the sample was then treated with 5.00 mL pre-cleaned CHCl_3 , mixed vigorously for 2 minutes, and allowed to settle and separate for 15-20 minutes. Due to the pH and the nature of the ligands, it took much longer for the CHCl_3 to separate from the aqueous layer than in the total Ag method, so gentle swirling during the settling process was required to help break up the resulting emulsion. The CHCl_3 layer was then collected into a cleaned 125 mL Teflon-FEP separatory funnel. Following this main extraction, a second 5.00 mL fraction of CHCl_3 was added to the same sample in the 500 mL separatory funnel, shaken for 2 minutes, and allowed to separate for 15-20 minutes, again with gentle swirling to help separate the layers. This second CHCl_3 layer was then collected into the same 125 mL separatory funnel. The aqueous layer remaining in the 500 mL funnel was checked for post-

extraction pH using a pH meter and was then discarded, as all Ag^+ could be assumed to have been taken up by the ligands and moved into the organic layer.

The CHCl_3 layers collected were washed with 5.00 mL of MQ water, to dilute any salts which might have been carried over in drops of aqueous layer which may have followed the CHCl_3 layer. Washing involved 30 seconds of shaking followed by at least one minute of separation, prior to collection of the CHCl_3 layer into an acid-cleaned 15 mL Teflon-FEP vial. This vial was capped and stored at room temperature until a suitable time for evaporation, no more than 4 hours.

Samples were digested and evaporated daily, as they were prepared. The 15-mL vials containing samples were uncapped, placed on a pancake griddle (Hamilton Beach StepSavor) which had been pre-heated to 200 °F, covered with 2.00 mL of ultra-pure nitric acid, and allowed to slowly evaporate. Keeping the temperature low until most of the CHCl_3 had evaporated was essential in order to avoid “bumping”, where the lower, more quickly-evaporating CHCl_3 would bubble through the nitric acid and cause sample loss through spitting. After about 1 hour (once the CHCl_3 had evaporated), the temperature was increased to 350 °F to facilitate the evaporation of the HNO_3 . Total evaporation time was usually about 1.5 hours. Tiny brown spots remained in each vial after evaporation. After removing from heat but without substantial cooling, 100 μL of concentrated ultra-pure HNO_3 were added to each vial, being careful to cover the sample spots, and evaporated down to dryness at 350 °F (about 10 minutes). This was repeated two more times. Each time, the sample pellet remaining became a little lighter or smaller

in size, but remained brownish in colour. At this point, samples were cooled and capped until a suitable time for bulking up. With the equipment available, six extractions could be performed to this point within 9-10 hours.

Sample vials were weighed, then heated to 200 °F on a griddle. 20 µL of concentrated ultra-pure HNO₃ were added to each hot vial, as heat was necessary to dissolve the brown pellets, but to avoid evaporation of the nitric acid, vials were immediately removed from the heat. Once dissolved and cooled, 20 µL of internal standard (containing 40 ppb Rh), and then 0.96 mL of MQ water were added gravimetrically, creating a total volume of 1.00 mL of sample suspended in 2% ultra-pure nitric acid. Vials were gently swirled to thoroughly mix contents. Sometimes, a small, visible amount of sticky residue was left in the vial.

The sample solutions were more viscous than their total silver counterparts, so samples were transferred via Eppendorf pipette to acid-cleaned 1.5 mL polypropylene snap-top vials (Sarstedt). Samples were analyzed manually on a Thermo X Series II ICP-MS spectrophotometer, with a 20s rinse of 2% ultra-pure hydrochloric acid followed by a 60s rinse of 2% ultra-pure nitric acid in between each sample. With the settings used and manual handling as opposed to autosampler, approximately 0.5 mL of sample was consumed with each analysis.

AIII.ii.ii Collection of well water and preparation of other reagents

“Fraquil” recipe water samples

For ligand exchange experiments with glutathione and EDTA, a modified Fraquil medium was prepared using the major salts as described at <http://www-cyanosite.bio.purdue.edu/media/nontable/fraquilnt/html>, substituting where necessary to make use of reagents on hand. Major stock solutions were prepared volumetrically by weighing the appropriate amount of salt and dissolving to make 100.00 mL of solution, and were stored in 125 mL LDPE bottles. These include 0.25 M calcium chloride (3.68 g $\text{CaCl}_2 \cdot 2\text{H}_2\text{O}$; Caledon), 0.15 M magnesium sulfate (1.81 g MgSO_4 ; ACP), 0.15 M sodium bicarbonate (1.26 g NaHCO_3 ; ACP), 0.1 M potassium nitrate (1.011 g KNO_3 ; ACP), and 0.01 M sodium phosphate dibasic (0.142 Na_2HPO_4 ; ACP). All stock solutions were stored at room temperature.

To make the Fraquil medium, 2.00 mL of each of the above solutions were pipetted into a 2.00 L Teflon-FEP bottle, then made up to 2000 g using MQ water. pH of the final Fraquil water was about 6, and the ionic strength of this solution was approximately 1.7×10^{-3} .

Samples involving well water as the medium

For experiments establishing the effectiveness of triclosan and T_3 as strong silver-binding ligands, well water obtained from PESC was used as the medium. Please see AIII.i.ii for details on well water collection, and Table 8 for details on titration set-up.

Competing Ligand	[Ag ⁺], pM	Sample volume, L	Moles Ag ⁺ required	Moles Ag ⁺ already	Moles Ag ⁺ to add	Volume of 100 nM Ag ⁺ required, μL
100 μM EDTA	10	1	1 x 10 ⁻¹¹	0	1 x 10 ⁻¹¹	100
	20	0.7	1.4 x 10 ⁻¹¹	7 x 10 ⁻¹²	7 x 10 ⁻¹²	70
	30	0.4	1.2 x 10 ⁻¹¹	8 x 10 ⁻¹²	4 x 10 ⁻¹²	40
	50	1	5 x 10 ⁻¹¹	0	5 x 10 ⁻¹¹	500
	100	0.7	7 x 10 ⁻¹¹	3.5 x 10 ⁻¹¹	3.5 x 10 ⁻¹¹	350
	200	0.4	8 x 10 ⁻¹¹	4 x 10 ⁻¹¹	4 x 10 ⁻¹¹	400
30 μg/L triclosan or 10 nM T ₃	20	1	2 x 10 ⁻¹¹	0	2 x 10 ⁻¹¹	200
	40	0.85	3.4 x 10 ⁻¹¹	1.7 x 10 ⁻¹¹	1.7 x 10 ⁻¹¹	170
	60	0.7	4.2 x 10 ⁻¹¹	2.8 x 10 ⁻¹¹	1.4 x 10 ⁻¹¹	140
	100	0.55	5.5 x 10 ⁻¹¹	3.3 x 10 ⁻¹¹	2.2 x 10 ⁻¹¹	220
	200	0.4	8 x 10 ⁻¹¹	4 x 10 ⁻¹¹	4 x 10 ⁻¹¹	400
	400	0.25	1 x 10 ⁻¹⁰	5 x 10 ⁻¹¹	5 x 10 ⁻¹¹	500

Table 8: Titration set-up for competitive ligand exchange experiments with well water from PESC.

For titrations involving EDTA, one 100-mL replicate of each scenario (without DDC⁻, with 10⁻⁶ M DDC⁻, and with 100 μM EDTA + 10⁻⁶ M DDC⁻) was prepared at each concentration point; therefore, each concentration point required 300 mL of water.

For titrations involving triclosan or T₃, one 50-mL replicate of each scenario (10⁻⁶ M DDC⁻ only, 30 μg/L triclosan + 10⁻⁶ M DDC⁻, and 10 nM T₃ + 10⁻⁶ M DDC⁻) was prepared at each concentration point; therefore, each concentration point required 150 mL of water.

frogSCOPE samples

Sampling was completed and coordinated by R. Skirrow at PESC. Speciation samples for the frogSCOPE program were prepared and analyzed by ICP-MS for total silver at PESC using PESC Method WICPMS Version 4.1 (based on EPA Method 200.8, “Determination of Trace Elements in Waters and Wastes by Inductively Coupled Plasma-Mass Spectrometry”, USEPA, 1994, http://www.caslab.com/EPA-Methods/PDF/200_8.pdf), on a Perkin Elmer Elan DRCII ICP-MS. Results were tabulated and provided by A. Carew, Department of Biochemistry and Microbiology, University of Victoria. After this work was completed, 250-mL aliquots were packaged in LDPE bottles, frozen at -80 °C, and sent to the University of Victoria Department of Biochemistry and Microbiology where they were stored at -80 °C for 15 months prior to Ag speciation analysis. All samples were kept at native pH to preserve any naturally-occurring Ag speciation. One week prior to analysis, samples were allowed to thaw in a dark cabinet at room temperature for 24 hours before being placed back in the refrigerator for storage.

The total silver concentration, as established at PESC, was used as a guideline for the concentration factor to use (i.e. how much water to treat with DDDC, and final solution volume for ICP-MS analysis). In the week prior to analysis, samples were thawed at room temperature for 24 hours in a darkened cabinet, and then were moved to the refrigerator, where they were stored throughout analysis. Samples containing silver used in toxicology studies for frogSCOPE were treated to the same preparation steps as previously outlined, but using different volumes of sample and reagents due to higher

concentrations. Please refer to Table 9 for sample details; Table 10 for details of reagent scaling, and Table 11 for details on titration experiment set-up.

1.0 M HEPPS Buffer Solution

Please refer to Section AII.ii.ii. for details.

NaDDC and DDDC Solutions

A master stock of 10^{-2} M DDC⁻ was prepared gravimetrically by dissolving about 0.115 g of NaDDC crystals (diethyldithiocarbamic acid, sodium salt trihydrate, Acros Organics) OR 0.1146 g of diethyldithiocarbamic acid, diethylammonium salt (Aldrich, 97% purity) to a total volume of 50.00 mL using 400 μ L of concentrated ammonium hydroxide and the balance MQ water. This solution was extracted with two aliquots of 4.00 mL of cleaned CHCl₃ to remove any organic silver complexes which might be present in the crystals. This stock was diluted to 10^{-5} , 10^{-4} , and 10^{-3} M by taking 10, 100, and 1000 μ L, respectively, and diluting to 10.00 mL with MQ water and 80 μ L concentrated ammonium hydroxide. These solutions, with a pH of about 10.8, were stored in the refrigerator and could be used within one week.

1 mM glutathione

0.0157 g of reduced glutathione was weighed directly into an acid-cleaned 60 mL LDPE bottle, then made up to 50.00 mL gravimetrically using MQ water. This solution was stored in the refrigerator and was used within one week.

Sample ID	Expected [Ag] _T	[Ag] _T by ICP-MS ¹	Volumes, mL		Conc. Factor	Expected Max. [Ag], nM
			Original Sample	ICP-MS Sample		
0.6 µg/L blank	0	<185 pM	50	1	50 X	<9.25
0.6 µg/L nanoAg ²	1.6 nM	742 pM	20	1	20X	14.8
0.6 µg/L AgNO ₃	5.6 nM	4.26 nM	10	5	2 X	8.52
6.0 µg/L blank	0	464 pM	50	1	50 X	23.2
6.0 µg/L nanoAg ²	16.3 nM	9.18nM	10	5	2 X	18.4
6.0 µg/L AgNO ₃	56 nM	13.6 nM	10	10	1 X	13.6

¹Analyzed at PESC and reported by A. Carew, Dept. of Biochemistry and Microbiology, University of Victoria.

²ViveNano nanoAg is 29.29% by mass Ag metal. ICP-MS data provided March 2010 by J. Dinglasan, ViveNano.

Table 9: Details on frogSCOPE samples examined by competitive ligand exchange.

This set consisted of two sets of six samples made from this same well water, but from experiments of high Ag exposures (6.0 µg/L; February 27, 2009) and medium Ag exposures (0.6 µg/L; March 12, 2009). Each set contained two blanks, two samples made with the given concentration of AgNO₃ (Fisher, ACS grade), and two samples made with the given concentration of nanosilver (ViveNano, 1.5 mg/mL).

Total silver concentrations reported here ([Ag]_T) were determined at PESC, and were used as a guideline for experimental set-up. The goal was to keep samples within the low-nanomolar range, so that titrations would not exceed a 60 nM final concentration at the ICP-MS.

Sample ID	Volume of sample to be extracted, mL	Reagent volumes, μL			
		10^{-3} M DDC ⁻	1 M HEPPS buffer	Conc. NH_4OH	Internal Standard ¹
“usual” samples (pM range)	100	100	1000	30	20
0.6 $\mu\text{g/L}$ blank	50	50	500	15	20
0.6 $\mu\text{g/L}$ nanoAg	20	20	200	6	20
0.6 $\mu\text{g/L}$ AgNO_3	10	10	100	4	10*
6.0 $\mu\text{g/L}$ blank	50	50	500	15	20
6.0 $\mu\text{g/L}$ nanoAg	10	10	100	4	10*
6.0 $\mu\text{g/L}$ AgNO_3	10	10	100	6 ²	20*

¹ Volumes without an asterisk (*) were from the 39.59 ppb Rh working standard; volumes with an * were from the University of Victoria ICP-MS lab 398.2 ppb Rh stock.

²Volume of NH_4OH was increased to offset the pH effect of adding larger volumes of the Ag^+ in 2% HNO_3 standard used in titrations.

Table 10: Details of reagent scaling for different concentration factors required by frogSCOPE samples, as compared with “usual” samples in the pM range (grey).

Sample	[Ag ⁺] to add	Sample vol., mL	Moles Ag ⁺ required	Moles Ag ⁺ already	Moles Ag ⁺ to add	Vol. Ag ⁺ standard ¹ required, μ L
0.6 μ g/L blank	50 pM	200	1×10^{-11}	0	1×10^{-11}	100
	100 pM	150	1.5×10^{-11}	7.5×10^{-12}	7.5×10^{-12}	75
	150 pM	100	1.5×10^{-11}	1×10^{-11}	5×10^{-12}	50
	200 pM	50	1×10^{-11}	7.5×10^{-12}	2.5×10^{-12}	25
0.6 μ g/L nanoAg	100 pM	100	1×10^{-11}	0	1×10^{-11}	100
	200 pM	80	1.6×10^{-11}	8×10^{-12}	8×10^{-12}	80
	300 pM	60	1.8×10^{-11}	1.2×10^{-11}	6×10^{-12}	60
	500 pM	40	2×10^{-11}	1.2×10^{-11}	8×10^{-12}	80
0.6 μ g/L AgNO ₃	2 nM	50	1×10^{-10}	0	1×10^{-10}	100*
	4 nM	40	1.6×10^{-10}	8×10^{-11}	8×10^{-11}	80*
	6 nM	30	1.8×10^{-10}	1.2×10^{-10}	6×10^{-11}	60*
	10 nM	20	2×10^{-10}	1.2×10^{-10}	8×10^{-11}	80*
6.0 μ g/L blank	50 pM	200	1×10^{-11}	0	1×10^{-11}	100
	100 pM	150	1.5×10^{-11}	7.5×10^{-12}	7.5×10^{-12}	75
	150 pM	100	1.5×10^{-11}	1×10^{-11}	5×10^{-12}	50
	200 pM	50	1×10^{-11}	7.5×10^{-12}	2.5×10^{-12}	25
6.0 μ g/L nanoAg	2 nM	50	1×10^{-10}	0	1×10^{-10}	100*
	4 nM	40	1.6×10^{-10}	8×10^{-11}	8×10^{-11}	80*
	6 nM	30	1.8×10^{-10}	1.2×10^{-10}	6×10^{-11}	60*
	10 nM	20	2×10^{-10}	1.2×10^{-10}	8×10^{-11}	80*
6.0 μ g/L AgNO ₃	5 nM	50	2.5×10^{-10}	0	2.5×10^{-10}	250*
	10 nM	40	4×10^{-10}	2×10^{-10}	2×10^{-10}	200*
	15 nM	30	4.5×10^{-10}	3×10^{-10}	1.5×10^{-10}	150*
	20 nM	20	4×10^{-10}	3×10^{-10}	1×10^{-10}	100*

¹Volumes without an asterisk (*) were from the 100 nM Ag⁺ working standard; volumes with an * were from the 1000 nM Ag⁺ working standard.

Table 11: Titration set-up for competitive ligand exchange experiments with frogSCOPE samples.

One replicate was prepared at each concentration point. Volumes were selected based on total silver analysis: the higher the total silver, the lower the volume used.

100 mM EDTA

Approximately 1.47 g of EDTA (Free Acid, Ultra Pure grade, Caledon) were weighed and quantitatively transferred into a 50 mL polypropylene volumetric flask. After adding about 25 mL of MQ water, 1400 μL of concentrated NH_4OH were added to dissolve the EDTA. The volume was then made up to 50.00 mL using MQ water. The pH of the final solution, as measured using a pH 0-14 strip, was 8-9. The solution is stable for months when refrigerated.

Triclosan and 3,3',5-Triiodothyronine (T_3)

Master stock solutions of triclosan (3.0 mg/L = 10.4 μM) and T_3 (10 μM) were prepared in 400 μM NaOH by A. Hinthner, Dept. of Biochemistry and Microbiology, University of Victoria. Solutions were stored refrigerated and used within one month.

Clean CHCl_3 , silver stock solutions and working standards

Please refer to Section AIII.i.ii for the details.

Internal standard

Please refer to Section AIII.i.ii and Table 10 for details.

External standards

Please refer to Section AIII.i.ii. Volumes of 100 nM Ag^+ were adjusted to create 2-10 nM Ag^+ in 1.00 mL of solution for most analyses, and 5-60 nM Ag^+ for the frogSCOPE samples.

AIII.iii Method Limitations

When comparing identical $[Ag^+]$ and [ligands], both the total Ag and Ag speciation methods using competitive ligand exchange-solvent extraction (CLE-SE) have been observed to exhibit considerable variation (see Appendix IV). Table 12 summarizes some of the key opportunities for sample losses and contamination which can create variation in both methods. In most cases, the percent Ag recovered in both the total Ag method and Ag speciation method is less than 100%, suggesting that sample loss is more prevalent. Since there are so many opportunities for both loss and gain of Ag, replicate analyses would be desirable to help mitigate these effects. However, the large volumes of sample required and the amount of time it takes to prepare a sample set for analysis makes replicate sample preparation difficult. In the literature where CLE-SE has been applied to Ag, one replicate has been the rule rather than the exception, and results have been interpreted accordingly (Adams & Kramer, 1999a; Miller & Bruland, 1995).

Kinrade and Van Loon (1974) performed experiments varying shaking time as well as equilibration time, and found that the Ag-PDC and Ag-DDC complexes might be broken apart with increasing shaking time. Kinrade and Van Loon (1974) also suggested that the Ag-ligand complexes are sensitive to vigor of shaking, and reported that inverting the separatory funnel containing chemicals at a constant rate for one minute gave better precision for silver than the vigorous shaking usually specified by other researchers

Opportunities for sample loss (lower Ag recovery)	Opportunities for sample contamination (higher Ag recovery)
<ul style="list-style-type: none"> • incomplete movement of AgDDC (and AgPDC in total method) into CHCl₃ layer • incomplete separation of organic and aqueous layers at any point in sample preparation • explosive loss of CHCl₃ when venting separatory funnels prior to shaking the contents • improperly or incompletely sealed sep. funnel caps during shaking • incomplete back-extraction of Ag in CHCl₃ layer to 8 M HNO₃ layer (total Ag method only) • spitting during digestion step (especially in speciation method) • Ag sticking in residue left behind in Teflon vials during weighing and transfer to 1.5 mL PP vials • bubbles, or dirty tubing which “grabs” Ag, in the ICP-MS sample introduction system 	<ul style="list-style-type: none"> • incompletely cleaned equipment, especially the Teflon separatory funnels and Teflon vials • incompletely cleaned CHCl₃, APDC/DDDC or DDDC solutions • impurities in reagents, which get magnified with organic extraction • pipetting any solution into the sep. funnel without a proper pipette tip rinse, or touching the pipette tip to anything at any point • touching the sep. funnel tip to anything at any point during extraction • spitting from a neighbouring sample during digestion • working over an uncapped sample at any time during preparation • Ag-contaminated ICP-MS sample introduction system (particularly probe, tubing, and nebulizer) following a run of high Ag samples by another researcher

Table 12: Opportunities for Ag loss and gain during sample preparation and analysis.

The number of steps in sample preparation provide, by far, the largest number of opportunities for picomolar levels of Ag to be lost or gained.

(Bruland et al., 1985; Bruland et al., 1979; Kramer, 2006; Miller & Bruland, 1994). As this sensitivity may extend to other natural (or introduced) ligands in the solution, it might be worth testing the effect of shaking time and vigor of shaking on the reproducibility and recovery of Ag for both the total Ag method and the Ag speciation method.

It was suggested by Kinrade and Van Loon (1974) that the use of ammonium acetate buffer might be inappropriate for both Ag and Pb, as they form stable Ag- and Pb-acetate complexes which are not extractable. This may have been the reason that only a few data points approached 90-100% recovery for Ag (see Appendix IV), whereas other soft metals extracted using the same PDC⁻/DDC⁻ mixture were consistently extracted in the 98-99% range (Bruland et al., 1979). The main reasons for using 3M ammonium acetate (pH of about 5.5) is that it buffers to the ideal pH for maximum Ag extraction and can be made very cleanly, an important feature for studying trace metals (Bruland et al., 1979). If there are further studies in how to increase total Ag recovery while reducing the need for large sample volumes or complicated calculations, then studying different buffers which can be made cleanly might be one area for further research.

AIII.iv References

- Adams, N. W. H., & Kramer, J. (1999a). Determination of silver speciation in wastewater and receiving waters by competitive ligand equilibration/solvent extraction. *Environmental Toxicology and Chemistry*, 18(12), 2674.
- Bruland, K. W., Coale, K. H., & Mart, L. (1985). Analysis of seawater for dissolved cadmium, copper, and lead: an intercomparison of voltammetric and atomic absorption methods. *Marine Chemistry*, 17, 285-300.
- Bruland, K. W., Franks, R. P., Knauer, G. A., & Martin, J. H. (1979). Sampling and analytical methods for the determination of copper, cadmium, zinc, and nickel at the nanogram per liter level in sea-water. *Analytica Chimica Acta*, 105(1), 233-245.
- Kramer, D. (2006). *An Exploration of the Marine Silver Cycle in Coastal and Open Ocean Environments of the North Pacific*. M.Sc. Thesis, University of Victoria, Victoria, B.C.
- Miller, L. A., & Bruland, K. W. (1994). Determination of copper speciation in marine waters by competitive ligand equilibration/liquid-liquid extraction: an evaluation of the technique. *Analytica Chimica Acta*, 284, 573-586.
- Miller, L. A., & Bruland, K. W. (1995). Organic Speciation of Silver in Marine Waters. *Environmental Science & Technology*, 29, 2616-2621.

Appendix IV: Data Tables

Table IV.i Experiment summary: effect of 0.5-5.0 nM [Ag⁺] on CdS fluorescence

Date (2009)	Slit Widths, excitation/emission	Average Synchronous Fluorescence Intensity at 304 nm using $\Delta\lambda = 305$ nm						Comments
		Blank	0.5 nM Ag ⁺	1.0 nM Ag ⁺	1.5 nM Ag ⁺	3.0 nM Ag ⁺	5.0 nM Ag ⁺	
Feb 19	5nm/10nm	757.542	780.170		771.385		763.266	First batch of synthesized CdS; Ag ⁺ made without any HNO ₃
Mar 2	5nm/10nm	789.044	755.050		685.593		952.663	Second batch of synthesized CdS; Ag ⁺ made with 2% HNO ₃
Apr 23	5nm/10nm	640.030	62.327		57.132	<50.000		First use of commercial CdS QDs: left toluene layer floating on top; results reflect little CdS getting into aqueous layer
Apr 28	10nm/20nm	717.996		678.332		665.972	564.513	First successful functionalization of commercial CdS in toluene
May 1	10nm/20nm	186.224		163.073		154.401	176.230	
May 8	10nm/10nm	426.830		385.860		395.006	375.458	
Jun 17	5nm/10nm	509.817	518.600		509.578		501.699	Last use of PBS as the buffer
Jun 26	10nm/10nm	557.532	538.553		548.865		507.588	First use of HEPPS as the buffer
Jul 24	10nm/10nm	506.070	449.563		486.166		473.058	Same functionalized CdS as used June 26
Jul 29A	10nm/10nm	867.954	862.364		869.323		849.157	Toluene evaporated prior to functionalization; Ag ⁺ stocks made with 0.04% HNO ₃

		Average Synchronous Fluorescence Intensity at 304 nm using $\Delta\lambda = 305$ nm						
Date (2009)	Slit Widths, excitation/emission	Blank	0.5 nM Ag ⁺	1.0 nM Ag ⁺	1.5 nM Ag ⁺	3.0 nM Ag ⁺	5.0 nM Ag ⁺	Comments
Jul 29B	10nm/10nm	649.658	623.909		629.126		605.020	Toluene not evaporated prior to functionalization; Ag ⁺ stocks made with 0.04% HNO ₃
Jul 31 A	10nm/10nm	907.977	896.978		921.171		914.602	Toluene evaporated prior to functionalization; Ag ⁺ stocks made with 0.04% HNO ₃ for all July 31 analyses
Jul 31 B	10nm/10nm	907.740	892.165		909.440		913.368	Toluene evaporated prior to functionalization
Jul 31 C	10nm/10nm	891.888	910.652		837.033		843.923	Toluene not evaporated prior to functionalization
Jul 31 D	10nm/10nm	890.635	876.524		808.196		819.132	Toluene not evaporated prior to functionalization
Aug 13	5nm/5nm	632.606	652.021		670.933	654.472	665.207	Ag ⁺ stocks made without any HNO ₃ for this and all subsequent analyses
Sep 15	5nm/5nm	620.112	606.091		613.473	608.039	632.073	Same functionalized CdS as used Aug 13
Sep 16	5nm/10nm	751.977	730.844		748.417	747.417	651.978	10X the usual [MAA] in CdS stock
Sep 29A	5nm/10nm	711.097	707.530		684.386		599.270	10X the usual [MAA] in CdS stock
Sep 29 B	5nm/10nm	729.528	670.822		713.398	686.701	598.892	10X the usual [MAA] in CdS stock

Table IV.ii CdS fluorescence experiments with a larger range of [Ag⁺]

	Average Synchronous Fluorescence Intensity at 304 nm using $\Delta\lambda = 305$ nm						
[Ag ⁺], nM	May 1	May 8	Apr 28	Aug 13	Sep 15	Sep 16	Sept 29
0	186.224	426.830	717.996	632.606	620.212	751.977	729.528
0.5				652.021	606.091	730.844	670.822
1	163.073	385.860	678.332				
1.5				670.933	613.473	748.417	713.398
2	152.757	382.177	732.781				
3	154.401	395.006	665.972	654.472	608.039	747.417	686.701
4	159.606	402.333	610.909				
5	176.230	375.458	564.513	665.207	632.073	651.978	598.892
6	177.002	395.790					
7	163.278	379.658					
8	227.130	383.392		660.889	612.788	736.781	722.367
9	180.146	389.675					
10	173.843	382.161		639.059	627.156	727.650	652.195
11	170.644	383.921					
12	205.119	389.964					
13	177.569	396.969					
14	167.341	379.151					
15	155.185	380.367					
Notes						10X usual [MAA]	
	Ag ⁺ stocks made with 2% HNO ₃			No HNO ₃ in Ag ⁺ stocks			

Table IV.iii Total silver experiments using APDC/NaDDC & organic extraction

Sample ID	[Ag ⁺] added, pM	[Ag] by ICP-MS, nM	Concentration Factor (M _{aq} /M _{ICPMS})	[Ag*], pM	% recovery	Final pH of (aq) layer
TT Blk 1	0.0	0.078061	200*	0.4	n/a	not taken
TT Blk 2	0.0	0.071783	200*	0.4	n/a	not taken
Method Blk 1	0.0	0.114729	200*	0.6	n/a	not taken
Method Blk 2	0.0	0.257596	200*	1.3	n/a	not taken
TT Blk 3	0.0	0.047217	200*	0.2	n/a	not taken
TT Blk 4	0.0	0.069608	200*	0.3	n/a	not taken
Method Blk 3	0.0	2.603383	200*	13.0	n/a	not taken
Method Blk 4	0.0	0.131801	200*	0.7	n/a	not taken
Method Blk 5	0.0	0.735445	200*	3.7	n/a	not taken
Method Blk 6	0.0	0.188104	200*	0.9	n/a	not taken
50 pM titration	50.6	2.997547	200*	15.0	30%	not taken
75 pM titration	76.4	6.847307	200*	34.2	45%	not taken
100 pM titration	103.9	6.789894	200*	33.9	33%	not taken
125 pM titration	125.3	12.15583	200*	60.8	49%	not taken
30 min hi pH 1	104.4	10.13837	200.55	50.6	48%	7.154
30 min hi pH 2	104.4	7.666839	197.51	38.8	37%	7.883
30 min hi pH 3	104.4	14.48604	198.77	72.9	70%	7.722
30 min lo pH 1	104.4	11.11168	190.63	58.3	56%	3.926
30 min lo pH 2	101.8	17.36457	201.13	86.3	85%	3.922
30 min lo pH 3	101.8	21.02556	194.18	108.3	106%	4.262
2 hour 1	101.8	14.06952	199.18	70.6	69%	4.598
2 hour 2	101.8	6.554468	198.07	33.1	33%	4.713
2 hour 3	101.8	12.06073	197.20	61.2	60%	4.797

Sample ID	[Ag ⁺] added, pM	[Ag] by ICP-MS, nM	Concentration Factor (M _{aq} /M _{ICPMS})	[Ag*], pM	% recovery	Final pH of (aq) layer
1 hour 1	101.8	13.21689	196.69	67.2	66%	4.487
1 hour 2	101.8	11.57841	197.93	58.5	57%	4.354
1 hour 3	101.8	13.42922	203.14	66.1	65%	4.384
4 hour 1	101.6	12.73334	199.40	63.9	63%	4.244
4 hour 2	101.6	8.809124	196.65	44.8	44%	4.265
5 min 1	101.6	16.09328	199.63	80.6	79%	4.199
5 min 2	102.2	14.46521	198.87	72.7	71%	4.251
5 min 3	102.2	14.62986	198.30	73.8	72%	4.196
TotAg Well H ₂ O	0.0	1.165162	199.79	5.8	n/a	3.932
TotAg Well H ₂ O + 10 pM Ag	9.5	0.421926	200.62	2.1	22%	3.949
TotAg Well H ₂ O + 20 pM Ag	21.0	1.006122	200.52	5.0	24%	3.787
TotAg Well H ₂ O rerun (RR)	0.0	0.960413	199.79	4.8	n/a	3.932
TotAg Well H ₂ O + 10 pM Ag RR	9.5	0.635664	200.62	3.2	33%	3.949
TotAg Well H ₂ O + 20 pM Ag RR	21.0	1.489055	200.52	7.4	35%	3.787
Well H ₂ O	0.0	1.280	202.14	6.3	n/a	4.257
Well H ₂ O + 20 pM Ag	20.3	3.222	203.06	15.9	78%	4.278
Well H ₂ O + 40 pM Ag	41.1	5.247	200.75	26.1	64%	4.251
Well H ₂ O + 60 pM Ag	59.9	11.206	199.70	56.1	94%	4.356
Well H ₂ O + 100 pM Ag	102.0	17.757	200.20	88.7	87%	4.264

*samples were prepared volumetrically, so exact concentration factors are unknown.

Double lines (=) between results denote separate analysis dates.

Table IV.iv Competitive ligand experiments using DDC⁻, various competing ligands, & organic extraction

Sample ID	[Ag ⁺], pM	[Ag] by ICP-MS, nM	Concentration Factor (M _{aq} /M _{ICPMS})	[Ag*], pM	% recovery	Final pH of (aq) layer
no ligands #1	100.6	0.100765	100.17	1.0	1%	8.761
10 ⁻⁷ M DDC ⁻ #1	99.2	0.148263	100.36	1.5	1%	7.833
10 ⁻⁶ M DDC ⁻ #1	100.4	6.648117	99.67	66.7	66%	7.773
no ligands #2	101.0	0.11345	100.70	1.1	1%	7.677
10 ⁻⁷ M DDC ⁻ #2	100.2	0.290142	100.58	2.9	3%	7.785
10 ⁻⁶ M DDC ⁻ #2	101.5	8.393909	98.90	84.9	84%	7.830
10 ⁻⁵ M DDC ⁻ #1	100.7	8.280327	100.30	82.6	82%	7.924
10 ⁻⁴ M DDC ⁻ #1	102.5	5.198508	99.11	52.5	51%	7.945
1 μM glutathione #1	101.5	0.141109	100.40	1.4	1%	7.861
10 ⁻⁵ M DDC ⁻ #2	101.6	9.135929	98.94	92.3	91%	7.761
10 ⁻⁴ M DDC ⁻ #2	102.2	7.025288	98.94	71.0	69%	7.780
1 μM glutathione #2	102.8	0.136136	99.84	1.4	1%	7.592
1 μM glut, 10 ⁻⁷ M DDC ⁻ #1	102.4	2.801785	99.50	28.2	27%	7.746
1 μM glut, 10 ⁻⁶ M DDC ⁻ #1	100.8	6.901608	100.30	68.8	68%	7.725
1 μM glut, 10 ⁻⁵ M DDC ⁻ #1	102.5	8.513267	93.13	91.4	89%	7.730
1 μM glut, 10 ⁻⁷ M DDC ⁻ #2	102.2	1.95458	99.34	19.7	19%	7.760
1 μM glut, 10 ⁻⁶ M DDC ⁻ #2	101.0	6.827873	99.14	68.9	68%	7.795
1 μM glut, 10 ⁻⁵ M DDC ⁻ #2	102.3	5.640802	99.51	56.7	55%	7.803
1 μM glut, 10 ⁻⁴ M DDC ⁻ #1	102.5	5.290258	99.22	53.3	52%	7.782
1 μM glut, 10 ⁻⁴ M DDC ⁻ #2	101.0	5.466417	99.80	54.8	54%	7.775
no ligands	100.4	-0.04565	99.43	-0.5	0%	7.762

Sample ID	[Ag ⁺], pM	[Ag] by ICP-MS, nM	Concentration Factor (M _{aq} /M _{ICPMS})	[Ag*], pM	% recovery	Final pH of (aq) layer
10 ⁻⁷ M DDC ⁻	102.6	0.611327	100.00*	6.1	6%	7.727
10 ⁻⁶ M DDC ⁻	101.2	8.864726	100.58	88.1	87%	7.621
10 ⁻⁵ M DDC ⁻	101.5	2.103402	99.96	21.0	21%	7.727
10 ⁻⁴ M DDC ⁻	102.4	2.261317	99.15	22.8	22%	7.800
100 μM EDTA	102.4	-0.07535	99.42	-0.8	-1%	7.619
100 μM EDTA, 10 ⁻⁷ M DDC ⁻	101.1	0.504868	99.66	5.1	5%	7.720
100 μM EDTA, 10 ⁻⁶ M DDC ⁻	102.4	6.764264	99.37	68.1	66%	7.763
100 μM EDTA, 10 ⁻⁵ M DDC ⁻	102.3	5.064609	99.32	51.0	50%	7.730
100 μM EDTA, 10 ⁻⁴ M DDC ⁻	101.0	4.566949	99.60	45.9	45%	7.761
1000 μM EDTA	101.6	-0.0283	99.76	-0.3	0%	7.569
1000 μM EDTA, 10 ⁻⁷ M DDC ⁻	101.3	0.189209	99.03	1.9	2%	7.679
1000 μM EDTA, 10 ⁻⁶ M DDC ⁻	100.7	4.81051	99.39	48.4	48%	7.683
1000 μM EDTA, 10 ⁻⁵ M DDC ⁻	102.2	2.284154	99.44	23.0	22%	7.678
1000 μM EDTA, 10 ⁻⁴ M DDC ⁻	100.1	2.355867	99.89	23.6	24%	7.665
no ligands #1	100.2	0.302343	99.29	3.0	3%	7.478
10 ⁻⁷ M DDDC #1	106.1	5.541646	99.25	55.8	53%	7.527
10 ⁻⁶ M DDDC #1	101.6	8.492365	99.72	85.2	84%	7.524
10 ⁻⁵ M DDDC #1	99.9	6.599064	99.78	66.1	66%	7.509
10 ⁻⁴ M DDDC #1	101.8	5.537878	100.15	55.3	54%	7.521

Sample ID	[Ag ⁺], pM	[Ag] by ICP-MS, nM	Concentration Factor (M _{aq} /M _{ICPMS})	[Ag*], pM	% recovery	Final pH of (aq) layer
10 ⁻⁷ M DDDC #2	100.4	3.818479	99.65	38.3	38%	7.506
10 ⁻⁶ M DDDC #2	101.1	7.002821	99.23	70.6	70%	7.491
10 ⁻⁵ M DDDC #2	102.6	7.242218	99.62	72.7	71%	7.483
10 ⁻⁴ M DDDC #2	101.0	7.142151	99.32	71.9	71%	7.497
1 μM glutathione	100.4	0.283688	99.95	2.8	3%	7.433
1 μM glut, 10 ⁻⁷ M DDDC	101.8	5.427707	100.21	54.2	53%	7.507
1 μM glut, 10 ⁻⁶ M DDDC	100.4	8.230469	100.54	81.9	82%	7.516
1 μM glut, 10 ⁻⁵ M DDDC	99.2	5.868819	99.15	59.2	60%	7.505
1 μM glut, 10 ⁻⁴ M DDDC	101.7	7.214083	99.19	72.7	72%	7.512
100 μM EDTA	102.5	0.336474	99.86	3.4	3%	7.396
100 μM EDTA, 10 ⁻⁷ M DDDC	100.4	2.066463	99.09	20.9	21%	7.553
100 μM EDTA, 10 ⁻⁶ M DDDC	100.7	0.716267	99.89	7.2	7%	7.555
100 μM EDTA, 10 ⁻⁵ M DDDC	101.0	9.557773	100.31	95.3	94%	7.553
100 μM EDTA, 10 ⁻⁴ M DDDC	100.9	5.373379	100.26	53.6	53%	7.520
well H ₂ O, 10 ⁻⁵ M DDDC	0.0	0.516998	98.54	5.2	n/a	7.723
well H ₂ O, 10 ⁻⁵ M DDDC, 100 pM Ag ⁺	105.7	10.46526	98.59	106.1	100%	7.706
no ligands	0.0	0.050666	98.21	0.5	n/a	7.787
DDC ⁻ only	0.0	0.42253	101.09	4.2	n/a	7.787
DDC ⁻ & EDTA	0.0	0.469625	98.70	4.8	n/a	7.796
10 pM Ag	10.2	0.011997	98.96	0.1	1%	7.787

Sample ID	[Ag ⁺], pM	[Ag] by ICP-MS, nM	Concentration Factor (M _{aq} /M _{ICPMS})	[Ag*], pM	% recovery	Final pH of (aq) layer
10 pM Ag	10.2	0.013326	98.96	0.1	1%	7.787
10 pM & DDC ⁻	9.8	1.896938	99.62	19.0	194%	7.826
10 pM, DDC ⁻ , EDTA	9.8	0.525474	98.81	5.3	54%	7.805
20 pM Ag	20.3	-0.00584	99.87	-0.1	0%	7.794
20 pM Ag	20.3	0.00762	99.87	0.1	0%	7.794
20 pM & DDC ⁻	20.3	2.229764	99.01	22.5	111%	7.807
20 pM, DDC ⁻ , EDTA	20.3	1.00302	99.86	10.0	49%	7.764
30 pM Ag	30.1	0.011553	99.43	0.1	0%	7.818
30 pM & DDC ⁻	30.1	2.81755	99.20	28.4	94%	7.776
30 pM & DDC ⁻	30.1	0.340254	97.77	3.5	12%	7.800
30 pM, DDC ⁻ , EDTA	30.1	1.715149	100.89	17.0	57%	7.785
50 pM Ag	50.5	0.007287	99.55	0.1	0%	7.811
50 pM & DDC ⁻	50.5	2.644543	100.05	26.4	52%	7.800
50 pM, DDC ⁻ , EDTA	51.6	1.703954	99.29	17.2	33%	7.840
100 pM Ag	103.5	0.051885	99.70	0.5	1%	7.836
100 pM & DDC ⁻	100.9	8.574853	99.88	85.9	85%	7.812
100 pM, DDC ⁻ , EDTA	100.9	6.691966	99.18	67.5	67%	7.790
30 pM & DDC ⁻	30.1	0.31848	97.77	3.3	11%	7.800
200 pM Ag	202.2	0.006179	98.77	0.1	0%	7.796
200 pM & DDC ⁻	202.2	11.77817	98.92	119.1	59%	7.775
200 pM, DDC ⁻ , EDTA	202.2	14.28391	99.04	144.2	71%	7.725
200 pM & DDC ⁻	202.2	11.45277	98.92	115.8	57%	7.775
no ligands	103.5	0.026733	99.31	0.3	0%	7.871
10 ⁻⁷ M DDC ⁻	99.7	5.843839	100.49	58.2	58%	7.932
10 ⁻⁶ M DDC ⁻	101.3	6.264781	99.77	62.8	62%	7.927
10 ⁻⁵ M DDC ⁻	99.2	9.564174	100.66	95.0	96%	7.930

Sample ID	[Ag ⁺], pM	[Ag] by ICP-MS, nM	Concentration Factor (M _{aq} /M _{ICPMS})	[Ag*], pM	% recovery	Final pH of (aq) layer
10 ⁻⁴ M DDC ⁻	99.6	9.30328	100.40	92.7	93%	7.909
no DDC ⁻ , 30 µg/L triclosan	100.8	0.025348	98.80	0.3	0%	7.783
10 ⁻⁷ M DDC ⁻ , 30 µg/L tric	102.2	6.197374	98.48	62.9	62%	7.926
10 ⁻⁷ M DDC ⁻ , 30 µg/L tric	99.9	0.506137	99.46	5.1	5%	7.849
10 ⁻⁶ M DDC ⁻ , 30 µg/L tric	100.2	7.081078	98.67	71.8	72%	7.907
10 ⁻⁵ M DDC ⁻ , 30 µg/L tric	102.8	9.654609	99.68	96.9	94%	7.902
10 ⁻⁴ M DDC ⁻ , 30 µg/L tric	99.8	5.736615	99.29	57.8	58%	7.923
no DDC ⁻ , 10 nM T ₃	100.3	0.037259	99.59	0.4	0%	7.802
10 ⁻⁷ M DDC ⁻ , 10 nM T ₃	101.0	4.503574	99.07	45.5	45%	7.949
10 ⁻⁶ M DDC ⁻ , 10 nM T ₃	99.3	6.367296	100.10	63.6	64%	7.868
10 ⁻⁵ M DDC ⁻ , 10 nM T ₃	101.2	5.985458	99.11	60.4	60%	7.909
10 ⁻⁴ M DDC ⁻ , 10 nM T ₃	99.9	9.179454	99.77	92.0	92%	7.842
Method Blank 2	0.0	0.195335	100.24	1.9	n/a	7.714
Method Blank 3	0.0	0.190459	100.15	1.9	n/a	7.702
Method Blank 4	0.0	0.052123	100.28	0.5	n/a	7.720
Method Blank 5	0.0	0.149021	99.97	1.5	n/a	7.695
Method Blank 6	0.0	0.153692	100.15	1.5	n/a	7.704
0.6 µg/L Blk	185.0	1.694251	50.00	33.9	18%	7.781
0.6 µg/L Blk + 50 pM Ag	235.5	3.804886	49.78	76.4	32%	7.807
0.6 µg/L Blk + 100 pM Ag	285.5	5.277169	49.77	106.0	37%	7.786
0.6 µg/L Blk + 150 pM Ag	334.0	6.026226	49.66	121.3	36%	7.753
0.6 µg/L Blk + 200 pM Ag	392.0	3.3654	49.90	67.4	17%	7.730

Sample ID	[Ag ⁺], pM	[Ag] by ICP-MS, nM	Concentration Factor (M _{aq} /M _{ICPMS})	[Ag*], pM	% recovery	Final pH of (aq) layer
6.0 µg/L Blk	464.0	0.233005	49.75	4.7	1%	7.746
6.0 µg/L Blk + 50 pM Ag	513.5	2.475591	49.70	49.8	10%	7.775
6.0 µg/L Blk + 100 pM Ag	562.4	4.639637	49.68	93.4	17%	7.756
6.0 µg/L Blk + 150 pM Ag	613.4	4.852579	49.73	97.6	16%	7.767
6.0 µg/L Blk + 200 pM Ag	666.7	5.199073	50.62	102.7	15%	7.740
0.6 µg/L nAg	742.0	1.409824	19.95	70.7	10%	7.576
0.6 µg/L nAg + 100 pM Ag	842.9	1.894515	19.98	94.8	11%	7.558
0.6 µg/L nAg + 200 pM Ag	943.8	3.052485	19.98	152.8	16%	7.835
0.6 µg/L nAg + 300 pM Ag	1044.9	5.167717	19.93	259.3	25%	7.628
0.6 µg/L nAg + 500 pM Ag	1245.4	6.144105	19.95	308.0	25%	7.527
0.6 µg/L AgNO ₃	4260.0	0.248821	2.003	124.2	3%	7.747
0.6 µg/L AgNO ₃ + 2 nM Ag	6303.3	4.218406	2.0094	2099.3	33%	7.773
0.6 µg/L AgNO ₃ + 4 nM Ag	8455.8	7.082534	2.004	3533.7	42%	7.626
0.6 µg/L AgNO ₃ + 6 nM Ag	10456	3.061194	2.022	1513.9	14%	7.856
0.6 µg/L AgNO ₃ + 10 nM Ag	14588	2.09159	2.016	1037.3	7%	7.808
6 µg/L nAg	9180.0	2.039781	2.002	1018.9	11%	7.627
6 µg/L nAg + 2 nM Ag	11217	2.415071	1.998	1208.6	11%	7.654
6 µg/L nAg + 4 nM Ag	13247	6.228015	1.988	3132.2	24%	7.944
6 µg/L nAg + 6 nM Ag	15273	9.634554	1.992	4837.1	32%	7.783
6 µg/L nAg + 10 nM Ag	19267	0.407851	2.008	203.1	1%	7.593

Sample ID	[Ag ⁺], pM	[Ag] by ICP-MS, nM	Concentration Factor (M _{aq} /M _{ICPMS})	[Ag*], pM	% recovery	Final pH of (aq) layer
6 µg/L AgNO ₃	13600	4.066872	1.001	4062.8	30%	7.809
6 µg/L AgNO ₃ + 5 nM Ag	18619	9.493261	0.9972	9520.1	51%	7.764
6 µg/L AgNO ₃ + 10 nM Ag	23645	3.735072	0.9956	3751.7	16%	7.632
6 µg/L AgNO ₃ + 15 nM Ag	28684	6.982648	0.9993	6987.4	24%	7.840
6 µg/L AgNO ₃ + 20 nM Ag	33724	13.90232	1.028	13523.3	40%	7.882
20 pM Ag	20.3	0.467	49.69	9.4	46%	7.750
20 pM Ag + 30 µg/L triclosan	20.3	0.275	49.71	5.5	27%	7.741
20 pM Ag + 10 nM T ₃	20.3	0.327	49.68	6.6	32%	7.739
40 pM Ag	40.5	1.390	49.79	27.9	69%	7.759
40 pM Ag + 30 µg/L triclosan	40.5	0.470	49.70	9.5	23%	7.775
40 pM Ag + 10 nM T ₃	40.5	1.263	49.70	25.4	63%	7.764
60 pM Ag	61.1	1.999	49.71	40.2	66%	7.715
60 pM Ag + 30 µg/L triclosan	61.1	0.808	49.61	16.3	27%	7.718
60 pM Ag + 10 nM T ₃	61.1	1.490	49.64	30.0	49%	7.718
100 pM Ag	101.7	2.981	49.74	59.9	59%	7.718
100 pM Ag + 30 µg/L triclosan	101.7	2.091	49.64	42.1	41%	7.704
100 pM Ag + 10 nM T ₃	101.7	2.796	49.72	56.2	55%	7.694
200 pM Ag	203.1	4.595	49.81	92.3	45%	7.728
200 pM Ag + 30 µg/L triclosan	203.1	3.215	49.77	64.6	32%	7.738

Sample ID	[Ag ⁺], pM	[Ag] by ICP-MS, nM	Concentration Factor (M _{aq} /M _{ICPMS})	[Ag*], pM	% recovery	Final pH of (aq) layer
200 pM Ag + 10 nM T ₃	203.1	2.325	49.82	46.7	23%	7.721
400 pM Ag	400.3	7.036	49.81	141.3	35%	7.721
400 pM Ag + 30 µg/L triclosan	400.3	6.616	49.78	132.9	33%	7.714
400 pM Ag + 10 nM T ₃	400.3	6.509	49.75	130.8	33%	7.719

*concentration factor is estimated as some of this sample was spilled just before weighing final volume.

Double lines (=) between results denote separate analysis dates.
Results highlighted were not used in further Ag analysis.

Table IV.v: Calculated values used for samples examined by Langmuir linearizations of titration data

Sample	[Ag _T], pM	[Ag*], pM	[Ag ⁺], pM	Σ[AgL _i], pM	$\frac{[Ag^+]}{\Sigma[AgL_i]}$	$\frac{\Sigma[AgL_i]}{[Ag^+]}$
Well water with 100 µM EDTA; $\alpha_{Ag^*} = 4.43E-03$	0	4.8	1.07E-03	-6.1	-1.76E-04	-5.69E+03
	9.8	5.3	1.20E-03	3.0	4.04E-04	2.47E+03
	20.3	10.0	2.27E-03	7.4	3.06E-04	3.26E+03
	30.1	17.0	3.84E-03	8.3	4.64E-04	2.15E+03
	51.6	17.2	3.87E-03	29.6	1.31E-04	7.63E+03
	100.9	67.5	1.52E-02	14.2	1.07E-03	9.35E+02
	202.2	144.2	3.25E-02	17.0	1.92E-03	5.21E+02
Well water & 30 µg/L triclosan; $\alpha_{Ag^*} = 6.61E-02$	20.3	5.5	8.36E-03	4.2	1.97E-03	5.06E+02
	40.5	9.5	1.43E-02	13.0	1.10E-03	9.08E+02
	61.1	16.3	2.46E-02	13.8	1.79E-03	5.58E+02
	101.7	42.1	6.37E-02	-20.7	-3.08E-03	-3.25E+02
	203.1	64.6	9.77E-02	15.4	6.34E-03	1.58E+02
	400.3	132.9	2.01E-01	14.2	1.42E-02	7.04E+01